AD NUMBER

AD865321

NEW LIMITATION CHANGE

TO

Approved for public release, distribution unlimited

FROM

Distribution authorized to U.S. Gov't. agencies and their contractors; Administrative/Operational Use; Nov 1969. Other requests shall be referred to Air Force Materials Lab, Attn: MAMC, Wright-Patterson AFB, OH 45433.

AUTHORITY

Air Force Materials Lab ltr, 12 Jan 1972

AFML-TR-68-190
PART II, VOLUME V

RESEARCH AND DEVELOPMENT OF REFRACTORY OXIDATION-RESISTANT DIBORIDES

PART II, VOLUME V:
THERMAL, PHYSICAL, ELECTRICAL AND OPTICAL PROPERTIES

EDWARD V. CLOUGHERTY
KENNETH E. WILKES
RONALD P. TYE
ManLabs, Inc.

TECHNICAL REPORT AFML-TR-68-190, PART II, VOLUME V

NOVEMBER 1969

AIR FORCE MATERIALS LABORATORY
AIR FORCE SYSTEMS COMMAND
WRIGHT-PATTERSON AIR FORCE BASE, OHIO

NOTICES

When Government drawings, specifications, or other data are used for any purpose other than in connection with a definitely related Government procurement operation, the United States Government thereby incurs no responsibility nor any obligation whatsoever; and the fact that the Government may have formulated, furnished, or in any way supplied the said drawings, specifications, or other data is not to be regarded by implication or otherwise as in any manner licensing the holder or any other person or corporation, or conveying any rights or permission to manufacture, use, or sell any patented invention that may in any way be related thereto.

This document is subject to special export controls and each transmittal to foreign governments or foreign nationals may be made only with prior approval of the Air Force Materials Laboratory (MAMC), Wright-Patterson Air Force Base, Ohio 45433.

Distribution of this report is limited for the protection of technology relating to critical materials restricted by the Export Control Act.

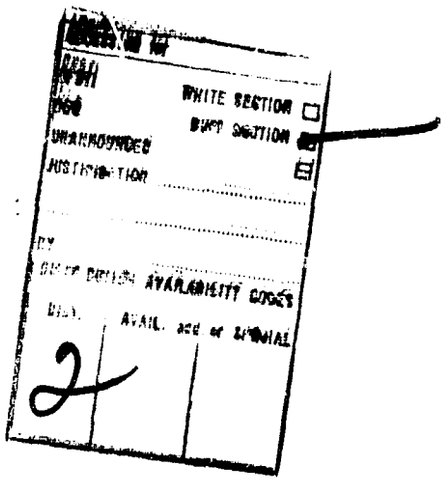

Copies of this report should not be returned unless return is required by security considerations, contractual obligations, or notice on a specific document.

500 - December 1969 - CO455 - 104-2292

RESEARCH AND DEVELOPMENT OF REFRACTORY OXIDATION-RESISTANT DIBORIDES

PART II, VOLUME V: THERMAL, PHYSICAL, ELECTRICAL AND OPTICAL PROPERTIES

EDWARD V. CLOUGHERTY

KENNETH E. WILKES

RONALD P. TYE

FOREWORD

This report was prepared by the Research Division, ManLabs Inc., with the assistance of Battelle Memorial Institute, Dynatech Corp. and Avco, Applied Technology Division under U.S. Air Force Contract No. AF33(615)-3671. The contract was initiated under Project 7350, "Refractory Inorganic Nonmetallic Materials," Task 735001, "Refractory Inorganic Nonmetallic Materials: Nongraphitic." The work was administered under the direction of the Air Force Materials Laboratory Ceramics and Graphite Branch with John R. Fenter acting as project engineer.

This report covers the period from 15 September 1967 to 15 May 1969.

ManLabs personnel participating in this study included F. V. Clougherty, H. Nesor and V. Kousky.

Battelle Memorial Institute personnel who participated in the work described in this report include H. Deem, E.A. Eldridge, A. S. Lower and K.E. Wilkes; Dynatech personnel, R.P. Tye; Avco personnel, R.J. Hill and R. Gannon.

The manuscript of this report was submitted by the authors in November 1969 for publication.

This technical report has been reviewed and is approved.

W. G. Ramke
Chief, Ceramics and Graphite Branch
Metals and Ceramics Division
Air Force Materials Laboratory

ABSTRACT

Thermal conductivity data were measured from 100° to 1000°C and were calculated from thermal diffusivity, specific heat and density data from 1000° to 2000°C for compositional and microstructural variations of ZrB_2 and HfB_2 with SiC and/or C additives varying in total content from 20 to 34 volume percent. All compositions displayed a negative temperature dependence with values of the order of 0.20 and 0.10 cal.cm/cm^{2}sec °C at room temperature and 2000°C, respectively. The specific heat data were obtained from drop calorimetry methods for selected compositions and by calculations from constituent values for other compositions.

Linear expansion data were obtained from room temperature to 2000°C by direct-view and differential dilatometry for compositions of ZrB_2 with SiC and/or C additives. Average CTE values are of the order of 7.0×10^{-6} in/in/°C. Density data at room temperature showed the effects of SiC and C; the additions produce a significant reduction in the density of HfB_2 from 11 to 8 grams/cc.

Electrical resistivity data were obtained from room temperature to 1000°C; all compositions displayed positive temperature coefficients. Room temperature values of the order of 10 to 15$\mu\Omega$cm were measured for all compositions.

Total normal emittance data were measured from 1600° to 2300°C for unoxidized diboride compositions.

TABLE OF CONTENTS

LIST OF ILLUSTRATIONS

LIST OF TABLES

I. INTRODUCTION AND SUMMARY

A. Introduction

The diborides of zirconium and hafnium are the outstanding candidates among high melting intermetallic compounds, graphite composites, oxides, and coated refractory metals for applications which require thermochemical stability and oxidation resistance at elevated temperatures. Earlier studies of diboride compounds provided a good working description of the chemical, physical and thermodynamic properties relevant to material response to high temperature oxidizing environments (1*, 2). Subsequently, extensive data derived from cold gas/hot sample furnace oxidation tests of polycrystalline composites containing ZrB_2 or HfB_2 with various additives designed to impart improved oxidation characteristics without sacrificing high temperature stability identified the SiC addition as the most beneficial composition (3). This study also generated mechanical property data for well characterized ZrB_2 and HfB_2 and diboride material response characteristics to hot gas/cold wall, arc plasma tests. The results of transverse bend tests showed that strength levels of 40,000 to 60,000 psi were attainable for fine grained high density ZrB_2 and HfB_2 over the range from room temperature to 1200°C in inert atmospheres. Results of limited arc plasma testing suggested favorable thermal stress and oxidation resistance. Thermal conductivity data for ZrB_2 and HfB_2 showed positive temperature coefficients with values of 0.09 and 0.05 cal $cm/cm^2 sec\ ^\circ C$ for dense ZrB_2 at 1000° and 1700°C respectively (2). Linear expansion data for ZrB_2 and HfB_2 provided CTE values of 7.0 to 8.0 x $10^{-6}\ ^\circ C^{-1}$. Electrical resistivity measurements to 1400°C demonstrated that dense ZrB_2 and HfB_2 have room temperature resistivities of the order of 4 to 10 $\mu\Omega$ cm with positive temperature coefficients of resistance.

The present investigation was undertaken to prepare a number of diboride materials containing either ZrB_2 or HfB_2 as the principal component with selected additives designed to enhance one or more of the following: oxidation resistance, mechanical properties, and thermal stress resistance. Diboride materials, including ZrB_2 and HfB_2 with no additive, were fabricated with microstructural variations of grain size and porosity, principally by conventional hot pressing procedures which are suitable for the production of components such as nose caps, leading edges, vanes and similar objects anticipated for use in high velocity flight or reentry conditions.

The program was broadly divided into three phases: (1) composition and microstructure screening, (2) extensive properties testing, and (3) simulated application evaluations and verification of properties in scaled-up fabrication. In Phase One, oxidation, mechanical, and thermal screening tests of a wide range of compositions and microstructures were used to select a limited number of materials for further study. In Phase Two, the selected compositions and microstructures were fully characterized over a wide temperature range in terms of oxidation resistance, strength, elastic modulus, linear expansion, thermal conductivity, and steady state thermal stress resistance. Finally, in Phase Three, properties were redetermined for materials prepared in scaled-up billet sizes, and several application oriented evaluations including a test of a leading edge configuration subjected to simulated hypersonic flight heating were performed.

---

*The underscored numbers in parenthesis refer to references which are listed at the end of this report.

B. Summary

The program progress during the first eighteen months, Part I, was primarily comprised of Phase One processing studies and thermal, oxidation and mechanical screening evaluations performed on samples obtained from hot pressed billets, 2 inch in diameter by 0.7 inch high. Data and results obtained in Part I were presented in a technical report (4).

Thermal, physical, electrical and optical property data were obtained in Part II for selected compositional and microstructural variations of ZrB_2 and HfB_2 with additions of SiC and/or C. Data were obtained for the following structures: Material I, ZrB_2 with no additive, fully dense and 90 per cent dense; Material III(5), HfB_2 with 5 volume per cent SiC, fully dense, Materials III and IV, HfB_2 with 20 and 30 volume per cent SiC respectively, both fully dense; Material V, ZrB_2 with 20 volume per cent SiC, fully dense and 90 per cent dense; Material VIII, ZrB_2 with 14 and 30 volume per cent SiC and C, respectively, fully dense; VIII (18,10), ZrB_2 with 18 and 10 volume per cent SiC and C, respectively, fully dense; Material XII(20), ZrB_2 with 20 volume per cent C, 95 to 100 per cent dense; Material XIV(18,10), HfB_2 with 18 and 10 volume per cent SiC and C, respectively, fully dense; and Material XV(20), HfB_2 with 20 volume per cent C, fully dense. The majority of the data were obtained from 3 inch diameter by 1 inch high hot pressed billets; specimens were also obtained from hot pressed billets 6 inch square by 1 to 2 inch high. The former billets were prepared in the Phase Two processing study; the latter billets, in the Phase Three scaled-up processing.

Thermal conductivity was measured from 100° to 1000°C using the cut-bar method; all data showed a slight negative temperature dependence. The magnitude of the dependence varied with composition and porosity. The thermal conductivity of dense Materials I, V and VIII (18,10) and 95 per cent dense XII(20) at 100°C are 0.199, 0.236, 0.275, and 0.204 cal $cm/cm^2 sec\,^{\circ}C$, respectively; the values at 1000°C are 0.192, 0.187, 0.176 and 0.153 cal $cm/cm^2 sec\,^{\circ}C$ respectively for the same structures.

Thermal diffusivity was measured from 1000° to 2000°C using the flash-laser technique; all data showed a slight negative temperature dependence. The thermal diffusivity of dense Materials I, V and VIII(18,10) and 95 per cent dense XII(20) at 1000°C are 0.205, 0.213, 0.190 and 0.179 cm^2/sec respectively; the values at 2000°C, 0.178, 0.163, 0.143 and 0.145 cm^2/sec, respectively for the same structures.

Drop calorimetry was employed to measure relative enthalpy, $H_T - H_{0\,^{\circ}C}$, for four compositional variations of ZrB_2, SiC and C over the range 1000° to 2000°C. The enthalpy data were used to obtain specific heat and relative entropy data ($S_T - S_{0\,^{\circ}C}$) over the same range. Specific heats calculated from composition and the component specific heat data compared favorably with the measured specific heats.

Thermal conductivity over the range 1000° to 2000°C was calculated from the diffusivity, specific heat and density data. The calculated data for 1000°C are in satisfactory agreement with the measured data obtained

by the cut-bar method. The slight negative temperature dependence observed between 100° and 1000°C persisted through 2000°C.

Linear expansion data were obtained for selected structures; both direct-view and differential dilatometry were employed to obtain data from room temperature to 2000°C. No major variation in expansion characteristics were observed for the structures examined; average CTE values for 20° to 1000°C were 6.5 to 7.5 x 10^{-6} in/in/°C.

Density data for the compositional variations of ZrB_2 and HfB_2 with SiC and C show the expected trends. The room temperature values for fully dense ZrB_2 compositions of Materials I, V, VIII(18,10) and XII(20) are 5.9 to 6.1, 5.5, 5.3 and 5.4 grams/cc, respectively. A larger reduction in density is effected by SiC and C in HfB_2 compositions. The room temperature values for dense Material II, III, IV, XIV(18,10) and XV(20) are 10.9 to 11.2, 9.2, 8.4, 8.7 and 9.0, respectively.

Electrical resistivity data were obtained from room temperature to 1000°C. Positive temperature coefficients were observed for all structures examined. Room temperature values for dense Materials I, V and VIII(18,10) and 95 per cent dense XII(20) are 12.1, 10.2, 14.6 and 13.6 μΩcm respectively; the values at 1000°C are 44.0, 54.5, 68.5 and 58.7 μΩcm, respectively, for the same structures.

Total normal emittance data were measured over the range 1600° to 2300°C for unoxidized surfaces of Material I, V, VIII, XII(20) and III. Values of 0.62 and 0.70 were obtained for Material I and V at 1600°C; 0.86 and 0.92 at 1700°C for Materials VIII and XII(20). All data show a gradual decrease with increase in temperature.

II. MATERIAL IDENTIFICATION AND STRUCTURE CHARACTERIZATION

Diboride materials in this program include ZrB_2 or HfB_2 with no intentional additive and several composite materials based on either ZrB_2 or HfB_2 with one or more additives designed to impart improvement in strength or oxidation resistance or thermal stress resistance or any combination of these properties. The phase constitution and base composition of all the materials considered for this program are identified by a Roman numeral designation as shown in Table 1.

The billet identification system extends the above designation to include the pressing number and the size of the billet. Reinforcing agents such as W filament, Thornel C yarn and SiC fibers are also identified by an extension of the original designation. Several billet designations are explained in Appendix I to familiarize the reader with this system. Compositional variations within a given identified material were also examined; representative designations for such variations are also provided in Appendix I.

III. THERMAL PROPERTIES

A. Introduction

Thermal property data required for thermal stress analyses and design considerations were obtained in the Phase Two property measurements. Thermal conductivity data were obtained from comparative cut-bar measurements performed in argon over the range 100° to 1000°C for twelve diboride structures consisting of compositional and microstructural variations of ZrB_2 or HfB_2 with SiC and/or C additives. Thermal diffusivity data were obtained from measurements employing the "flash-laser" technique in argon over the range 1000° to 2000°C for ten diboride structures. In order to provide a comparison of the conductivity and diffusivity data, drop calorimetry measurements were obtained for the four principal compositional variations of ZrB_2, SiC and C to provide enthalpy data over the range 1000° to 2000°C. The enthalpy data were employed to calculate specific heat and entropy values over the same temperature range. Thermal conductivity data calculated for the 1000° to 2000°C range for the four principal compositional variations from the specific heat, the thermal diffusivity and independently measured density (at temperature) were compared with the measured data over the range 100° to 1000°C.

The thermal conductivity measurements in the 100° to 1000°C range were performed at Dynatech Corporation, Measurements Laboratory under the direction of Mr. Ronald P. Tye. The thermal diffusivity and the drop calorimetry measurements and the calculations of specific heat, entropy and thermal conductivity were performed at Battelle Memorial Institute, Thermophysical Properties Division under the supervision of Mr. Kenneth E. Wilkes.

B. Measurement Techniques

1. Thermal Conductivity (100° to 1000°C)

The thermal conductivity specimens were in the form of cylinders approximately 0.875 inch diameter and 0.900 inch long with two small holes 0.065 inch diameter drilled half-way through the specimen and centered 0.650 inch apart.

The thermal conductivity measurements were undertaken in an argon atmosphere employing the comparative cut-bar technique shown schematically in Figure 1. Fine guage platinum-10 percent rhodium/platinum thermocouples in twin bore alumina insulation and protected by a closed end stainless steel hypodermic tubing were forced into the holes in the specimen as a tight fit. The specimen was then sandwiched between two similar samples of Armco iron of known thermal conductivity which were similarly instrumented. To minimize contact resistances at the interfaces each surface was prepared to as good a surface finish as possible. Platinum or silvermetal foils could not be used at the interfaces since contamination of the sample would occur at the higher temperature. The specimen assembly was placed between an upper heater and a lower heat sink consisting of a heater and a fluid cooled base and a reproducible load in excess

of 50 psi applied to the stack to help reduce contact resistance. A guard tube with thermocouple instrumentation along its length which could be heated at several positions along its length was placed around the system and the whole of the interspace and surroundings filled with a good heat insulating powder.

By means of suitable adjustments to the power in the various heaters a steady axial temperature gradient distribution was maintained in the system and undue radial loss was prevented by keeping the guard tube gradient matched closely to that in the sample stack.

At equilibrium conditions the temperature at various points in the specimen and guard were evaluated from thermocouple readings and the heat flow derived in terms of that flowing through each reference specimen. The thermal conductivity was evaluated from the above quantities and the dimensions of the sample as

$$K = \frac{1}{2\Delta T_{Sample}} \left[(k\Delta T)_{Top\ Standard} + (k\Delta T)_{Bottom\ Standard} \right] \quad (1)$$

The K value for the standard is the thermal conductivity at the mean measuring temperature obtained from calibration curves.

The errors in the measurements and procedure are estimated to provide thermal conductivity data accurate to ± 5 percent.

2. Thermal Diffusivity (1000° to 2000°C)

The thermal diffusivity specimens were in the form of right circular cylindrical discs, 0.500 inch diameter by 0.100 inch high with ends flat and parallel to ± 0.001 inch.

Thermal diffusivity measuremens were made by the "flash-laser" technique. The thin disk-shaped specimen was positioned in an isothermal zone of a furnace and the front face was irradiated by a short-duration laser pulse. As the heat pulse traveled through the specimen the back-face temperature rise was recorded as a function of time. This temperature-time history of the back face is directly related to the thermal diffusivity of the specimen as

$$\alpha = \frac{0.139 L^2}{t_{1/2}} \quad (2)$$

where α = thermal diffusivity, L = specimen thickness and $t_{1/2}$ = time required for back face of specimen to reach one-half its maximum temperature rise.

This relationship involves several simplifying assumptions:

(1) The heat flow is one-dimensional from the front face directly to the back face.

(2) The incident heat pulse is of negligible duration compared to the time required for significant heat propagation through the specimen.

(3) The incident heat pulse is uniformly absorbed on the front face of an opaque specimen.

(4) Heat losses off the faces are negligible.

(5) The temperature rise within the specimen is small enough to consider the thermal properties as constant.

In the present case, all assumptions except that of negligible heat losses are valid. Battelle has studied the effect of radiation losses on the measured thermal diffusivity and can apply appropriate adjustments on a routine basis. The maximum adjustments ranged from 2 percent at 1000°C to 8 percent at 2000°C.

A photograph of the Battelle-Columbus thermal-diffusivity apparatus is provided in Figure 2; a section drawing showing some internal details in Figure 3.

The specimen and heater were protected by an atmosphere of argon at about 3/8 atmosphere pressure. The specimens were held in a boron nitride holder inside a double-walled tantalum tube heater. Specimen temperatures were measured using a calibrated optical pyrometer. Thermal-radiation shielding surrounded the heater.

The radiation detector is positioned to view the back face of the specimen as shown in Figure 3. A lead sulfide cell is used as the radiation detector. The radiation detector is placed in one arm of a bridge circuit, the unbalance of which is shown on an oscilloscope and photographed by a camera. The time required for the back-face temperature to reach one-half of its maximum is obtained from measurements of the photograph. This time and the specimen thickness are used to calculate thermal diffusivity using Eq. 2.

The error of thermal-diffusivity values measured by the method described is estimated not to exceed ±5 percent below 1800°C and ±8 percent above 1800°C. These estimates are based on a weighted average of standard materials over a wide temperature range. Both the directly determined diffusivity and derived thermal conductivity have been compared to accepted literature values to arrive at these estimates.

3. Drop Calorimetry (1000° to 2000°C)

Specific heat data were determined from enthalpy data measured in a Bunsen ice calorimeter. A photograph of the

apparatus and a sketch of the calorimeter well are provided in Figures 4 and 5, respectively. The specimens were in the form of right circular rods 0.50 inch diameter by 2.00 inch long.

In the Bunsen ice calorimeter, heat given up by the specimen and capsule melts ice which is in equilibrium with water in the closed calorimeter well. As the icemelts to water there is a reduction in volume. Mercury entering the system from an external accounting system to make up the volume change is accurately weighed. Both Battelle-Columbus and the National Bureau of Standards have measured the ice-calorimeter heat-quantity versus mercury-weight constant to be 270.48 joules per gram. This is the constant of the measuring method and should not vary among Bunsen ice calorimeters. This value is a function of the volume change of ice melting to water and the heat of fusion involved in the change of state. All heat transfer is measured at the ice point as ice melts to water; temperatures are not measured in the calorimeter.

The specimens were encapsulated in graphite and were heated under a vacuum of approximately 5×10^{-5} mm Hg in a tantalum tube furnace above the calorimeter well. The specimen was then dropped into the well and allowed to cool. Separate runs with an empty capsule of the same material and surface emittance conditions as the specimen capsule determined the contribution of heat of the specimen by difference. The process was repeated through the temperature range of interest to establish an enthalpy-versus-temperature curve. Specific heat, entropy, and other parameters of interest were obtained with a digital computer using enthalpy and temperature data as input.

Specimen temperatures were measured by an optical pyrometer which can view the capsule. Calibration of the apparatus is checked frequently with National Bureau of Standards Al_2O_3 as the specimen standard. Measured enthalpies agree routinely with NBS values for this standard to within 1 percent.

The nominal uncertainty in the specific heat values computed in the above manner is approximately ± 2 percent.

C. Results and Discussion

1. Thermal Conductivity (100° to 1000°C)

Thermal conductivity data for twelve compositional and microstructural variations of ZrB_2 or HfB_2 with SiC and/or C additives are provided in Table 2.

The magnitude of the conductivity is higher than anticipated from earlier data (2) obtained using the method developed by M. Hoch (5) at the University of Cincinnati. However, other data for TiB_2 (6) show the same order of magnitude and the same temperature dependence as were obtained in this program.

The presence of SiC and C appear to increase the negative slope of the variation of thermal conductivity with temperature. Porosity should decrease thermal conductivity, however, the available data are not sufficient to confirm this trend. The high room temperature conductivity for 90 percent dense, I07F D0905K could be a consequence of the high ZrO_2 content of the I07F, ZrB_2 material.

2. Thermal Diffusivity (1000° to 2000°C)

The results of the thermal-diffusivity measurements for ten diboride structures are shown in Table 3 and Figures 6 through 15. Smooth curves were drawn through the data points. Agreement between heating and cooling data is good except for specimens IV09F D0811K and V07F D0851K where the cooling data are about 5 and 10 percent higher than the heating data. Most of the specimens containing carbon and silicon carbide changed from a dark grey color to a metallic luster following exposure to high temperatures. In most cases this would appear to be due to loss of carbon or silicon carbide from the surfaces of the specimen. The dimensional and weight change data both before and after the thermal diffusivity measurements in Table 4 show approximately 0.4 percent weight loss for these two specimens and considerably less variation for the remaining specimens.

A tungsten-rhenium thermocouple was used to measure the temperature of specimen V07F D0902K. However, a reaction between the thermocouple and specimen led to the use of an optical pyrometer for temperature measurements on the other nine specimens. The good agreement between heating and cooling data for this specimen makes it difficult to determine if the reaction affected the measured thermal diffusivity.

The data for all the structures show the diffusivity decreasing with increasing temperature.

3. Enthalpy, Specific Heat and Entropy Data (1000° to 2000°C)

The drop calorimetric measurements produce enthalpy values relative to 0°C, $H_T - H_{0°C}$ and analogous entropy values, $S_T - S_{0°C}$; absolute specific heat data, C_T are, however, obtained.

The enthalpy, specific heat and entropy data for Materials I, V, VIII(18,10) and XII(20) are provided in Tables 5 through 8 for 100° increments between 1000° and 2000°C. The specific heat data are also provided in graphical form in Figures 16 through 19.

4. Calculated Thermal Conductivity (1000° to 2000°C)

The thermal diffusivity, specific heat and density data for Materials I, V, VIII(18,10) and XII(20) in the temperature range 1000° to 2000°C were employed in Eq. 3 to calculate thermal conductivity.

$$K = \alpha C_T d \qquad (3)$$

The density at temperature was obtained from the room temperature value and the appropriate expansion data in Figures 33 through 41 by assuming isotropic expansion. The calculated conductivities obtained in this way are considered accurate to ± 8 percent; the results are provided in Table 9 and presented graphically along with the thermal conductivity data measured over the range 100° to 1000°C in Figures 20 through 23. The agreement at 1000°C is considered satisfacotry.

Specific heat data calculated for the compositions of Materials I, V, VIII(18,10) and XII(20) using literature data for SiC (7), graphite (7), ZrB_2 (1) and HfB_2 (1) are provided in Table 10 and compared therein with the experimental heat capacity data. The agreement is satisfactory. Hence, diffusivity data for dense Materials III(5), IV, VIII, XIV(18,10) and XV(20) and 88.5 percent dense Material V were employed with density and expansion results to provide reliable calculated thermal conductivity data to 2000°C which are provided in graphical form with the available thermal conductivity values measured over the range 100° to 1000°C in Figures 24 through 29.

IV. PHYSICAL PROPERTIES

A. Introduction

Linear expansion is the chief physical property considered for this program. Data were obtained in argon from room temperature to 2000°C; measurements were performed at ManLabs and at Battelle Memorial Institute. Density data were obtained for hot pressed billets by immersion methods at Avco Corp. as part of the fabrication effort (8).

The expansion data are required as input for thermal stress test data interpretation and for thermal stress calculations and analyses (10). Expansion data are also employed with room temperature density to calculate density at temperature which is required for thermal conductivity calculations based on measured thermal diffusivity data as illustrated in Section III-C.

Earlier expansion data and the results of X-ray and linear thermal expansion measurements for several diborides including ZrB_2 and HfB_2 are provided in a previous report (2); more recent results for ZrB_2 and HfB_2 and for mixtures of these diborides with several rare earth and alkaline earth hexaborides were obtained in a refractory coating development program for graphite substrates (11).

B. Measurement Techniques

1. Direct View-Dilatometer

Linear thermal expansion measurements at Battelle were performed in a direct view dilatometer as illustrated in Figures 30 and 31. In this method, two telemicroscopes fitted with optical extenders are used to view suitable fiducial marks on the specimen. The distance between fiducial marks is approximately 2.75 inches. The telemicroscopes are fitted with filar eyepieces in which each division of the filar equals about 0.00002 inch. Provision is made to view the fiducial marks at temperatures below which they become self-luminous by providing illuminated backgrounds.

Heating and cooling rates of the specimens (0.25 inch by 0.25 inch by 2.0 to 3.0 inch long) are controlled by a tantalum resistance furnace, which heats the specimens at a rate of approximately 5° to 8°C per minute. The specimens were held for approximately one half hour at temperature prior to each length measurement. All measurements were made in argon at 0.5 atmosphere pressure.

Errors in this apparatus are determined by the measurement of standard materials of known linear thermal expansion, supplied by the National Bureau of Standards. Errors associated with the reported data are ±1 percent of the total expansion.

2. Differential Dilatometer

Linear expansion measurements at ManLabs were performed in a differential dilatometer as illustrated in the schematic cross sectional view in Figure 32. This apparatus was modeled after the high temperature graphite dilatometer described by Criscione, et al. (11). The ManLabs dilatometer shown schematically in Figure 32 was fabricated from AUC graphite supplied by the National Carbon Company; the AGW graphite originally used by Criscione et al. was not available from National Carbon. The dilatometer assembly was heated in flowing argon by radiation from a resistance heated 0.75 inch i.d. by 15 inch long graphite tube furnace. Thermocouples located on the surface of the dilatometer as shown in Figure 32 provided temperature measurements up to 1200°C; a two color pyrometer was used for the higher temperature measurements. The latter were performed directly on the specimen by sighting through the hole in the bottom of the dilatometer. The apparatus was calibrated against tungsten (12), quartz (12) and aluminum oxide (13).

C. Results

1. Direct-View Dilatometer Data

The measured linear expansion versus temperature data for specimens of Materials I05 R44L, V07F R26L, VIII(18,10)07F D0920K and XII(20)07F D0812K are provided in Figures 33 through 36, respectively. Interpolated values obtained from these curves are listed in Table 11.

The slight disagreement between heat and cooling data for Material V07F R26L apparently represents a real change in the material resulting from the thermal cycle. Pre- and post-measurement length dimension measurements confirmed this change. This behavior was not observed for Material V similarly heated in the expansion measurements obtained at ManLabs which were described in the previous section.

2. Differential Dilatometer Data

The measured linear expansion versus temperature data for specimens of Materials I07F D0700K, V07F D706K, V07F D0845K, VIII07F D0761K, XII07F D0809K and IV09F D0804K are provided in Figures 37 through 42, respectively.

3. Summary of Expansion Data

The coefficients of thermal expansion calculated from both direct-view and differential dilatometric data for selected temperature increments for all the diboride materials are provided in Table 12. Some of the earlier reported data are also listed for comparison. The overall agreement is satisfactory.

4. Density Data

Room temperature density data for selected compositions of ZrB_2 or HfB_2 with and without SiC and C additives are presented in Table 13. These data are representative of hot pressed billets with less than one percent porosity for the indicated compositions.

V. ELECTRICAL PROPERTIES

A. Introduction

Electrical resistivity measurements were performed at Dynatech Corporation over the range from room temperature to 1000°C to provide data to complement the thermal conductivity obtained in the same temperature range. Previous resistivity data dense specimens of ZrB_2 and HfB_2 showed room temperature values between 4 and 10μΩ cm and positive temperature coefficients (2, 3). Electrical resistivity data were not available for the SiC and C bearing compositions; the excellent oxidation resistance of these materials (14) suggests potential application as a high temperature conductor suitable for oxidizing and otherwise corrosive atmospheres. The availability of high temperature electrically conductive materials was reviewed and summarized in a separate study (15).

B. Measurement Techniques

The specimens for the electrical resistivity measurements were in the form of 0.250 inch square rods some 2.00 inch long with two small holes (0.031 inch diameter) drilled 1.250 inches apart in the central section.

The current electrodes were fitted to each end of the bar and a fine guage chromel/alumel thermocouple fitted tightly into each hole. The sample was then placed on knife edges a given distance apart. A steady current was passed through the rod and the potential difference across the knife edges and each pair of "like" thermocouple arms were measured in addition to that across a standard calibrated resistance in series with the test sample. The current was reversed and the potential differences measured again in order to eliminate thermal voltages. The sample was then taken off the knife edges and placed at the central section of a uniform wire wound resistance furnace and heated in argon at a very slow uniform rate to any given fixed temperature and the measurements repeated on heating to 1000°C and on cooling back to 20°C.

The electrical resistivity was derived in terms of the ratio of the measured potential differences, the standard resistance and the dimensions of the sample.

C. Results

The electrical resistivity data for twelve compositional variations of ZrB_2 or HfB_2 with SiC and/or C from 20° to 1000°C in 100°C increments are provided in Table 14. All material compositions show positive temperature coefficients of resistance. The effects of porosity are marked by the presence of ZrO_2 in the 90 percent dense I07F R382 relative to fully dense I05 R44L which has a low oxide content. The effect of porosity is evident for 88.5 percent dense V07F D0851K with $\rho[20°C]$ = 15.5μΩcm compared to 99 percent dense V07F D0902K with $\rho[20°C]$ = 10.2μΩcm. Variation of relative density and composition can produce a limited range resistivity versus temperature profiles.

VI. OPTICAL PROPERTIES

A. Introduction

Total normal emittance measurements were performed at Avco, Applied Technology Division for selected unoxidized diboride compositions. The data were generally obtained between 1600° and 2200°C. Considerable emittance data for diborides and other high temperature materials were generated in a separate program (16); the data obtained in the latter program refers to oxidized surfaces. Emittance data are employed in high temperature optical pyrometry and in thermal stress calculations (10).

B. Measurement Techniques

The method of measurement follows directly from the definition of emittance for an opaque solid which is the ratio of the radiation from an area of its surface to that of the same area of a blackbody radiator at the same absolute temperature. The radiation emitted by the specimen surface is measured directly using a Barnes bolometer system calibrated against both radiation and absolute temperature using a blackbody source. The blackbody radiation is measured indirectly. The temperature of the sample is measured with an optical pyrometer sighted into a blackbody cavity in the center of the specimen. The blackbody radiation is then calculated from the Stefan-Boltzmann law. The ratio of the measured total radiation, to the calculated blackbody radiation is the total normal emittance of the surface.

The sample is heated by RF induction using a Lepel generator. The induction source and sample holding mechanism consists of several concentric units as illustrated in Figure 43. The induction coil of the RF generator is wrapped around a pyrex chamber which allows measurements in controlled atmospheres. A fused silica window is located at the end of the chamber to permit radiation measurements. A water cooled RF concentrator patterned after Blau (17) is positioned within. The cylindrical concentrator is open at one end; a plate with a hole in the center covers the other end. A slot-hole geometry serves to increase the current density induced in the sample's front surface. The specimen is mounted in a zirconia rod at the center of the hole in the concentrator.

The specimen is a small disc 5/16 inch diameter and 1/8 inch thick with a stem attached to permit mounting in a hollow zirconia rod as shown in Figure 44. The specimen is mounted in the concentrator so that the disc is in the main RF field and the stem is heated by conduction only. A blackbody cavity 0.020 inch in diameter and 0.080 inch deep is drilled into the center of the front surface of the disc. Because of its depth to diameter ratio and wall roughness, such a cavity has been found to be an effective blackbody (18). The occurrence of a difference in temperature between the specimen surface and the walls of the cavity was considered as a possible source of error by DeVose (19) and Marple (20). Both studies eliminated this as a major source of error.

Radiation measurements are made with a Barnes detector-preamplifier system. The detector is a Barnes low impedence high sensitivity stem bolometer. The pre-amplifier is a Barnes DP-7 having a voltage gain of 15,000. It has been designed to operate with Johnson noise-limited transducers and thus the maximum use is obtained with a Pyro optical pyrometer which has been calibrated for the expected temperature range. The temperature of such small targets as the blackbody hole in the specimens can be measured with ease with the telescopic optical system.

C. Results

Total normal emittance data for Materials I, V, VIII, XII(20) and III in the range 1600° to 2300°C are provided in Figures 45 through 49, respectively.

Considerable vaporization was observed upon heating the Material I specimen. During the first two heating cycles, to temperatures above 2000°C, 23 mg was lost during each run; the original specimen weight was 1.810 grams. In the final two runs, the temperature was maintained below 2000°C and no weight loss nor other signs of vaporization was detected. The vaporization caused pitting of the surface which may have affected the emittance values presented in Figure 45. Results of the initial heating cycle were disregarded due to difficulties experienced in focusing on the blackbody hole. At the sixth data point (2070°C) the hole became clear and no further difficulties were experienced. The problem may have been caused by foreign matter (machine oil, etc.) trapped in the small hole; a preheat cycle at low temperatures was incorporated in the procedure for the remaining measurements.

The Material V specimen was heated in vacuum ($\sim 5 \times 10^{-6}$ torr) three times, once to 1865°C and twice to above 2100°C, without signs of vaporization. Data were obtained during the three temperature increases and during one cooling cycle. Specimens of Materials VIII, XII(20) and III were tested in the same manner; no experimental difficulties were encountered. All data show the same general trend of a somewhat gradual decrease in emittance with increasing temperature over the range studied. The compositions containing SiC and/or carbon displayed significantly higher emittance values than Material I (ZrB_2 with no additive) at all temperatures. This effect is most striking at 1600°C.

Results of emittance measurements in oxidizing atmospheres (16) provide values of 0.6 independent of temperature in the range studied in the present program.

VII. CONCLUSIONS

1. Hot pressed diboride compositions containing ZrB_2 or HfB_2 as the principal component with up to 20 to 34 volume percent total addition of SiC and/or C possess high thermal conductivities at room temperature of the order of 0.20 cal. cm/cm^{2}sec°C. The compositions also display high values at 2000°C of the order of 0.10 cal. cm/cm^{2}sec°C.

2. Measured thermal diffusivity data in the range 1000° to 2000°C combined with measured or calculated specific heat values and room temperature density data corrected for expansion can be employed to calculate thermal conductivity of the diboride compositions.

3. The diboride compositions displayed metallic like electrical resistivity at room temperature and positive temperature coefficients. Variations of composition and porosity can be used to produce materials with varying room temperature resistivities and temperature coefficients.

4. The total normal emittance of the unoxidized diboride compositions are higher than observed for the oxidized materials which show values of 0.60.

REFERENCES

1. Kaufman, L. and Clougherty, E.V., "Investigation of Boride Compounds for Very High Temperature Applications", RTD-TDR-63-4096, Part I, December 1963 .

2. Kaufman, L. and Clougherty, E.V., "Investigation of Boride Compounds for Very High Temperature Applications", RTD-TDR-63-4096, Part II, February 1965 .

3. Kaufman, L. and Clougherty, E.V., "Investigation of Boride Compounds for Very High Temperature Applications", RTD-TDR-63-4096, Part III, March 1966 .

4. Clougherty, E.V., Kalish, D. and Peters, E.T., "Research and Development of Refractory Oxidation Resistant Diborides", AFML-TR-68-190 May 1968..

5. Hoch, M. et al., "New Method for the Determination of Thermal Conductivity between 1000° and 3000°C" in Progress in International Research on Thermodynamic and Transport Properties, Academic Press, Inc., New York, N.Y. (1962).

6. Powell, R.W. and Tye, R.P., "The Thermal Conductivities of Some Electrically Conducting Compounds", Special Ceramics, 1964 Edited by P. Popper, Academic Press, London, pp 243-257 (1965).

7. JANAF Thermochemical Data Tables

8. Clougherty, E.V., Hill, R.H., Rhodes, W.H. and Peters, E.T., "Research and Development of Refractory Oxidation Resistant Diborides, Part II, Volume II: Processing and Characterization", AFML-TR-68-190, Part II, Volume II, November 1969 .

9. Clougherty, E.V., Niesz, D.E., Mistretta, A.L., "Research and Development of Refractory Oxidation Resistant Diborides Part II Volume VI: Thermal Stress Resistance", AFML-TR-68-190 Part II Volume VI, November 1969 .

10. Clougherty, E.V., Mistretta, A.L. and Anthony, F.M., "Research and Development of Refractory Oxidation Resistant Diborides, Part II Volume VII: Application Evaluations and Design Considerations", AFML-TR-68-190 Part II Volume VII, November 1969 . (Secret report)

11. Criscione, J.M., et al., "High Temperature Protective Coatings for Graphite", ML-TDR-64-173, Part IV, November 1966 .

12. Goldsmith, A., Waterman, T.E. and Hirschborn, H.F., Handbook of Thermophysical Properties of Solid Materials, MacMillan Co. (1961).

13. Lynch, J.F., Ruderes, C.G., Duckworth, W.H., Engineering Properties of Ceramics, AFML-TR-66-52, June 1962 .

14. Clougherty, E.V. and Peters, E.T., "Research and Development of Refractory Oxidation Resistant Diborides, Part II, Volume III, Thermochemical Stability Characteristics", AFML-TR-68-190 Part II, Volume III, November 1969.

15. Fuschillo, N. and Lindberg, R.A., "Electrical Conductors at Elevated Temperatures", ASD-TDR-62-481, January 1963 .

16. Perkins, R., Kaufman, L. and Nesor, H., "Stability Characterization of Refractory Materials under High Velocity Atmospheric Flight Conditions", AFML-TR-69-84 Part III Volume II: Experimental Results of High Velocity Cold Gas/Hot Wall Tests, September 1969 .

Kaufman, L. and Nesor, H., "Stability Characterization of Refractory Materials under High Velocity Atmospheric Flight Conditions", AFML-TR-69-84 Part III Volume III: Experimental Results of High Velocity Hot Gas/Cold Wall Tests, September 1969 .

17. Blau, H.H., Jr., et al., "High Temperature Thermal Radiation Properties of Solid Materials", AFCRC-TN-60-165, March 1960 .

18. Buckley, H., Phil Mag. (1927), 4, 753, Ibid., (1928), 6, 447, Ibid., (1934), 17, 576.

19. DeVos, J., Physica (1954), 20, 690.

20. Marple, D.T.F., J. Opt. Soc., (1956), A, 46, 490.

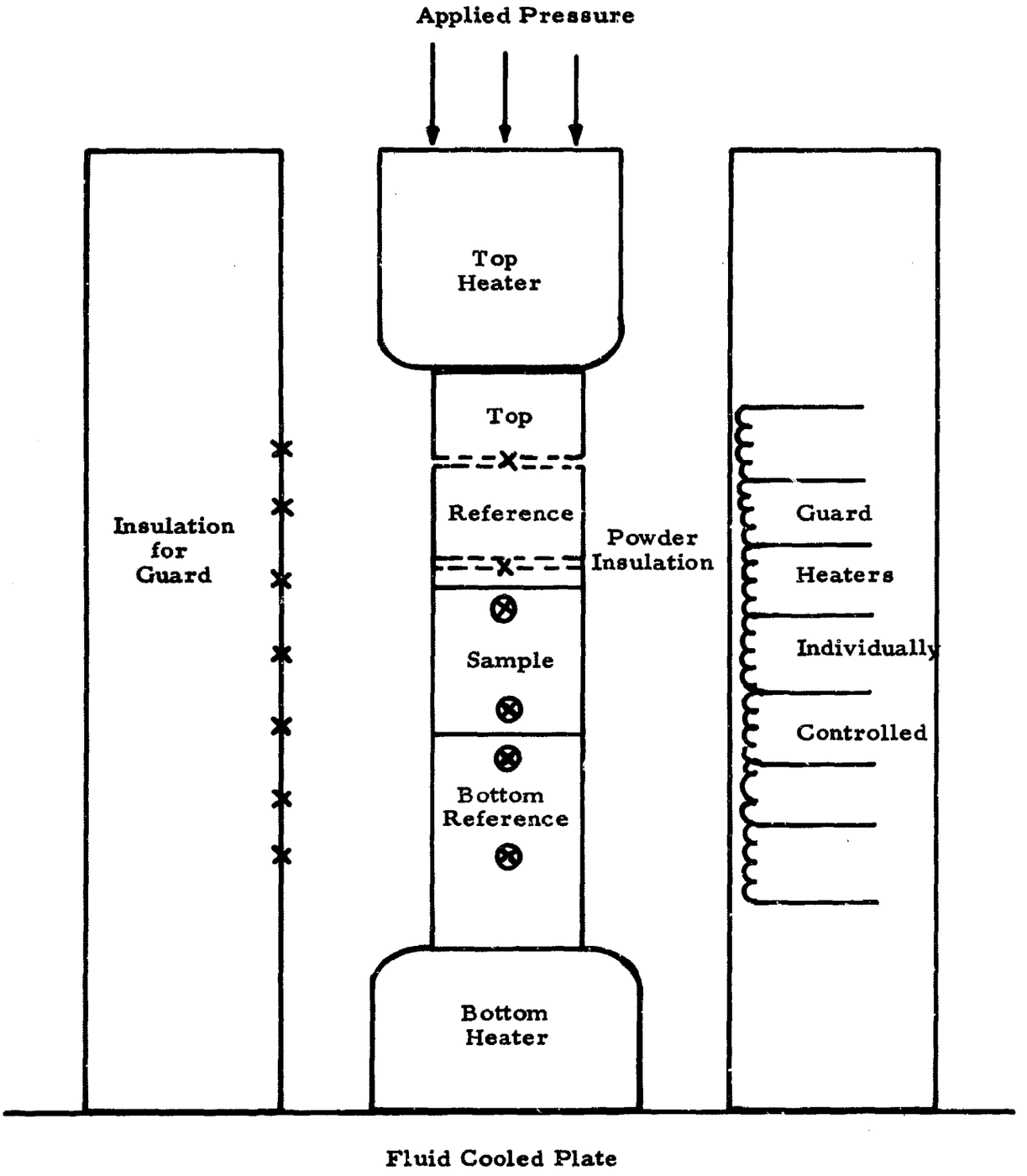

Figure 1. Schematic Assembly of Comparative Cut-Bar Method Apparatus (Dynatech Corp.)

Figure 2. Thermal Diffusivity Apparatus (Battelle Memorial Institute).

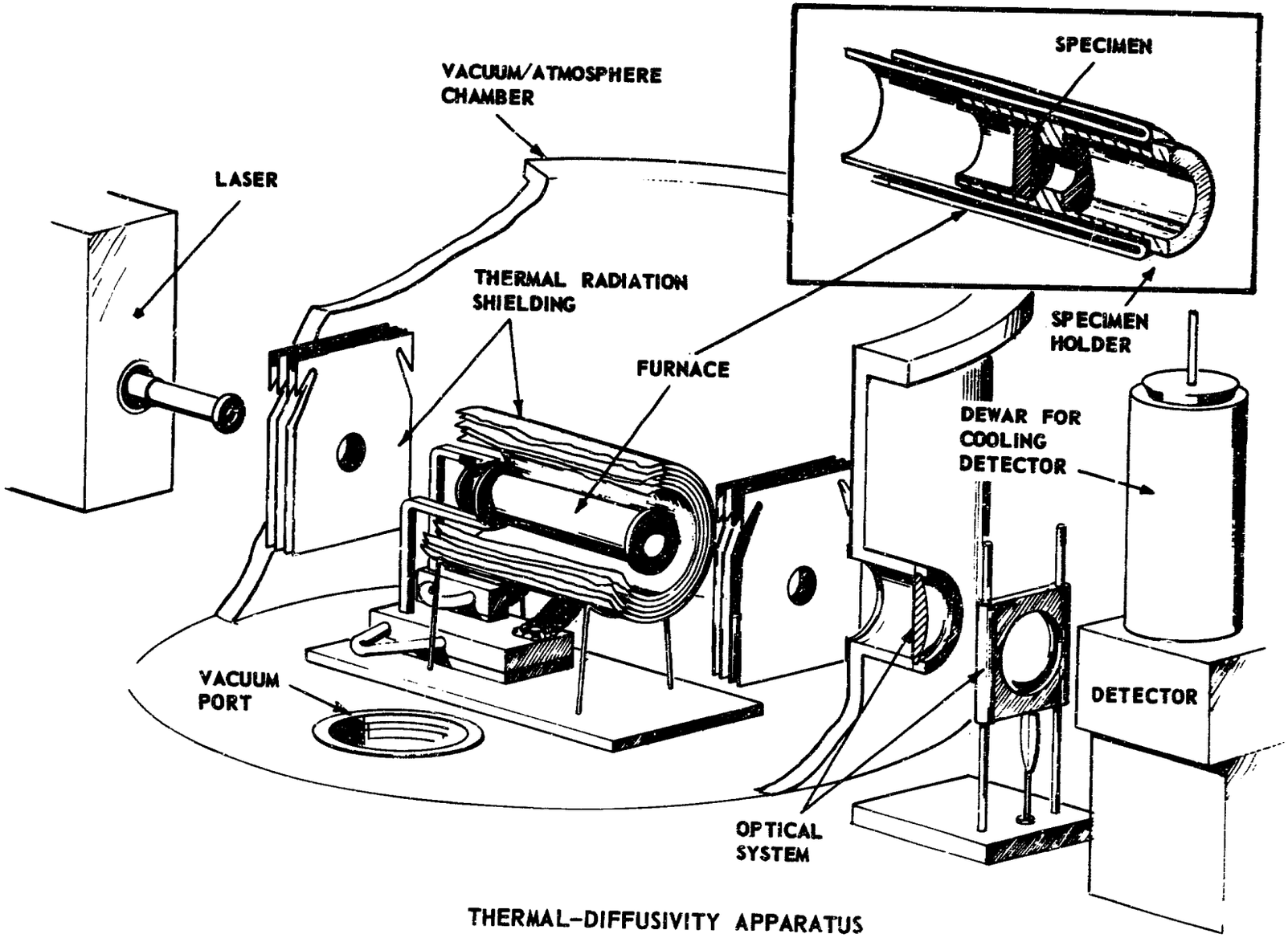

Figure 3. Section Drawing of Thermal Diffusivity Apparatus (Battelle Memorial Institute).

Figure 4. Drop Calorimeter Assembly (Battelle Memorial Institute).

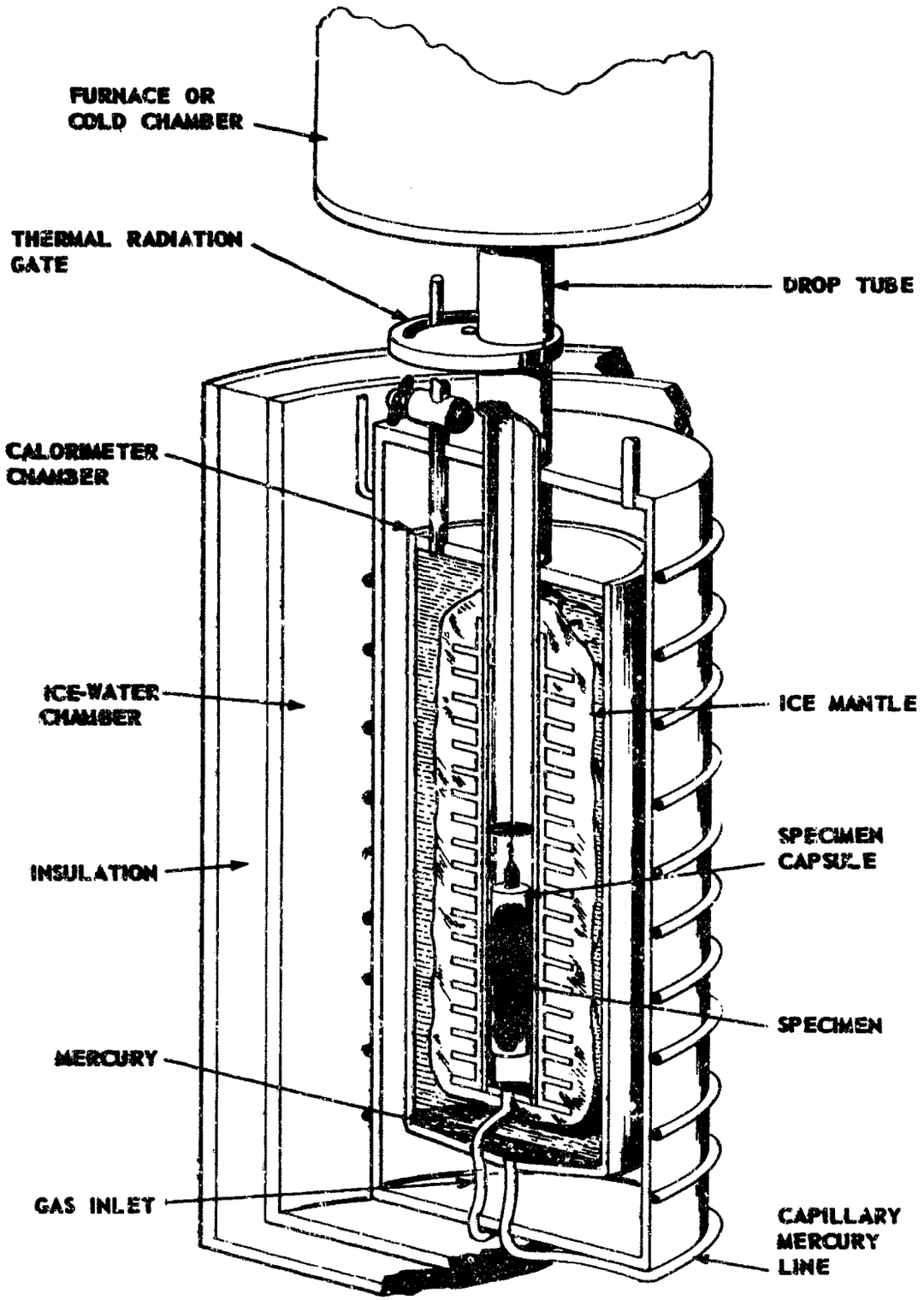

Figure 5. Section Drawing of Drop Calorimeter (Battelle Memorial Institute).

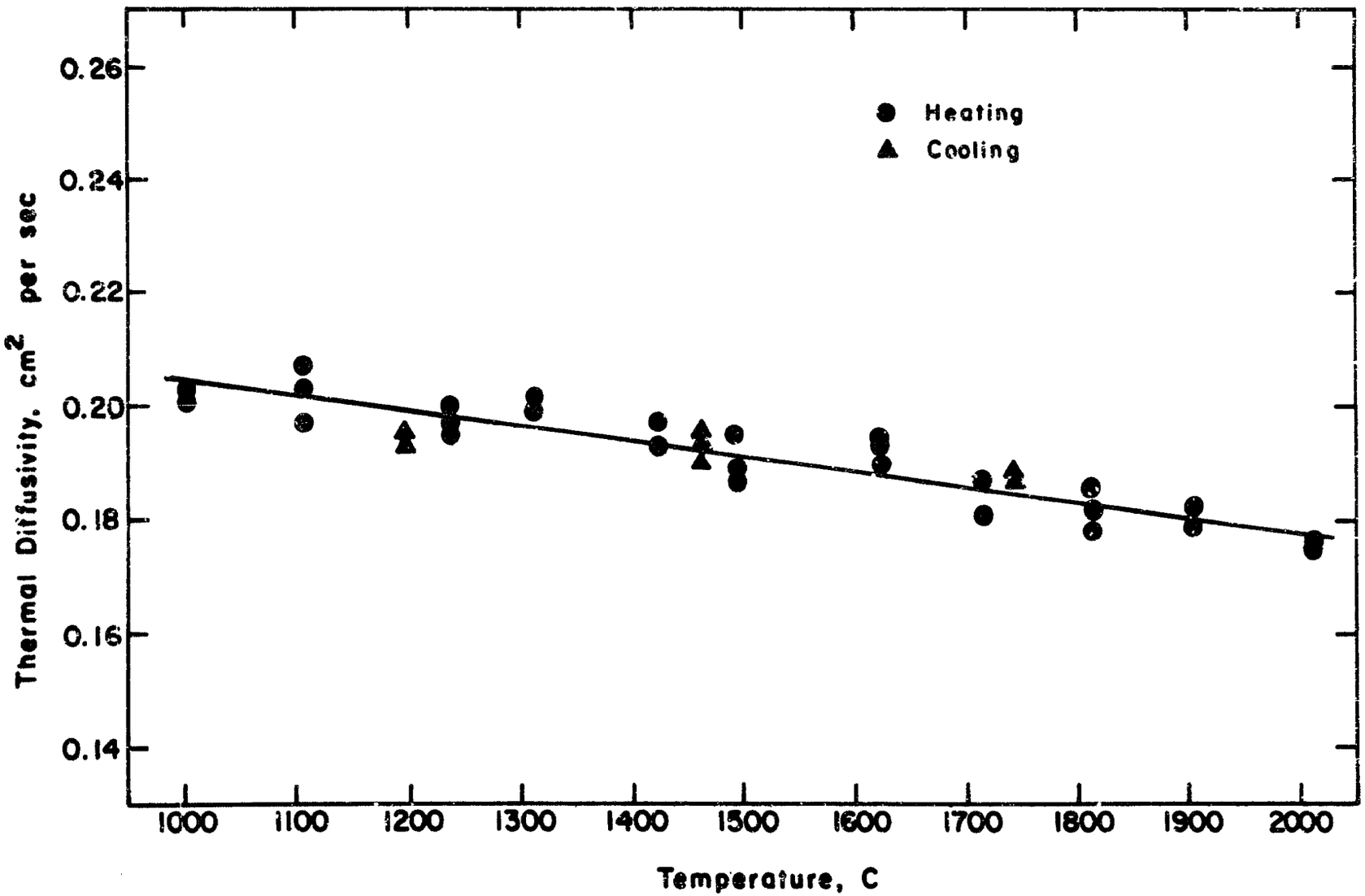

Figure 6. Thermal Diffusivity of Material I05 R44L.

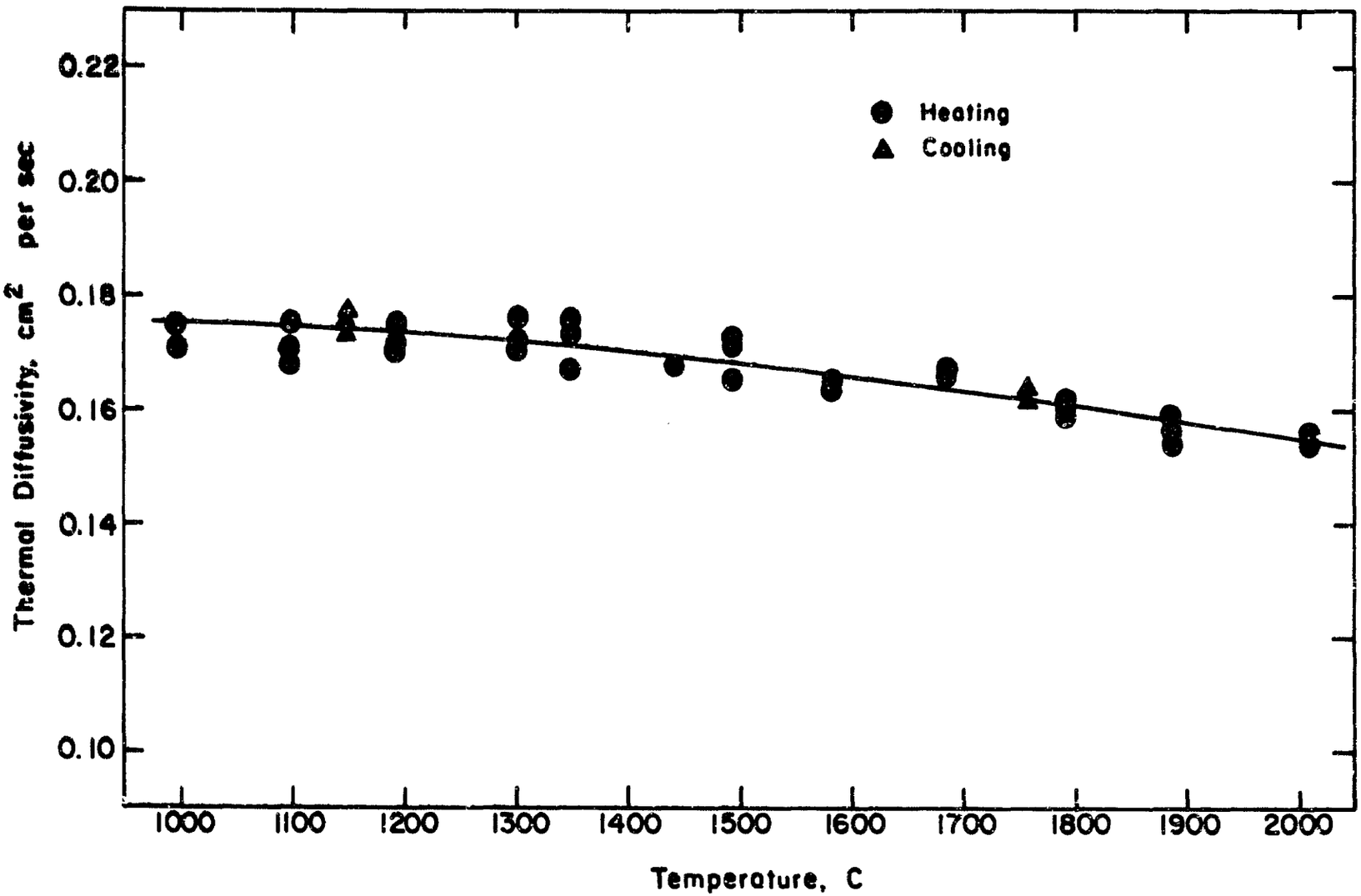

Figure 7. Thermal Diffusivity of Material III(5)09F D1061.

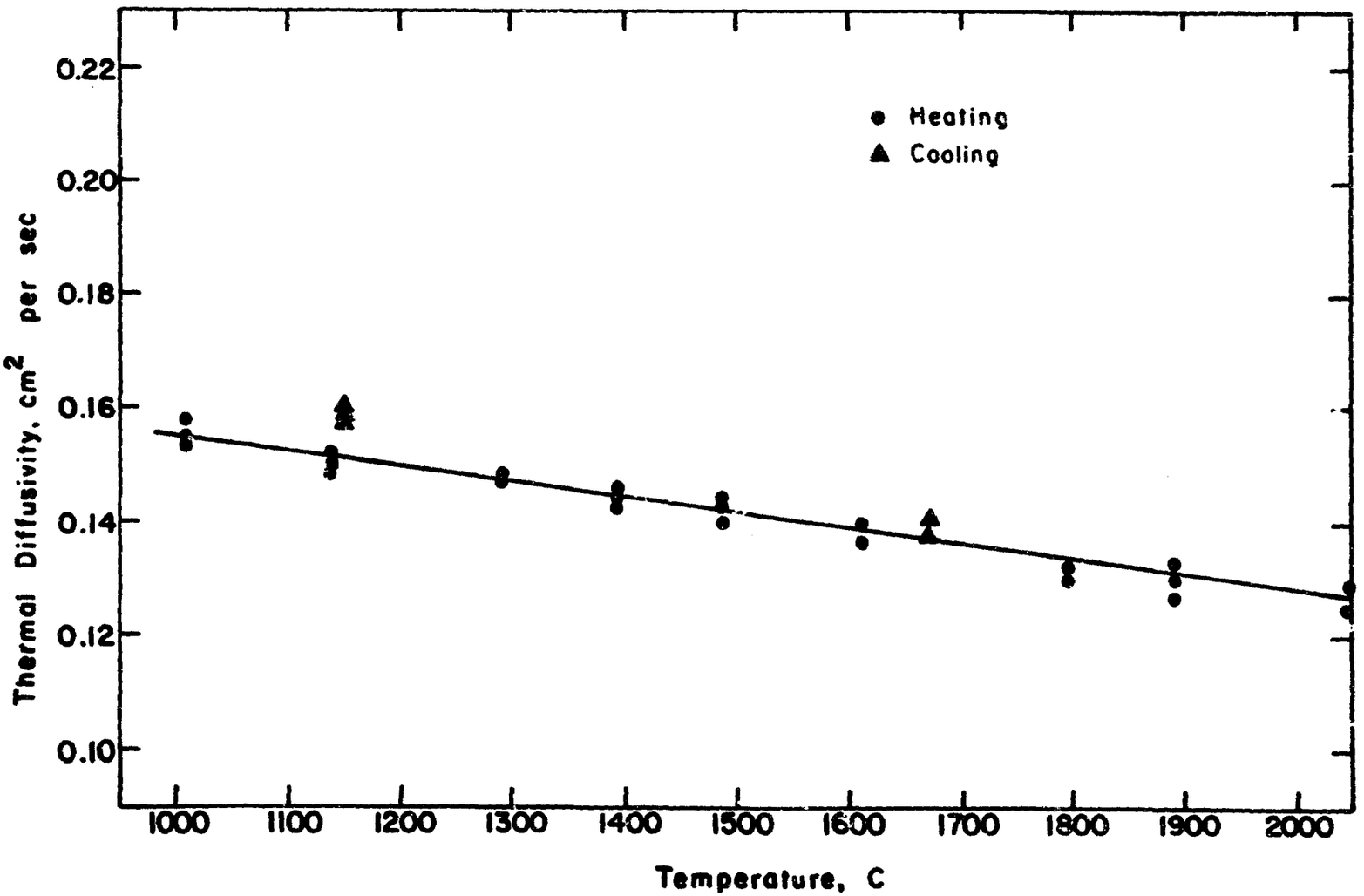

Figure 8. Thermal Diffusivity of Material IV09F D0811K.

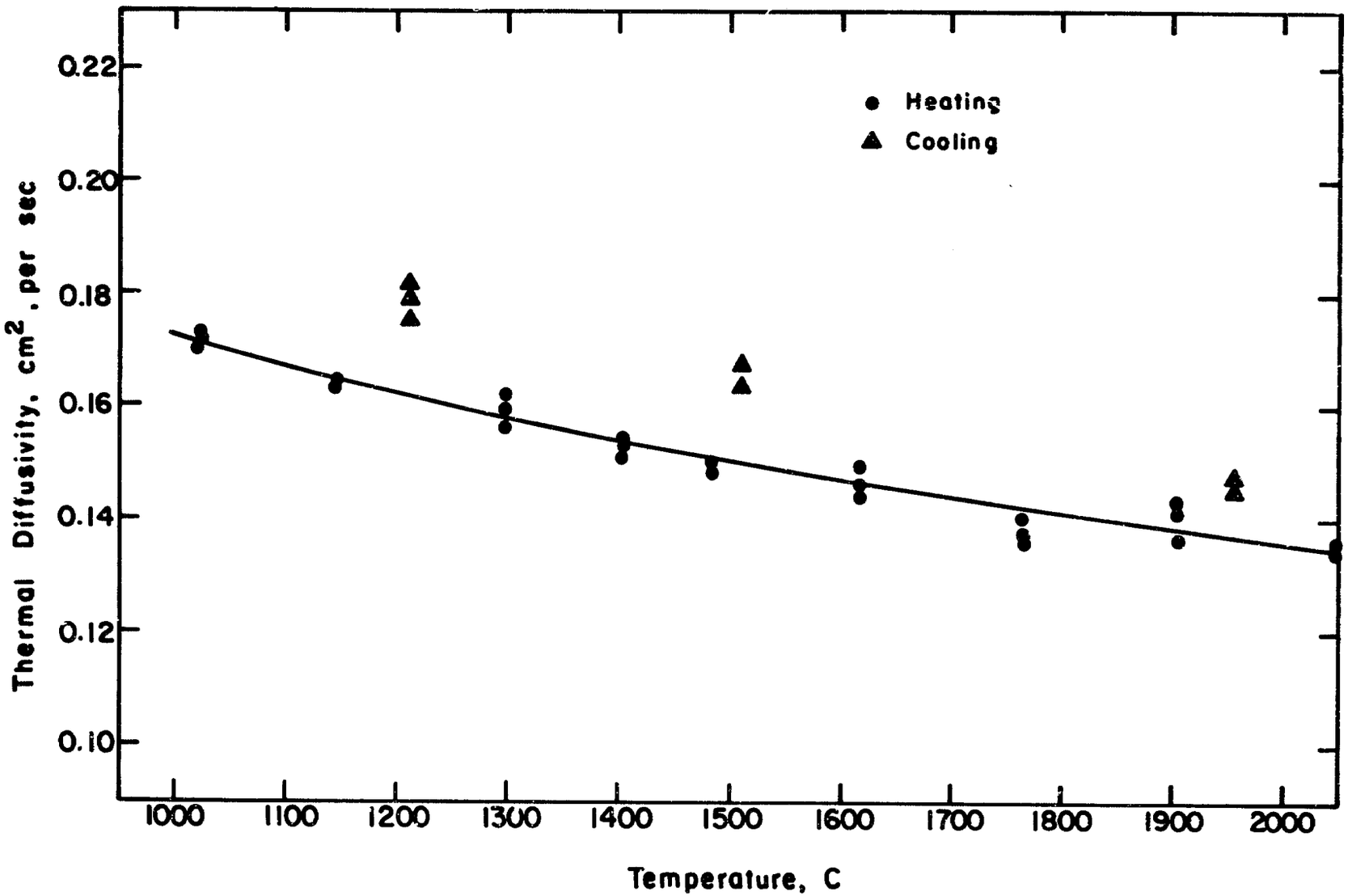

Figure 9. Thermal Diffusivity of Material V07F D0851K.

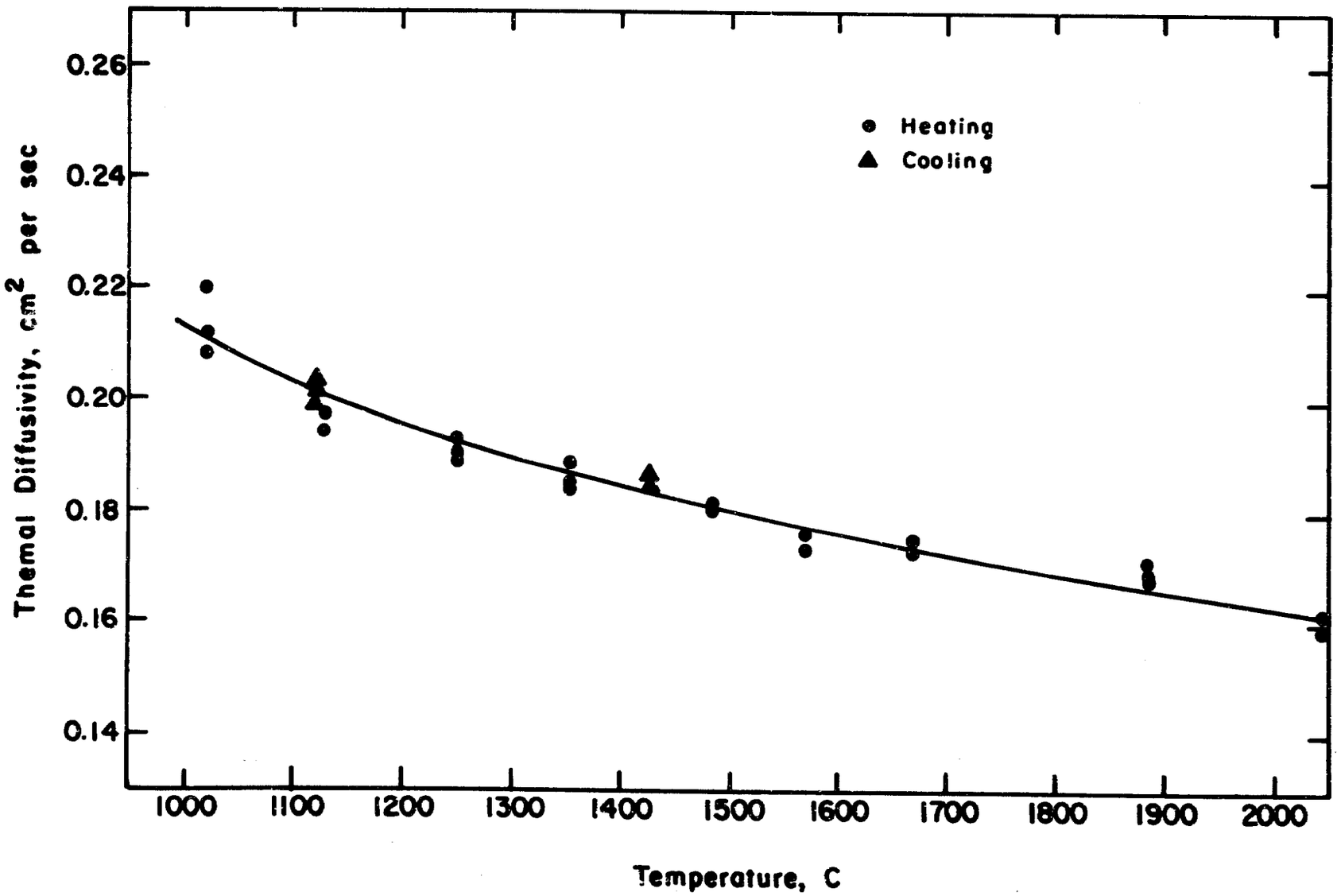

Figure 10. Thermal Diffusivity of Material V07F D0902K.

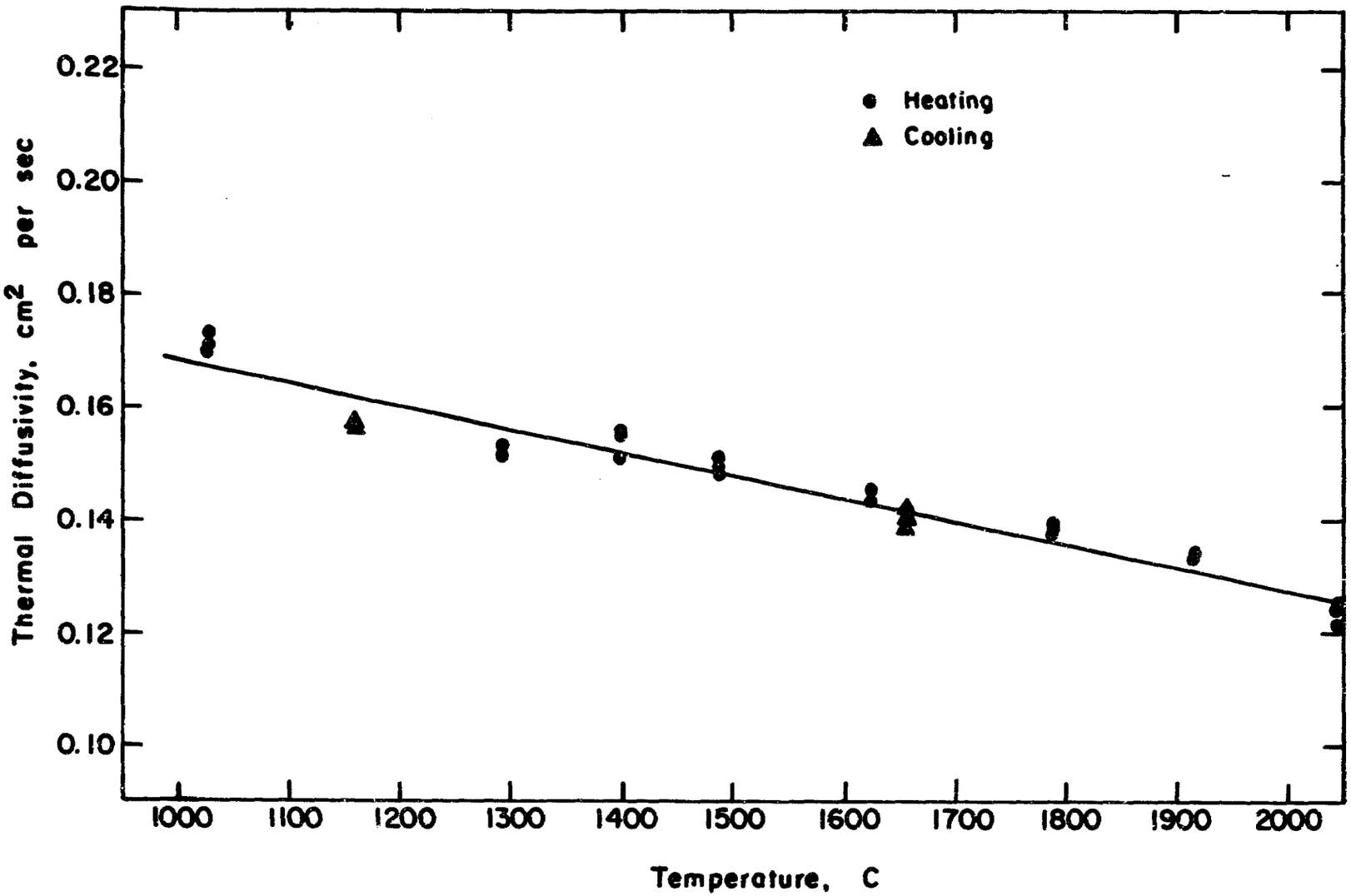

Figure 11. Thermal Diffusivity of Material VIII07F D0975K.

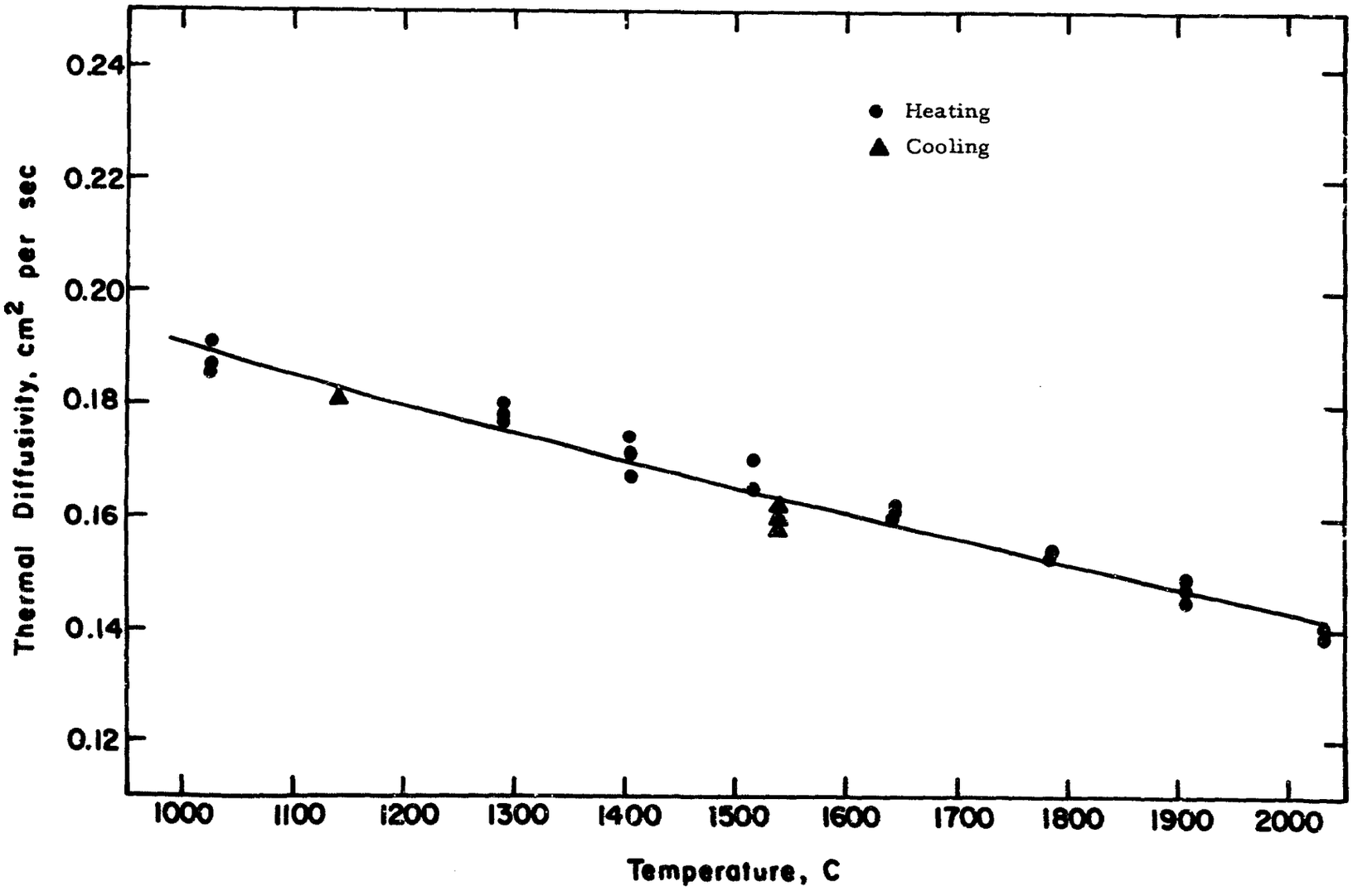

Figure 12. Thermal Diffusivity of Material VIII(18,10)07F D0920K.

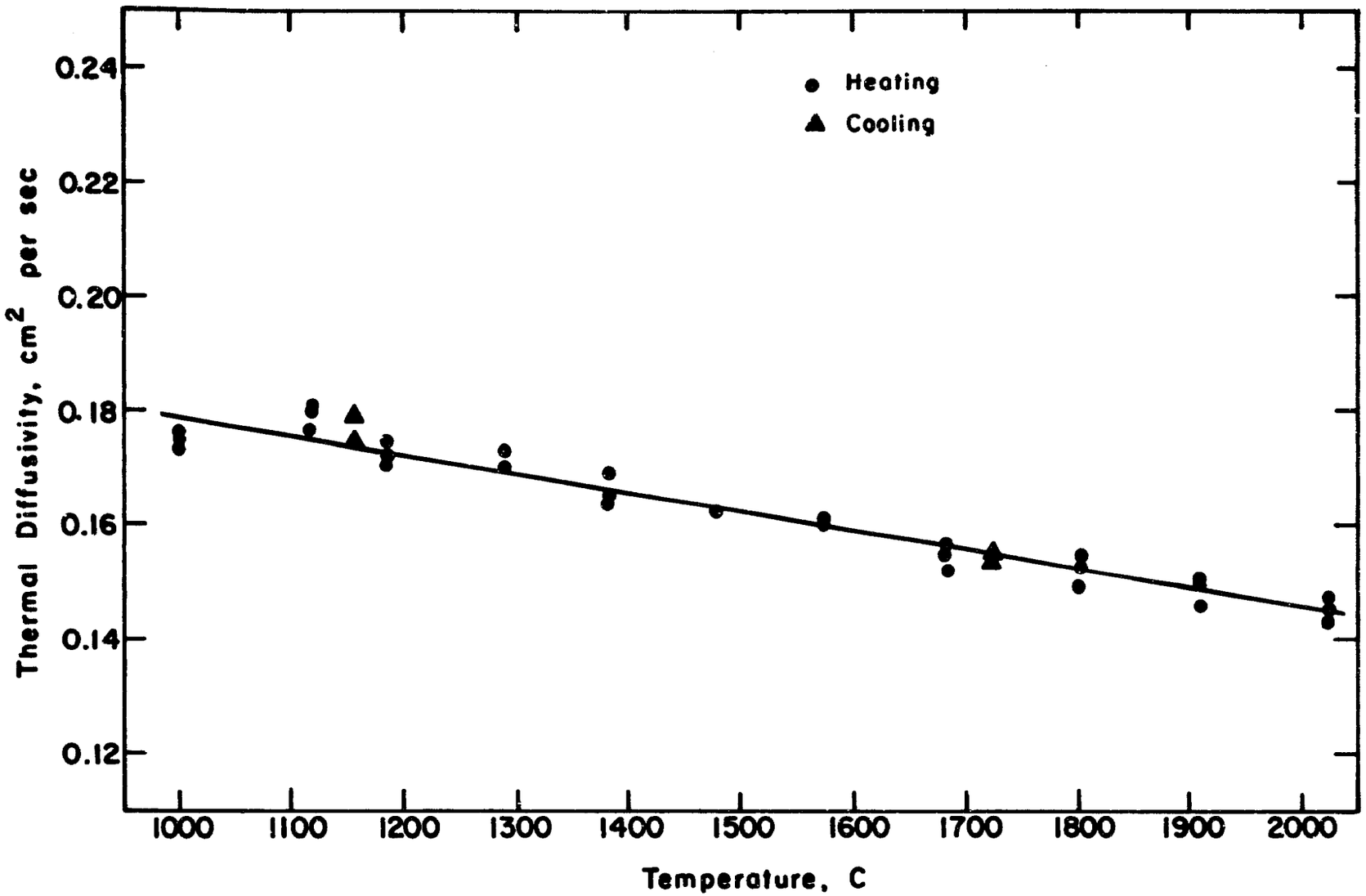

Figure 13. Thermal Diffusivity of Material XII(20)07F D0812K.

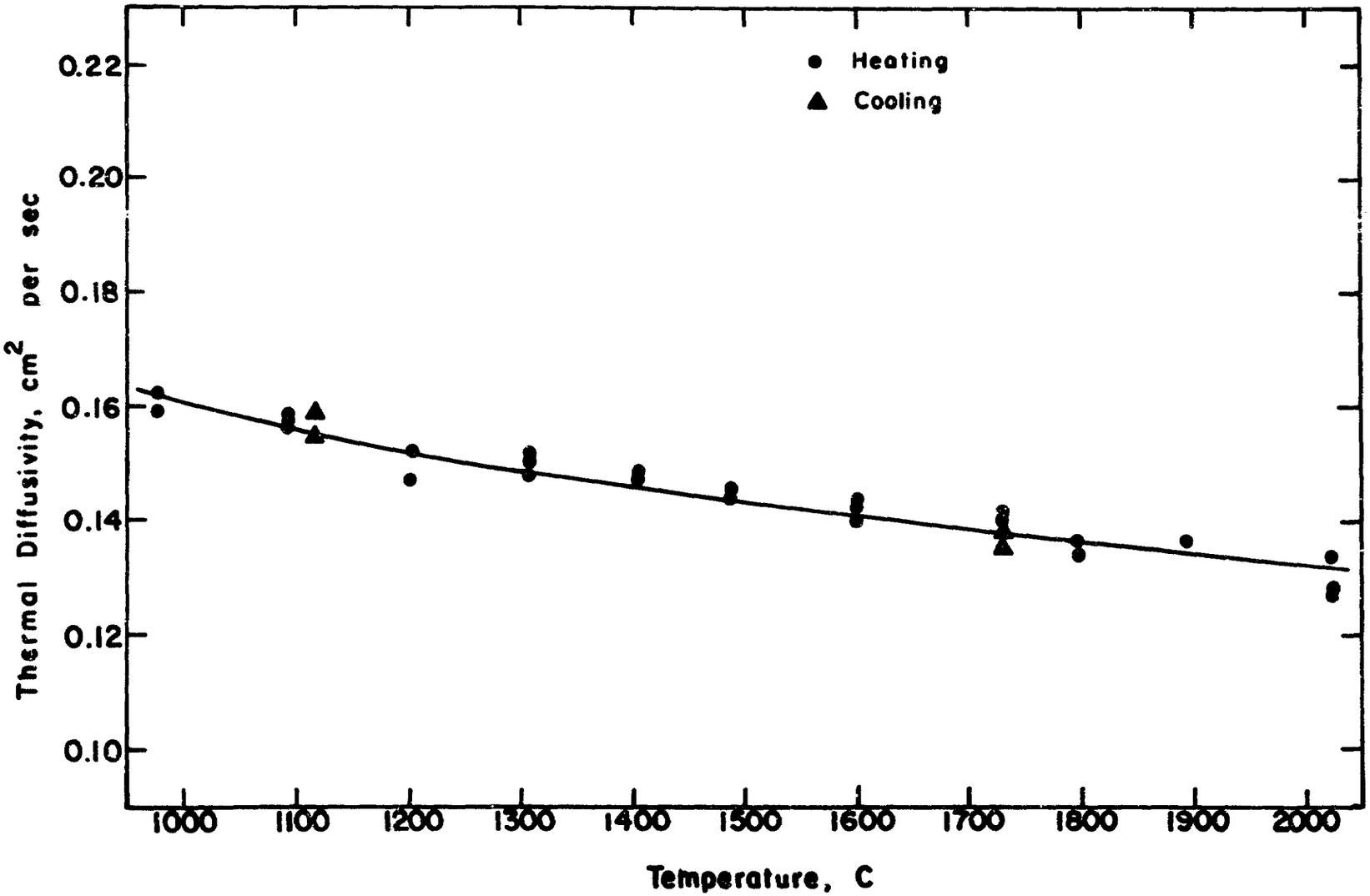

Figure 14. Thermal Diffusivity of Material XIV(18,10)09F D1037K.

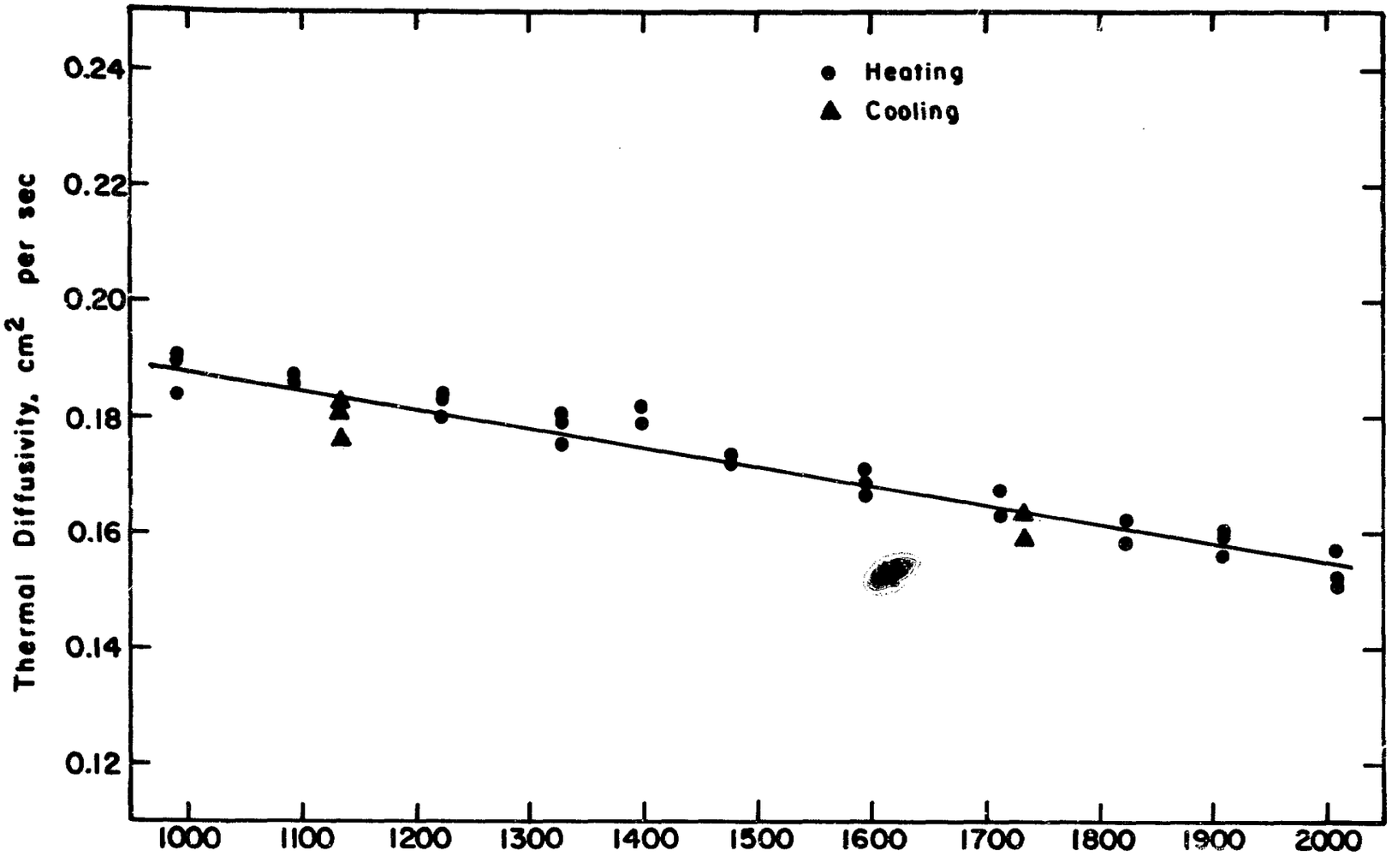

Figure 15. Thermal Diffusivity of Material XV(20) 10D105-4K.

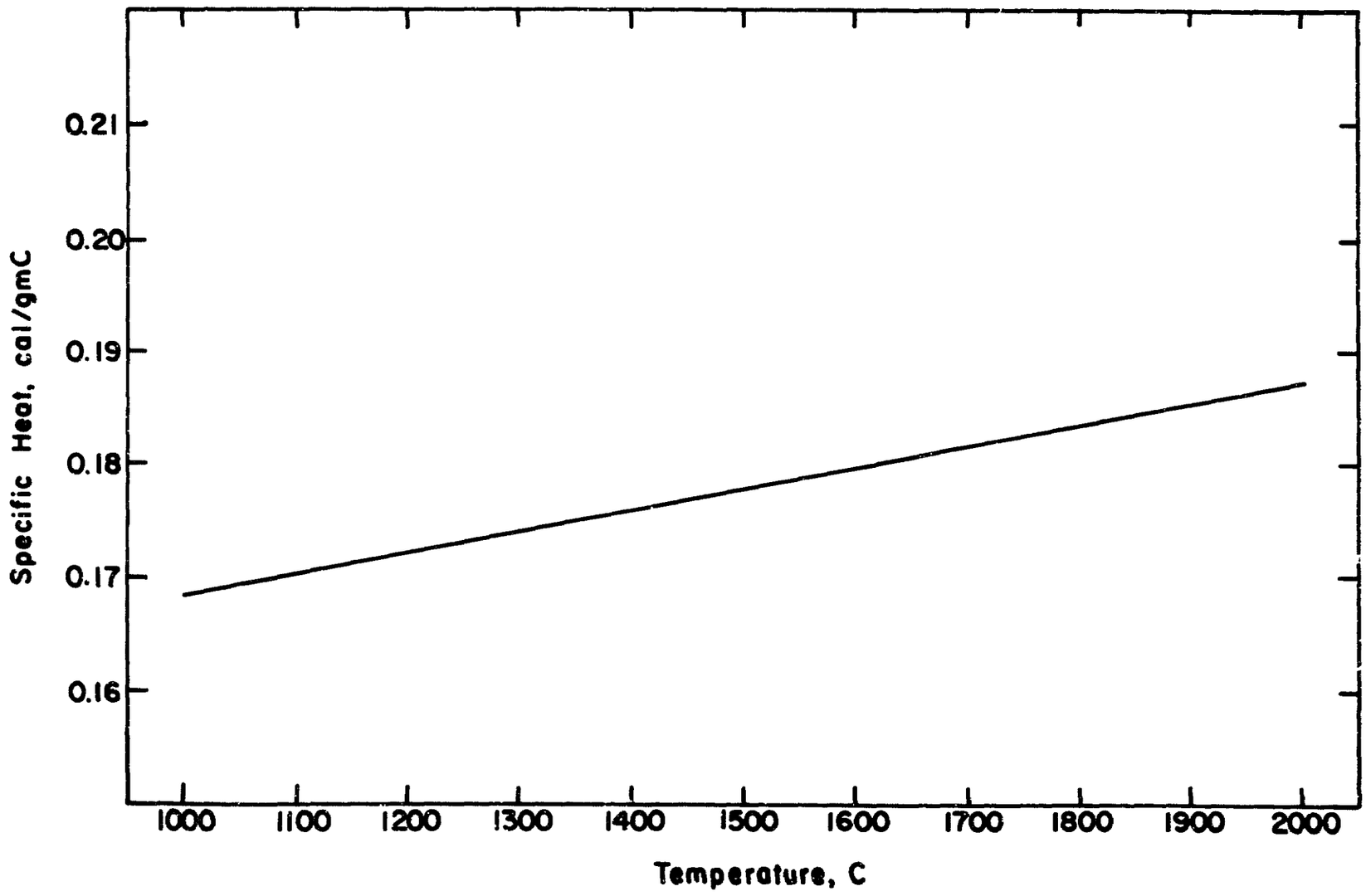

Figure 16. Specific Heat of Material 105 R44L.

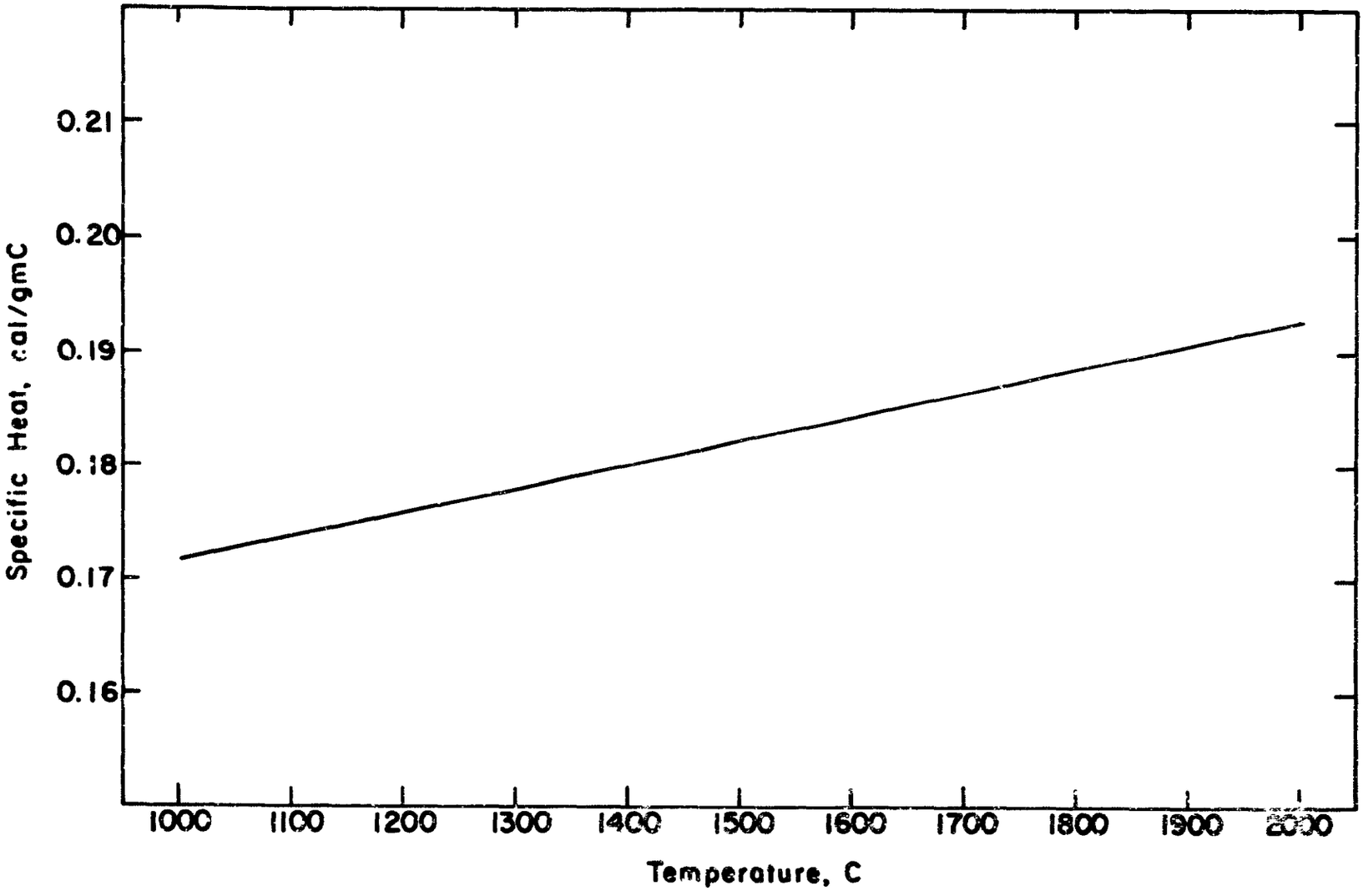

Figure 17. Specific Heat of Material V07F D0902K.

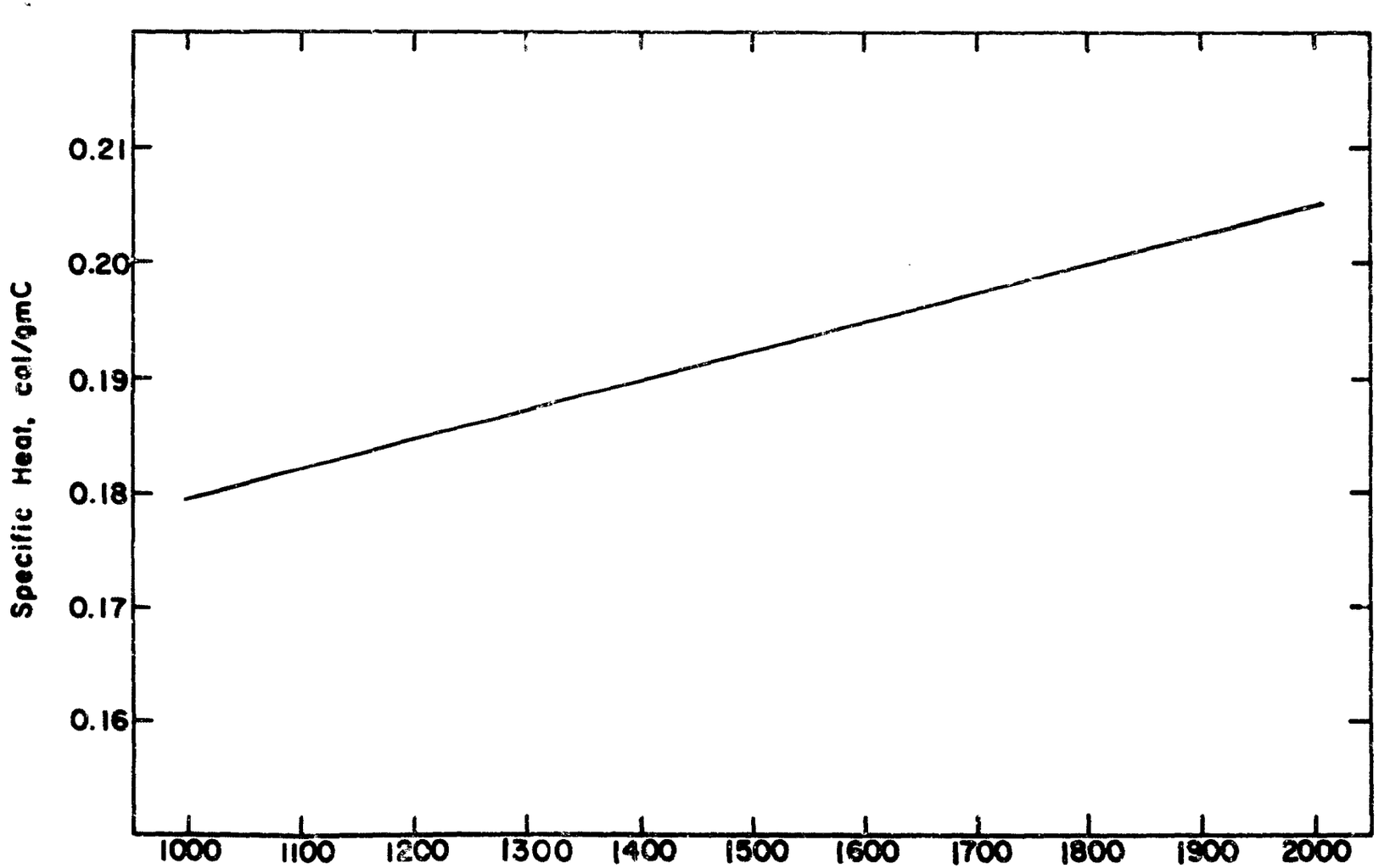

Figure 18. Specific Heat of Material VIII(18,10)07F D0920K.

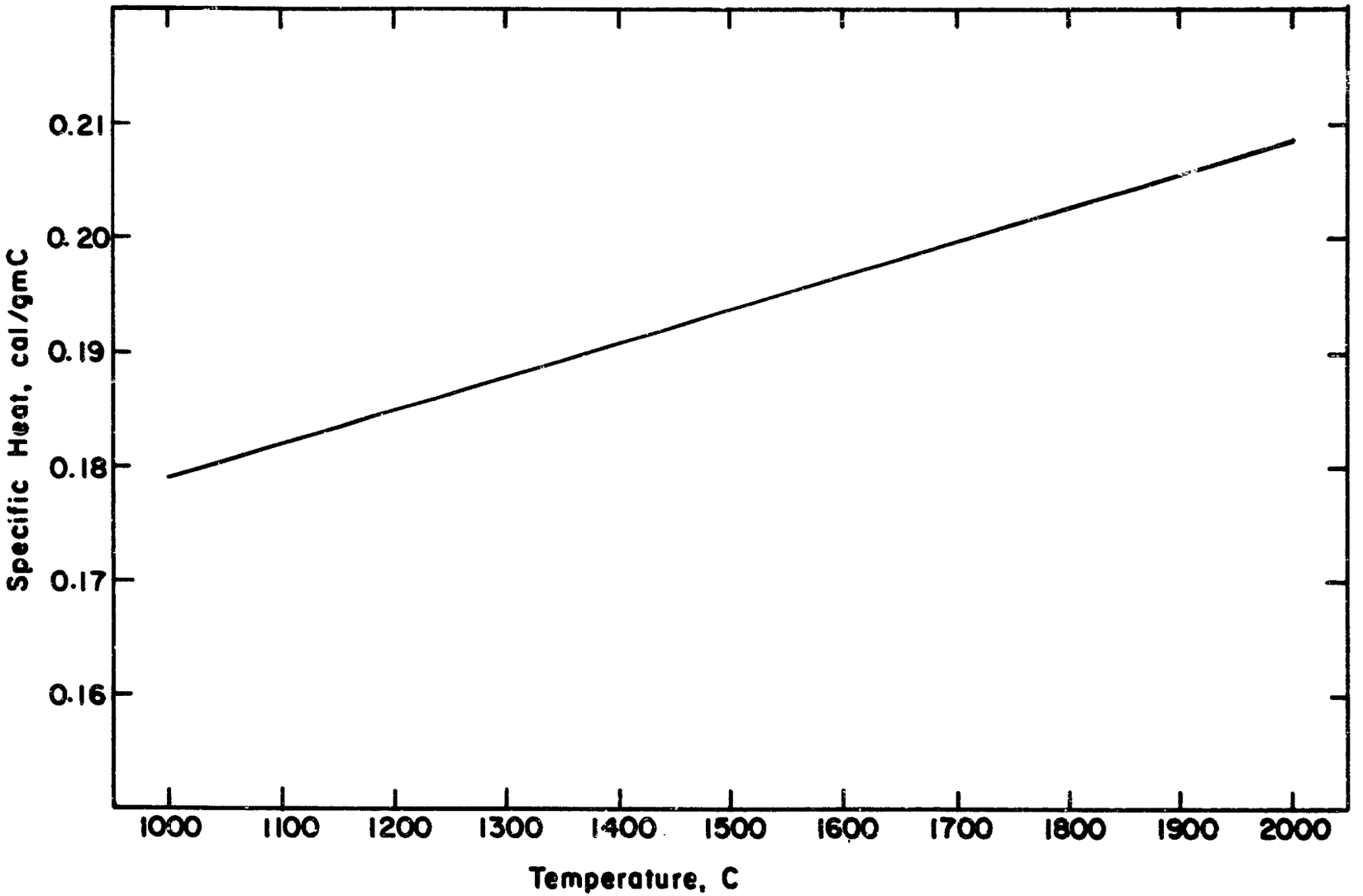

Figure 19. Specific Heat of Material XII(20)07F D0812K.

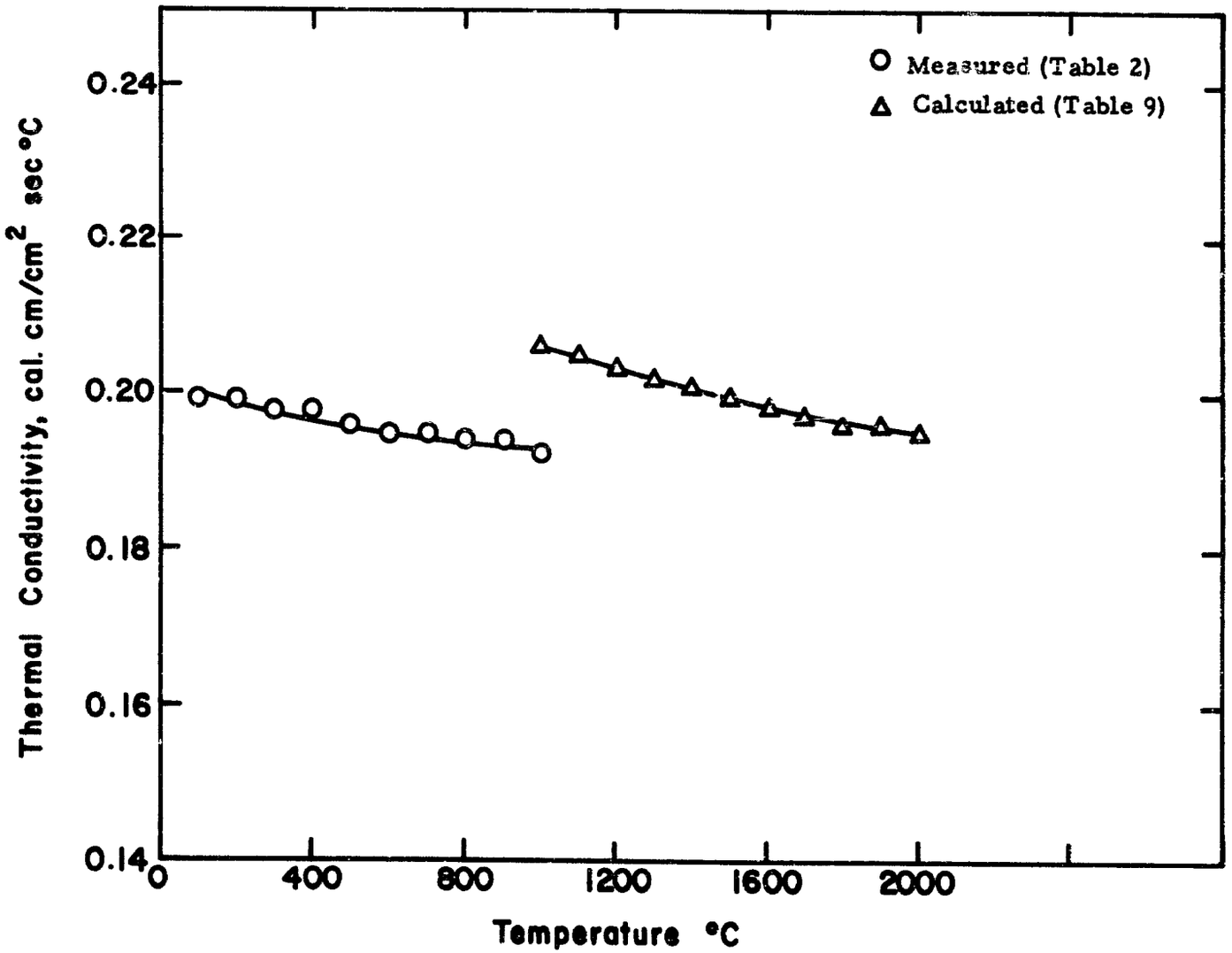

Figure 20. Measured and Calculated Thermal Conductivity, 100° to 2000°C for Material I.

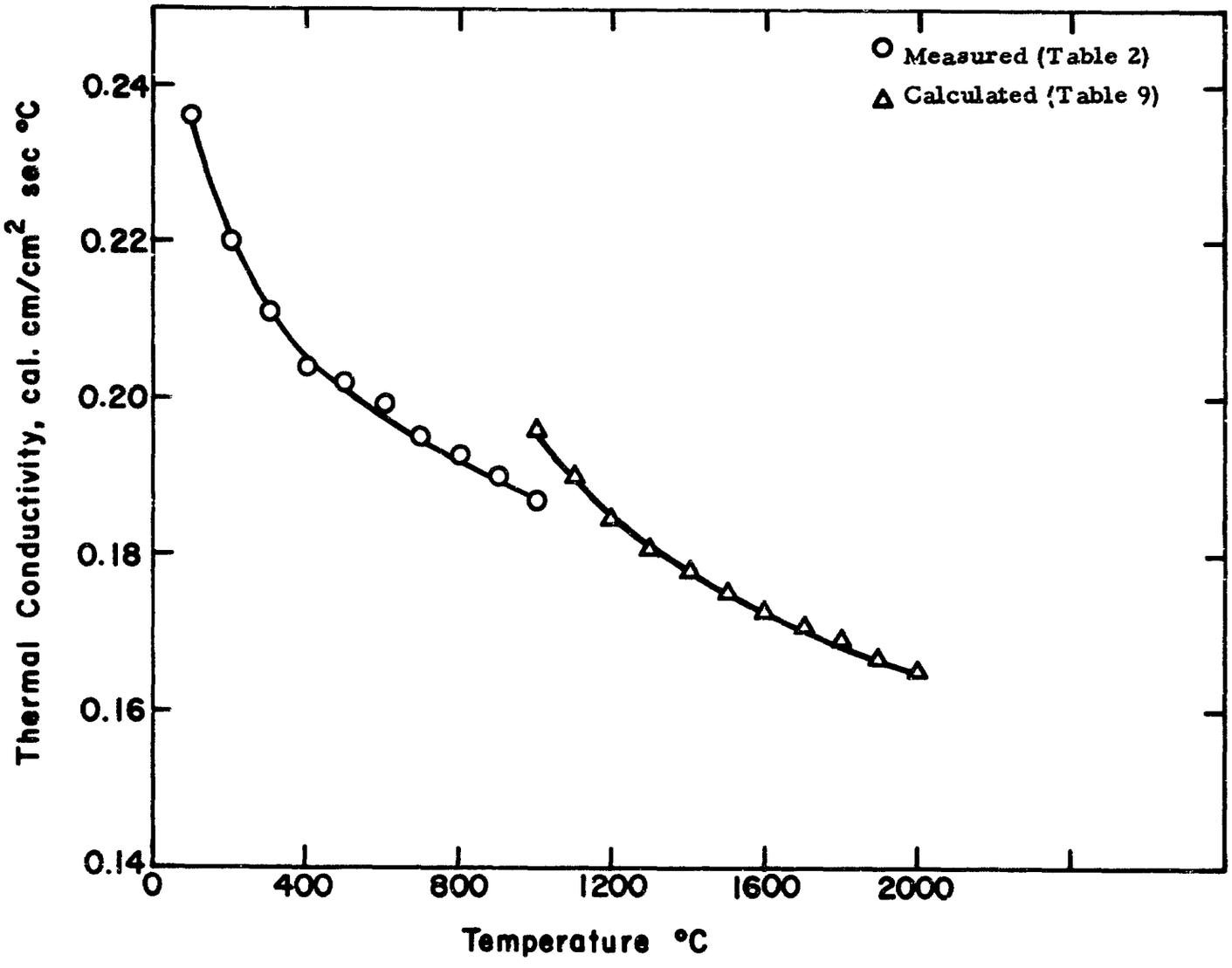

Figure 21. Measured and Calculated Thermal Conductivity, 100° to 2000°C for Material V.

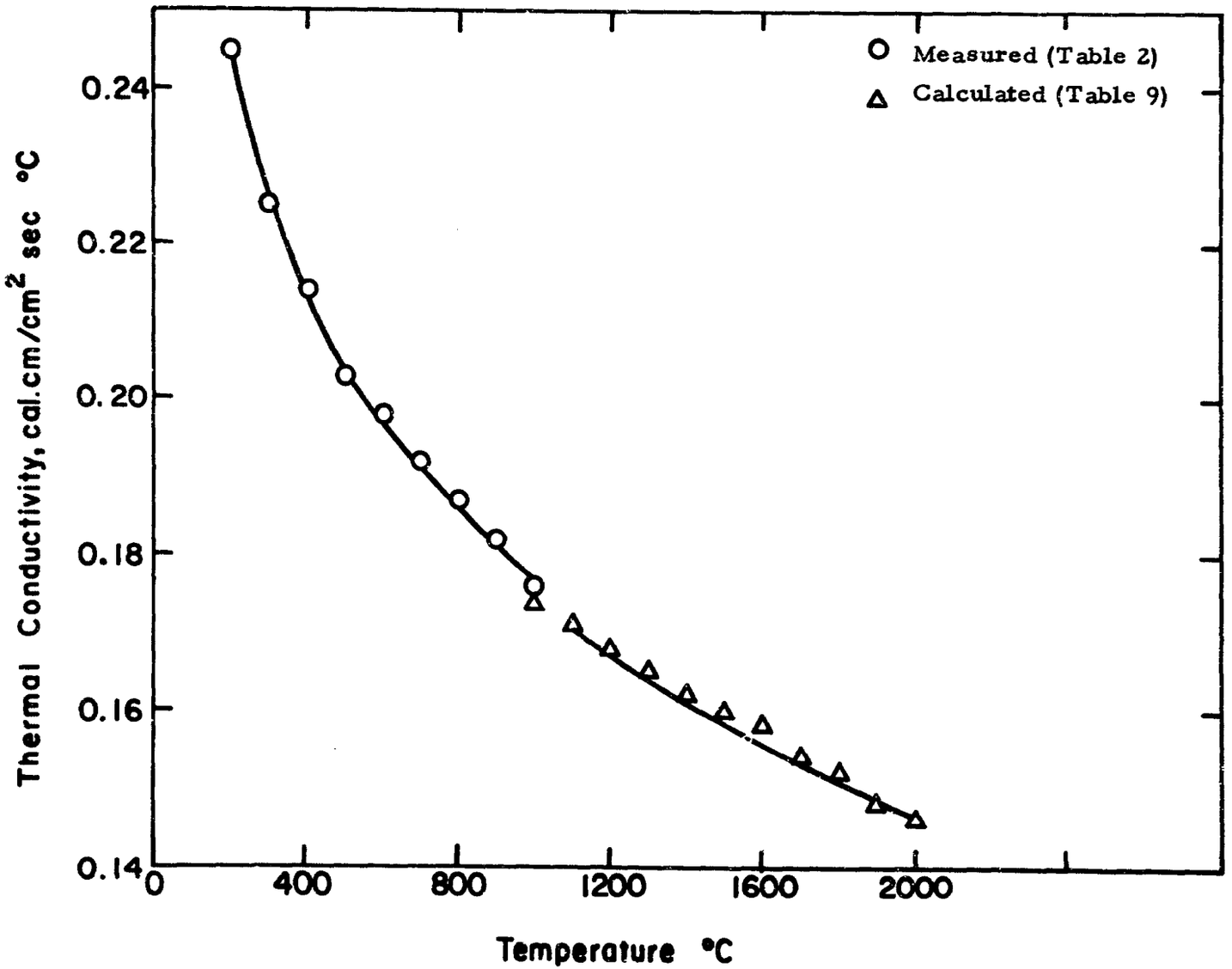

Figure 22. Measured and Calculated Thermal Conductivity, 100° to 2000°C for Material VIII(18,10).

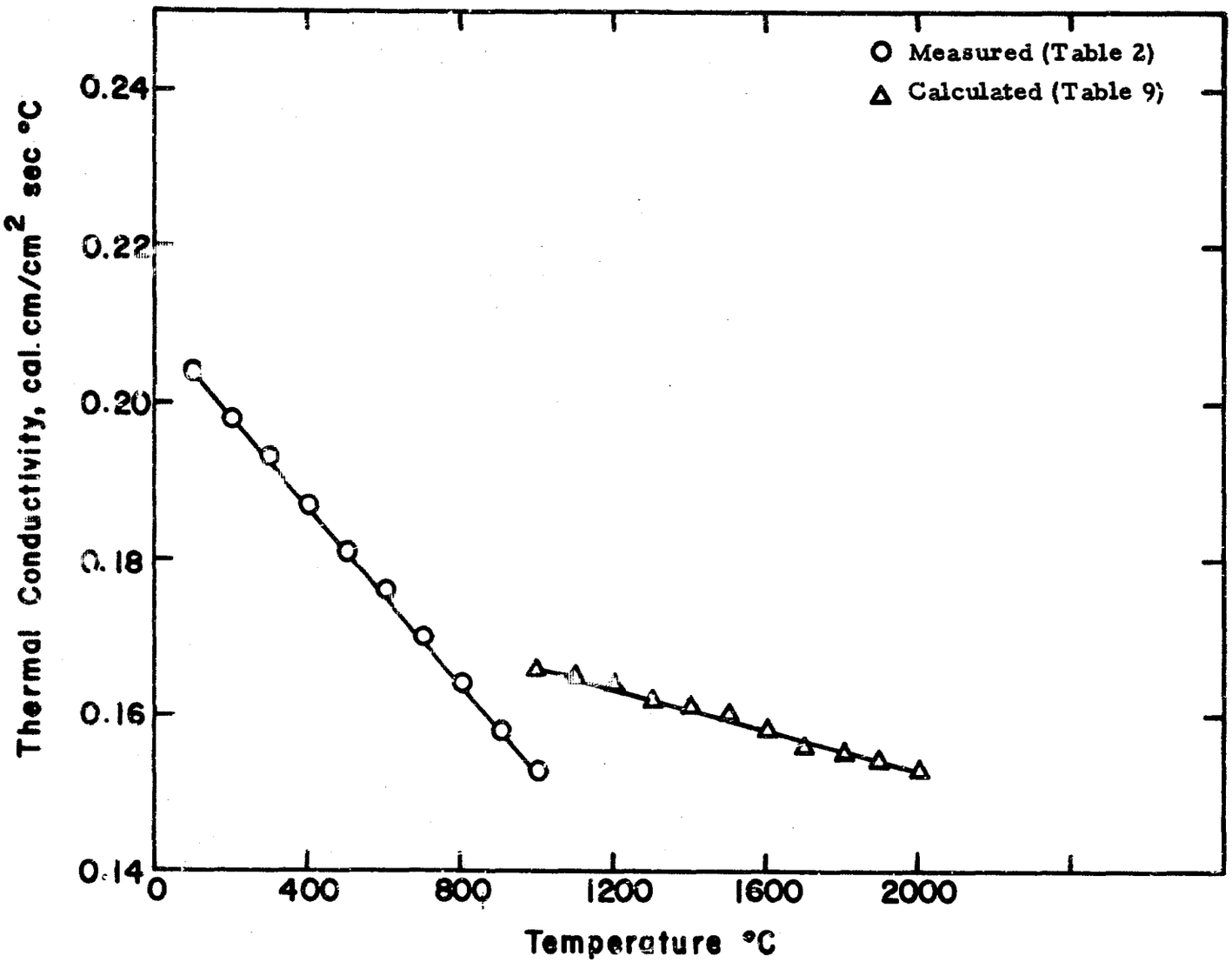

Figure 23. Measured and Calculated Thermal Conductivity, 100° to 2000°C for Material XII(20).

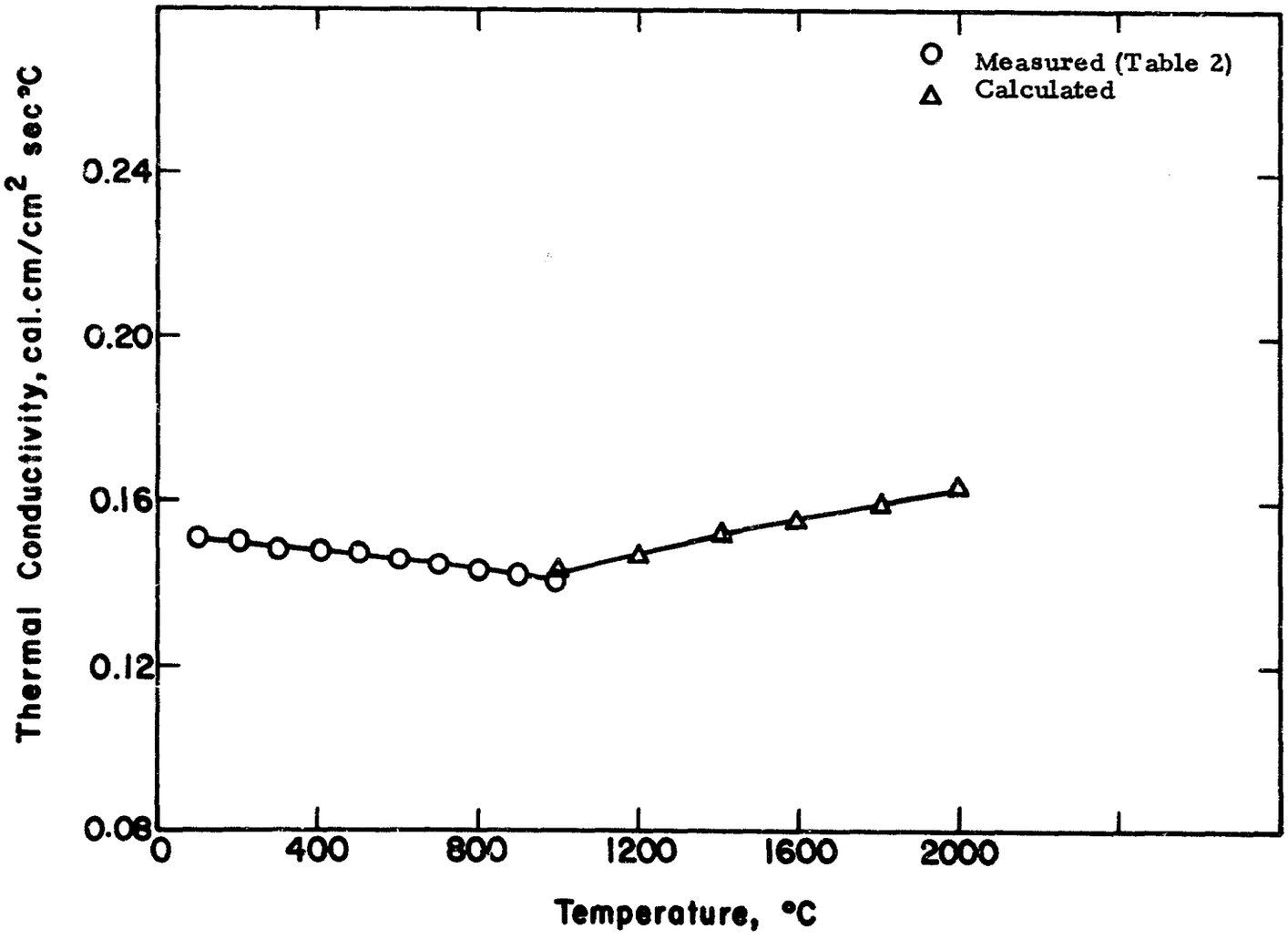

Figure 24. Measured and Calculated Thermal Conductivity, 100° to 2000°C for Material III(5).

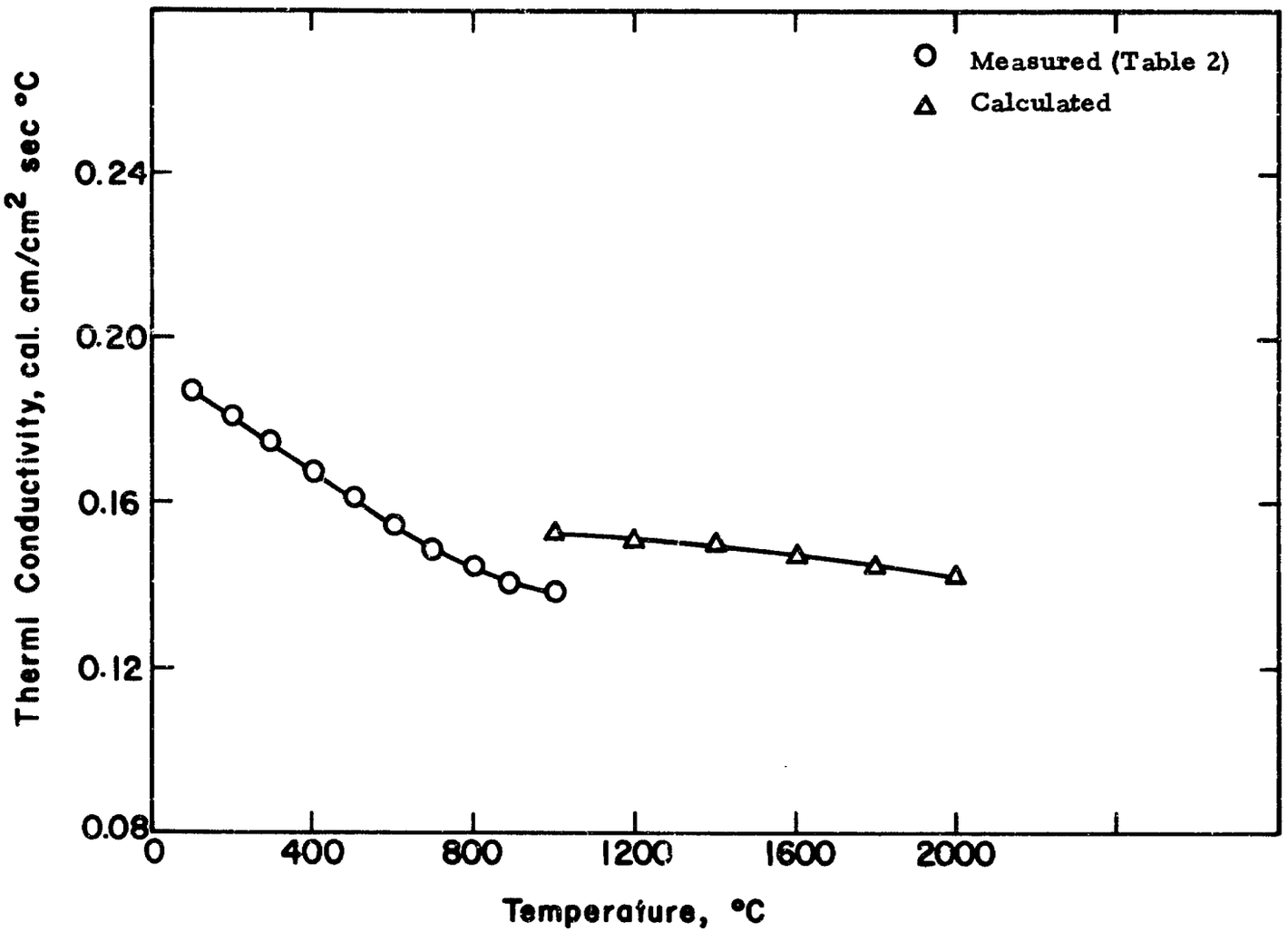

Figure 25. Measured and Calculated Thermal Conductivity, 100° to 2000°C for Material IV.

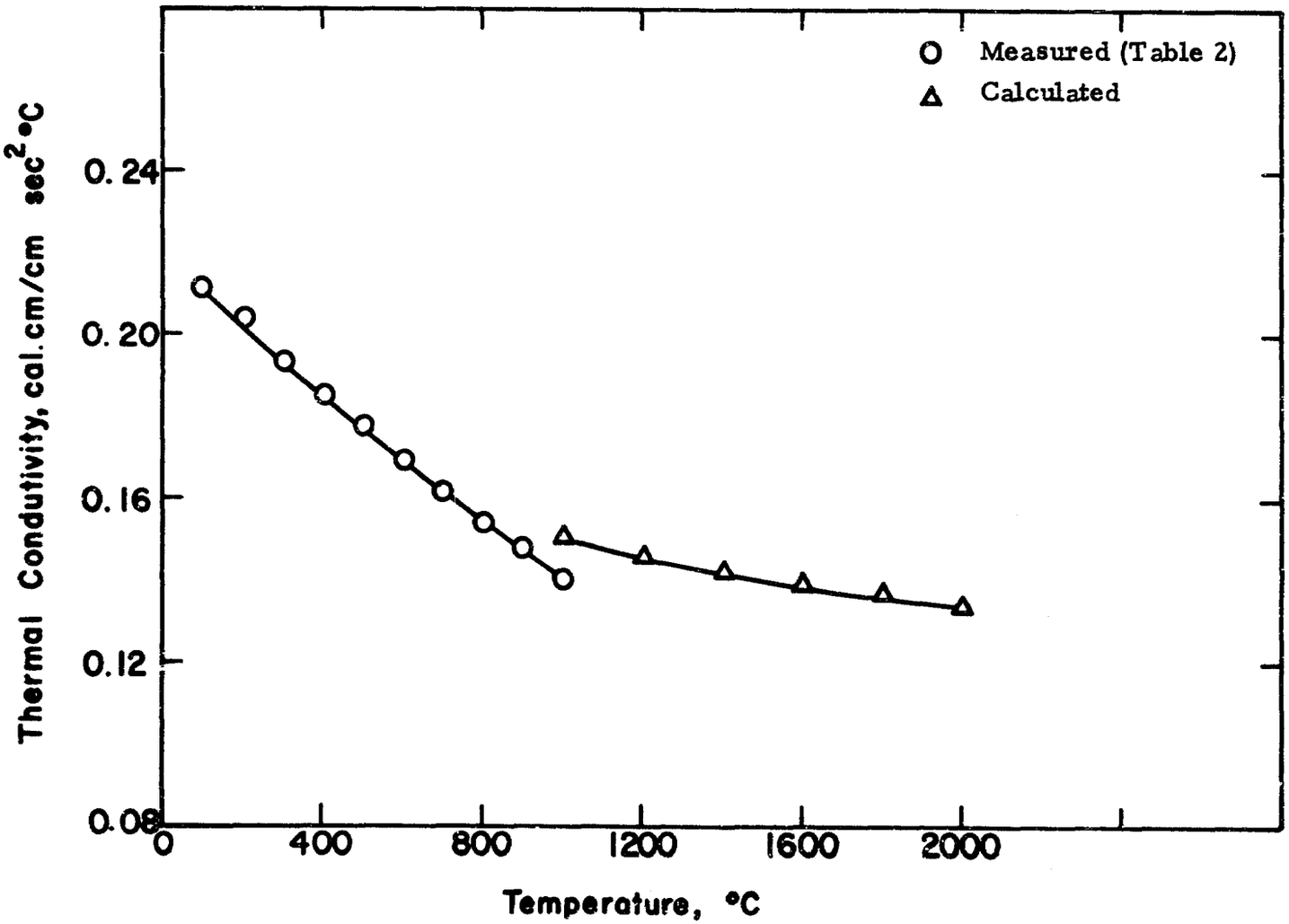

Figure 26. Measured and Calculated Thermal Conductivity, 100° to 2000°C for Material V, 88.5 Percent Dense.

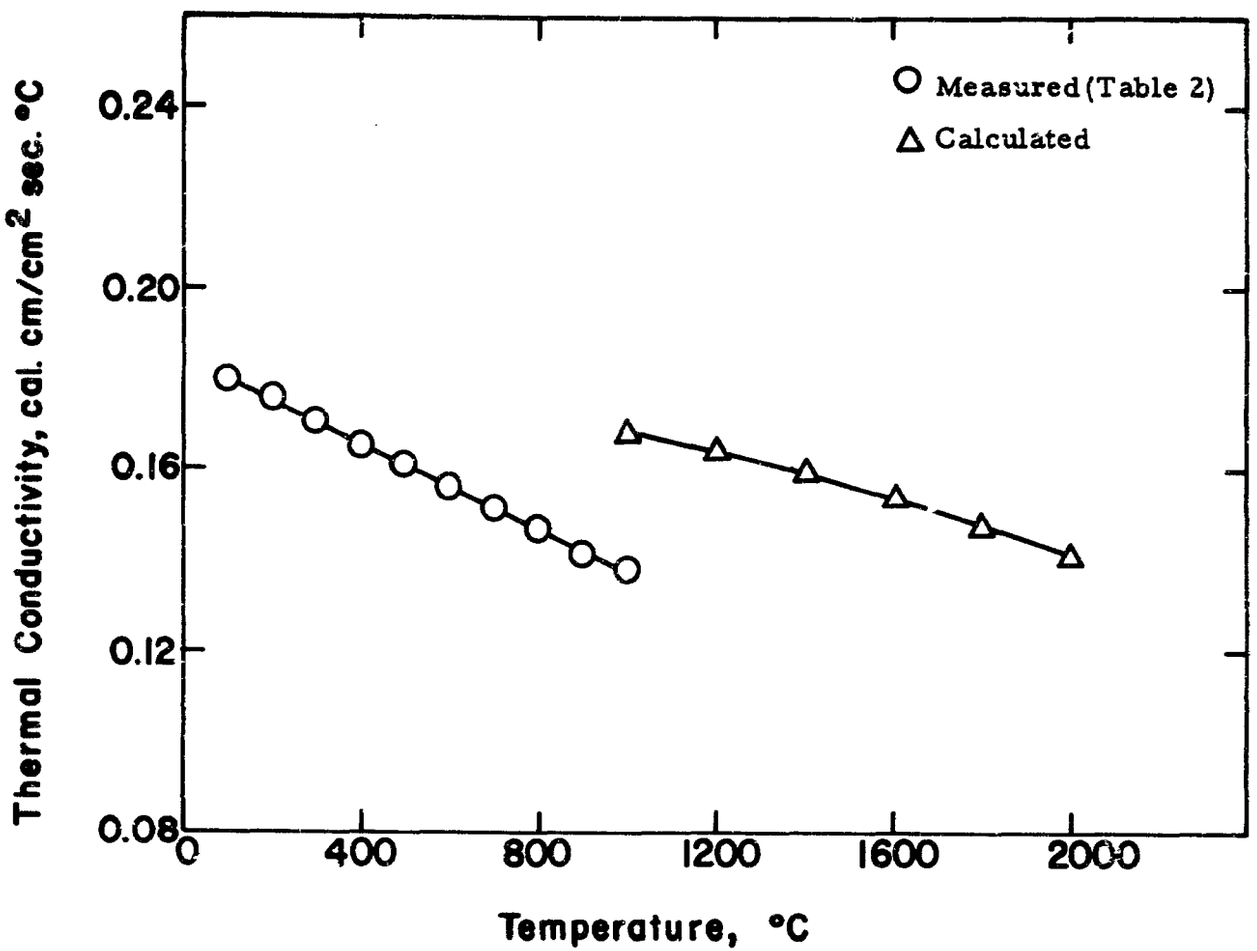

Figure 27. Measured and Calculated Thermal Conductivity, 100° to 2000°C for Material VIII.

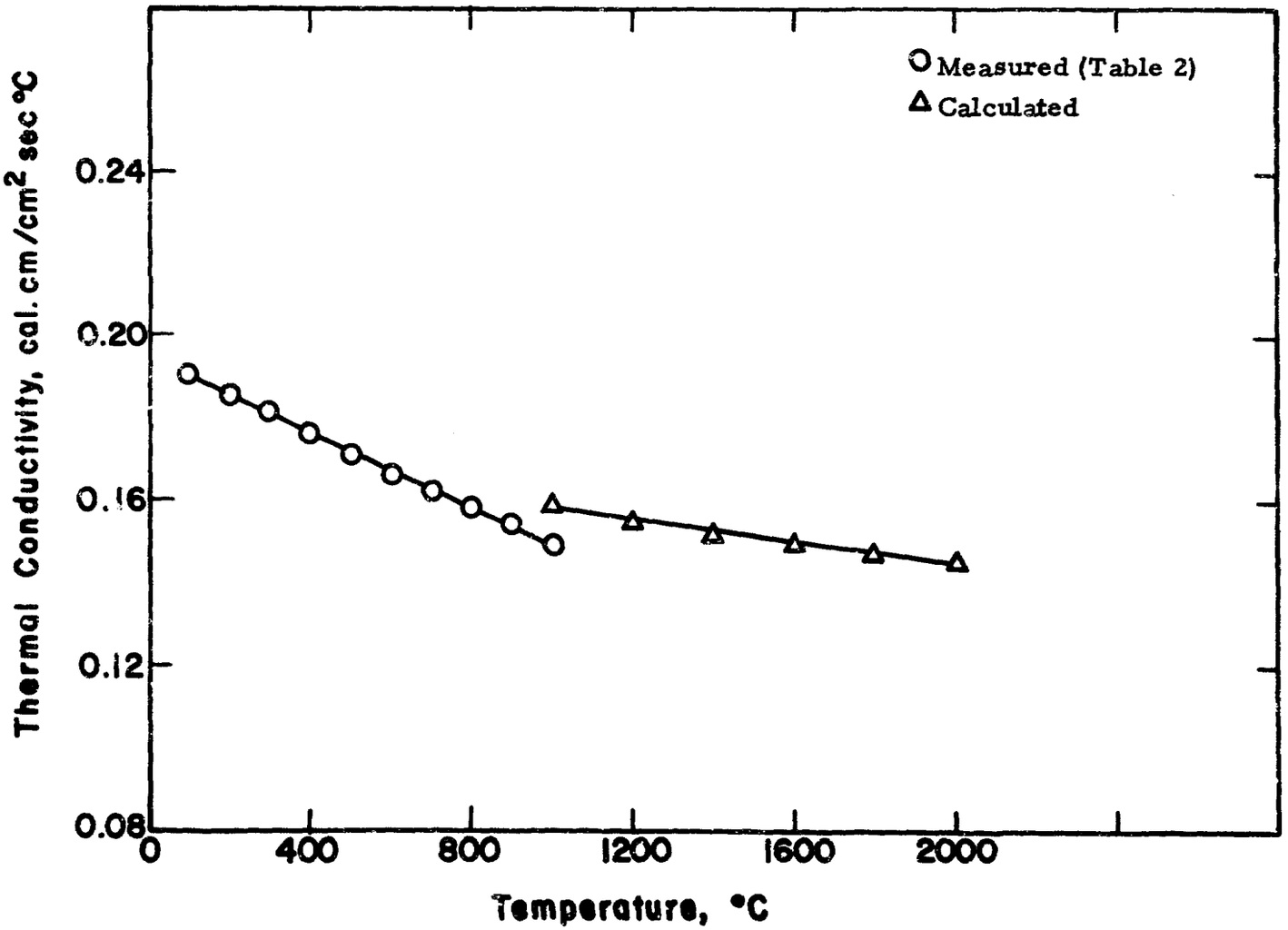

Figure 28. Measured and Calculated Thermal Conductivity, 100° to 2000°C for Material XIV(18, 10).

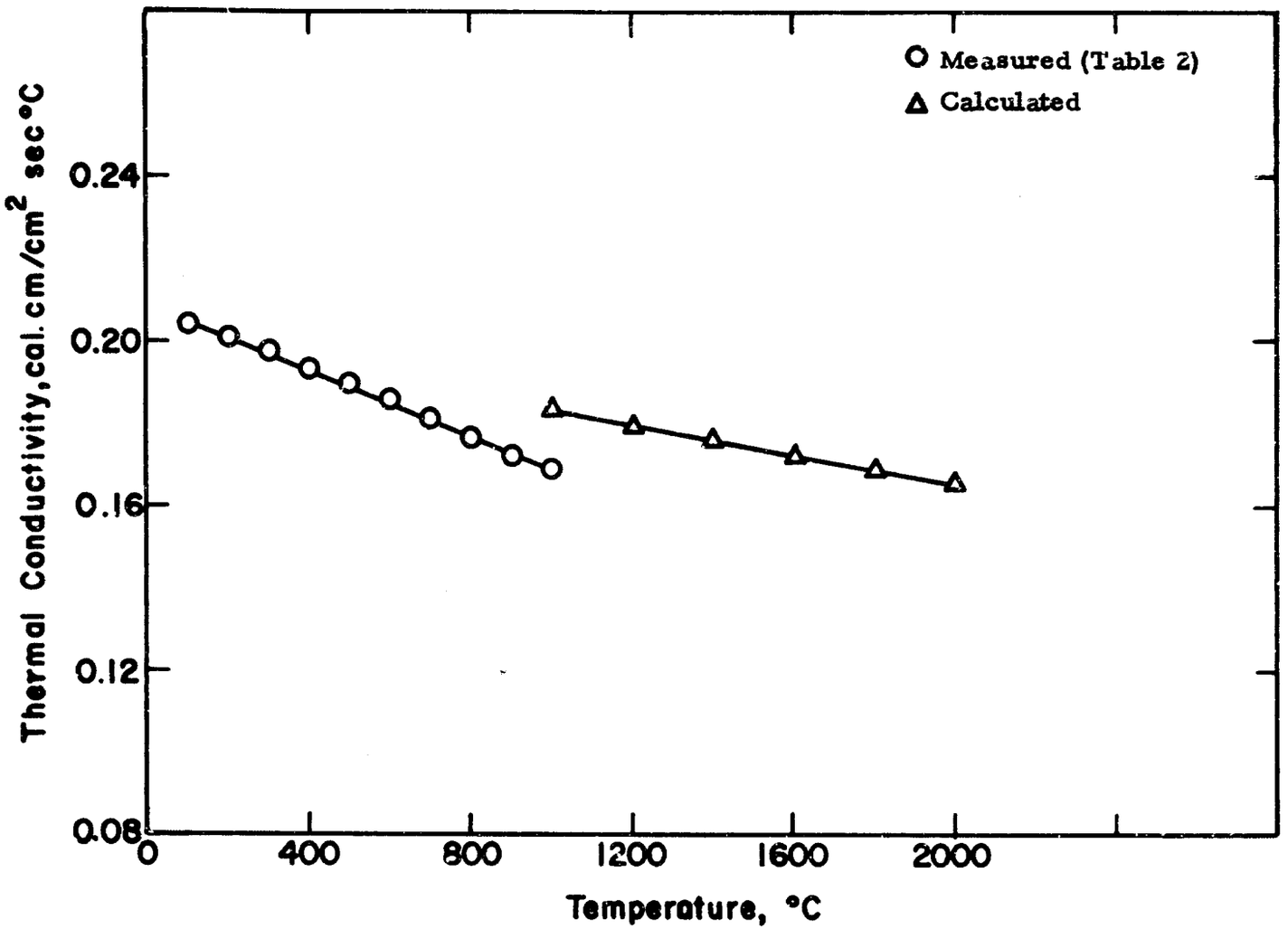

Figure 29. Measured and Calculated Thermal Conductivity, 100° to 2000°C for Material XV(20).

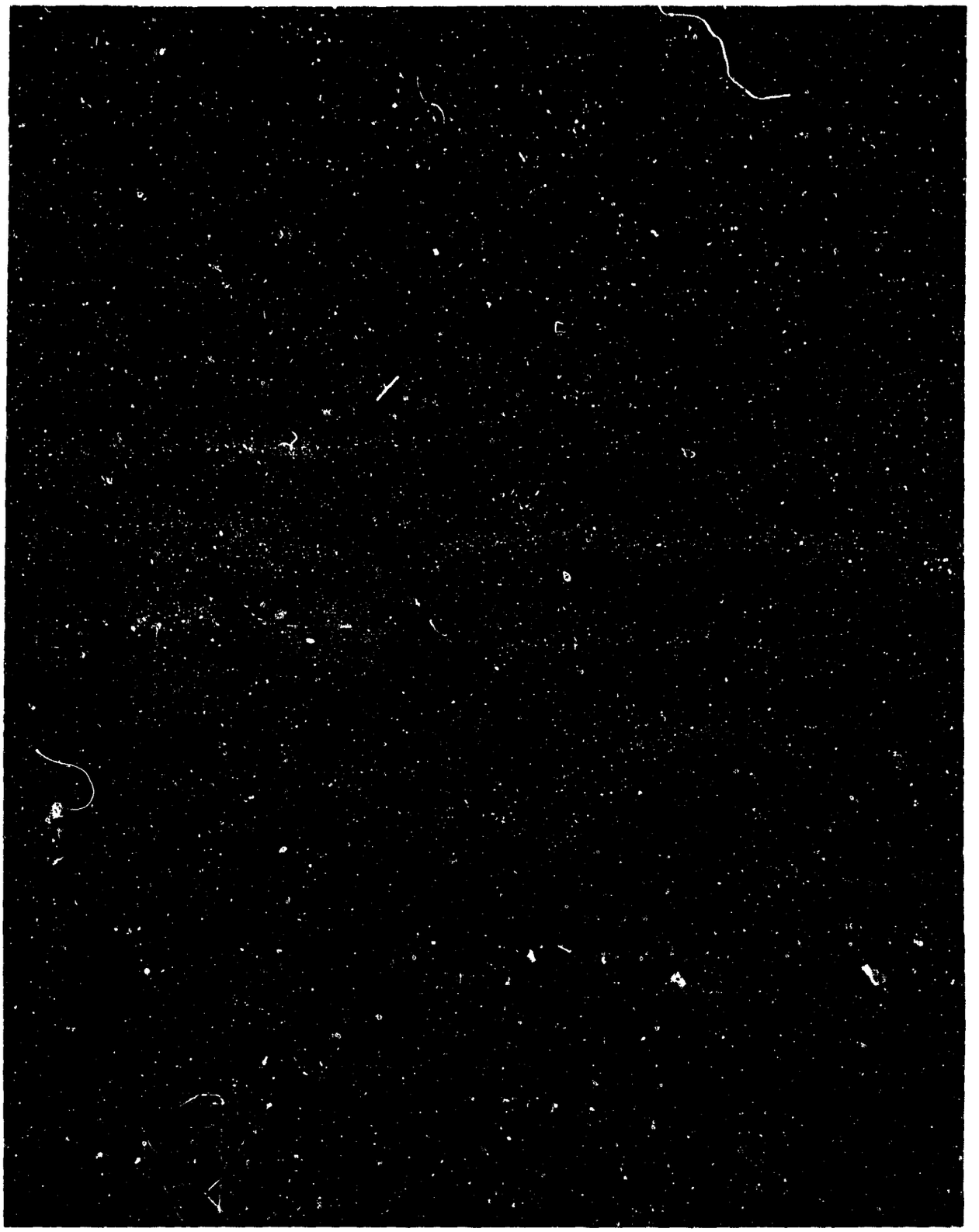

Figure 30. High Temperature Recording Dilatometer Apparatus (Battelle Memorial Institute).

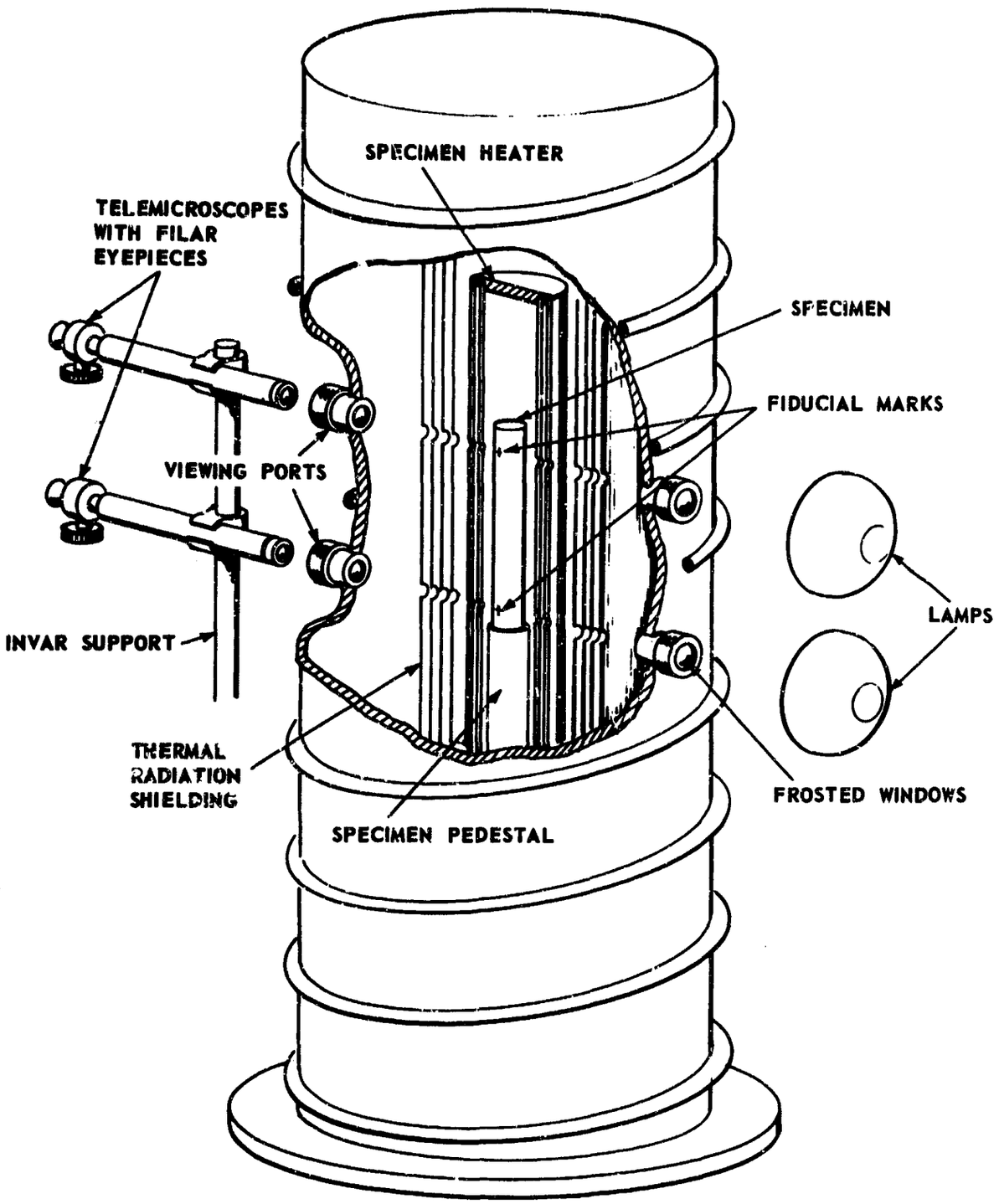

Figure 31. Section Drawing of Direct-View Dilatometer.

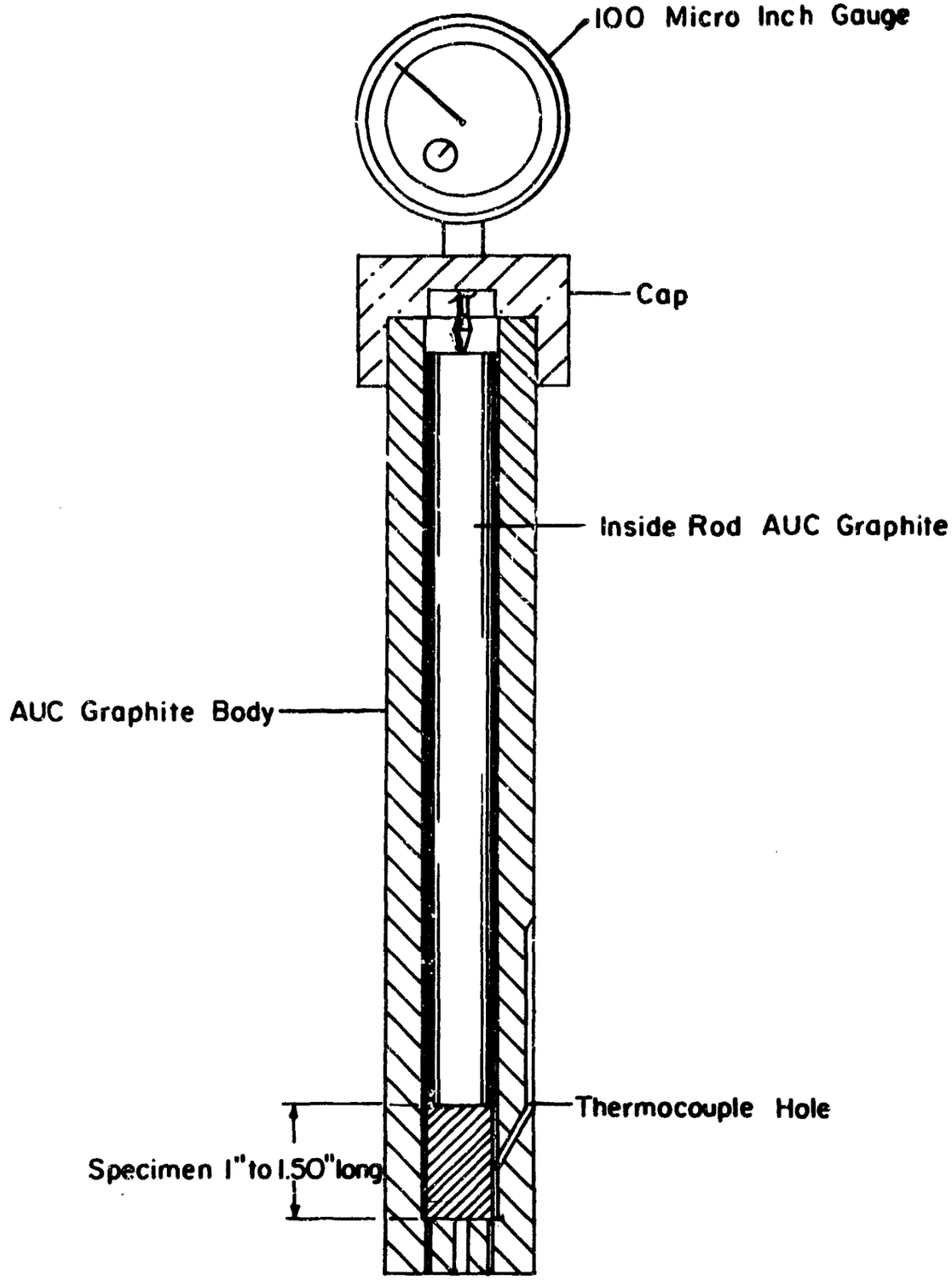

Figure 32. Cross Sectional View of ManLabs Graphite Dilatometer

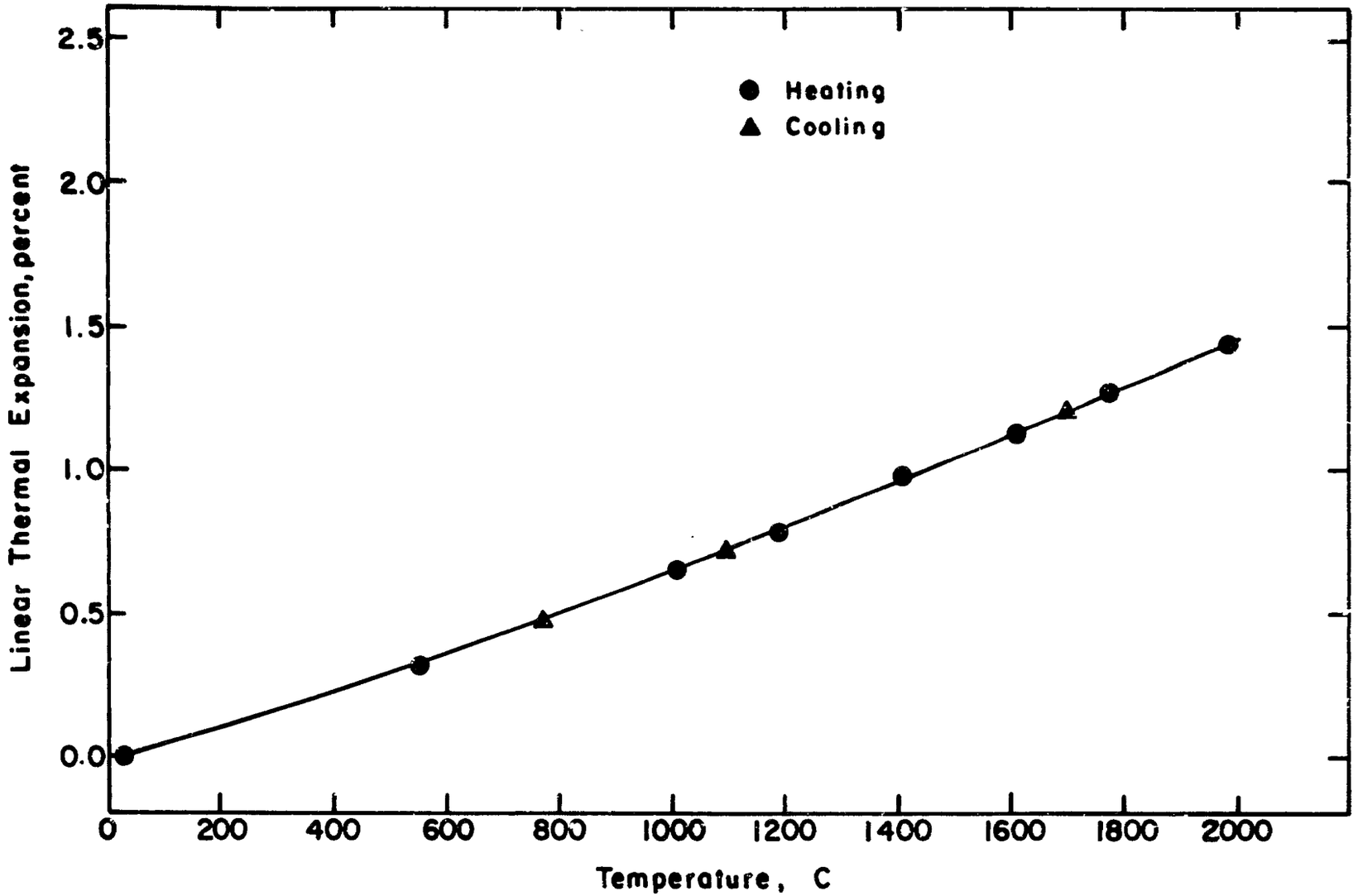

Figure 33. Direct-View Linear Expansion Data for Material I05 R44L, 100 Percent Dense.

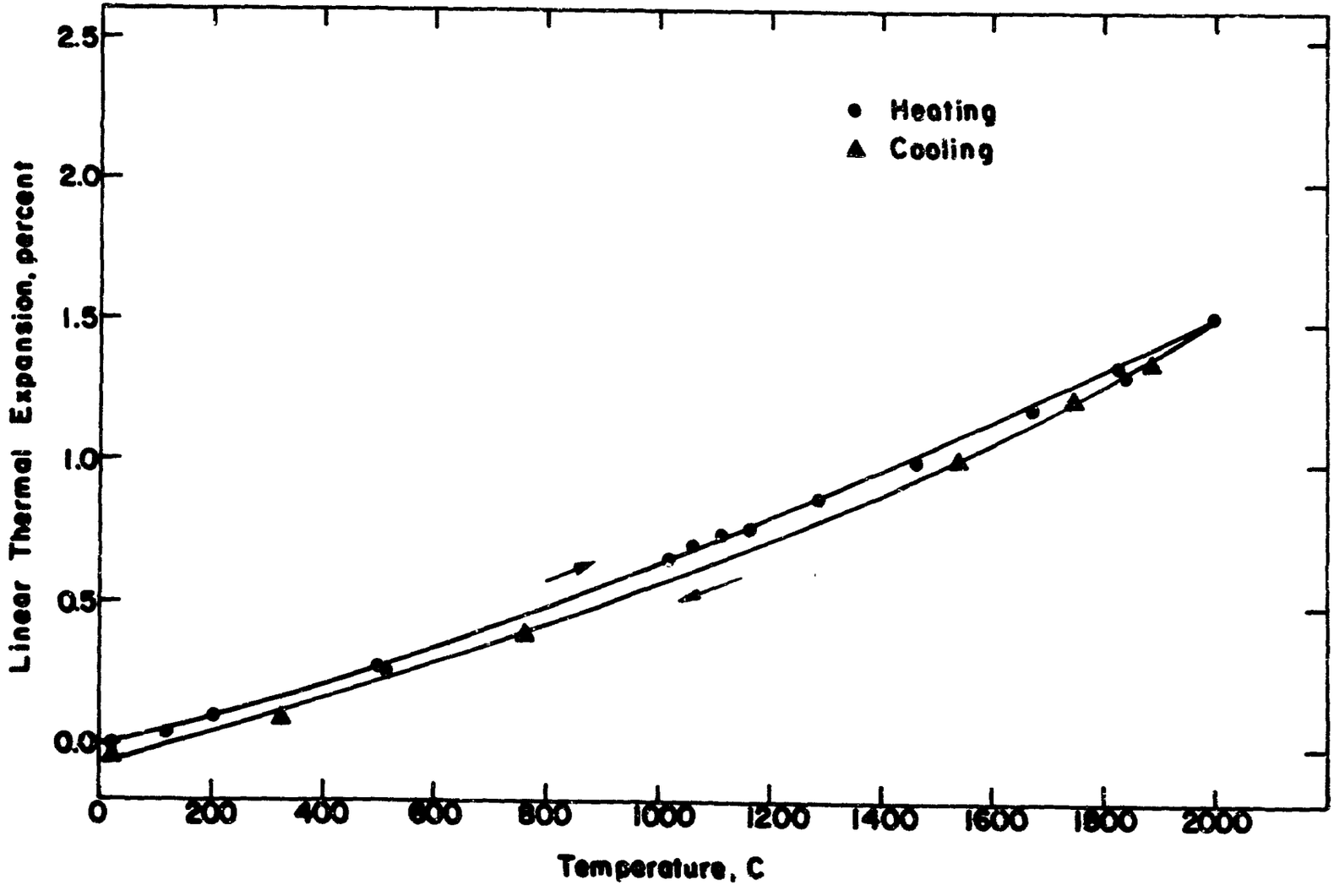

Figure 34. Direct-View Linear Expansion Data for Material V07F R26L, 99 Percent Dense.

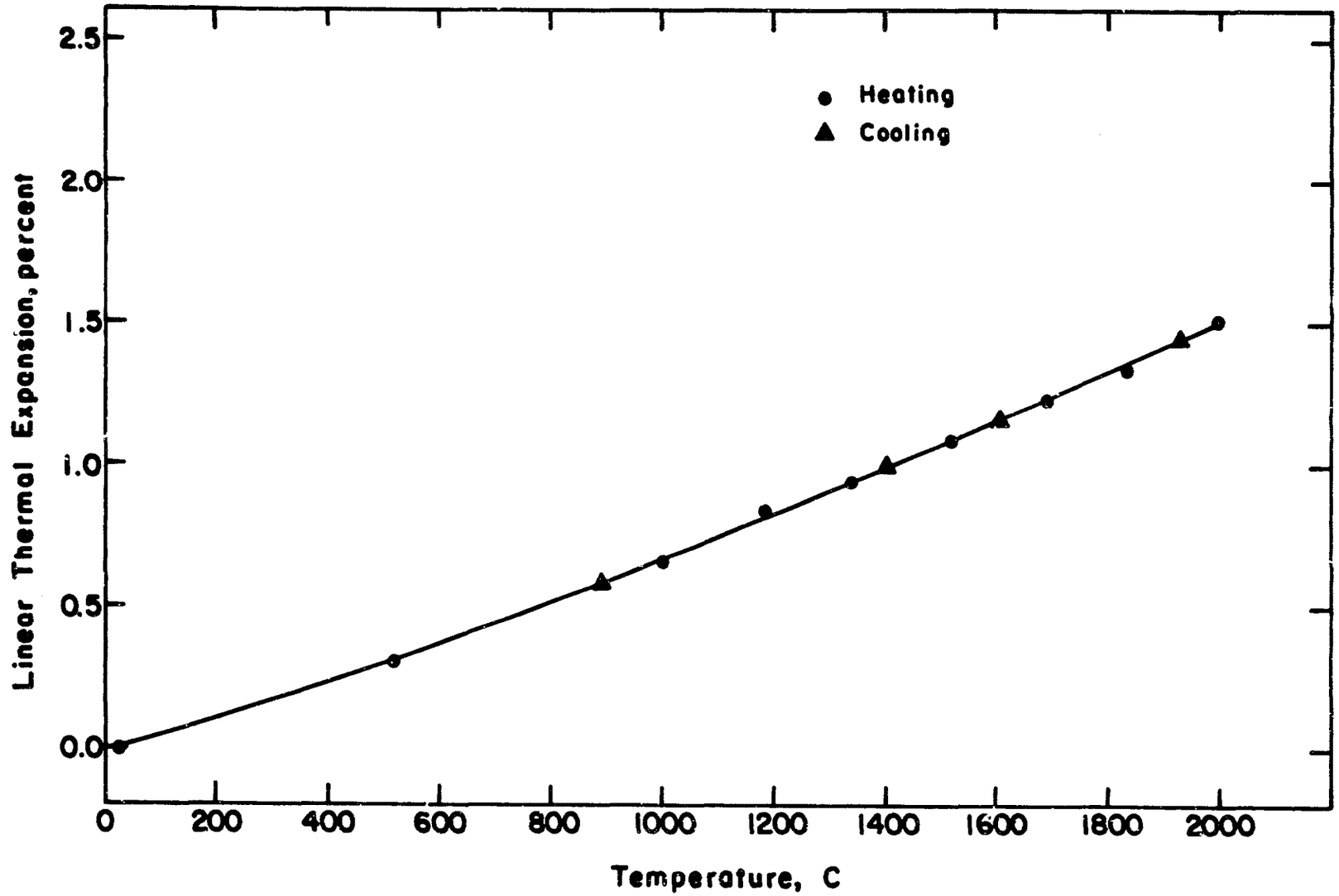

Figure 35. Direct-View Linear Expansion Data for Material VIII(18,10) D0920K, 100 Percent Dense.

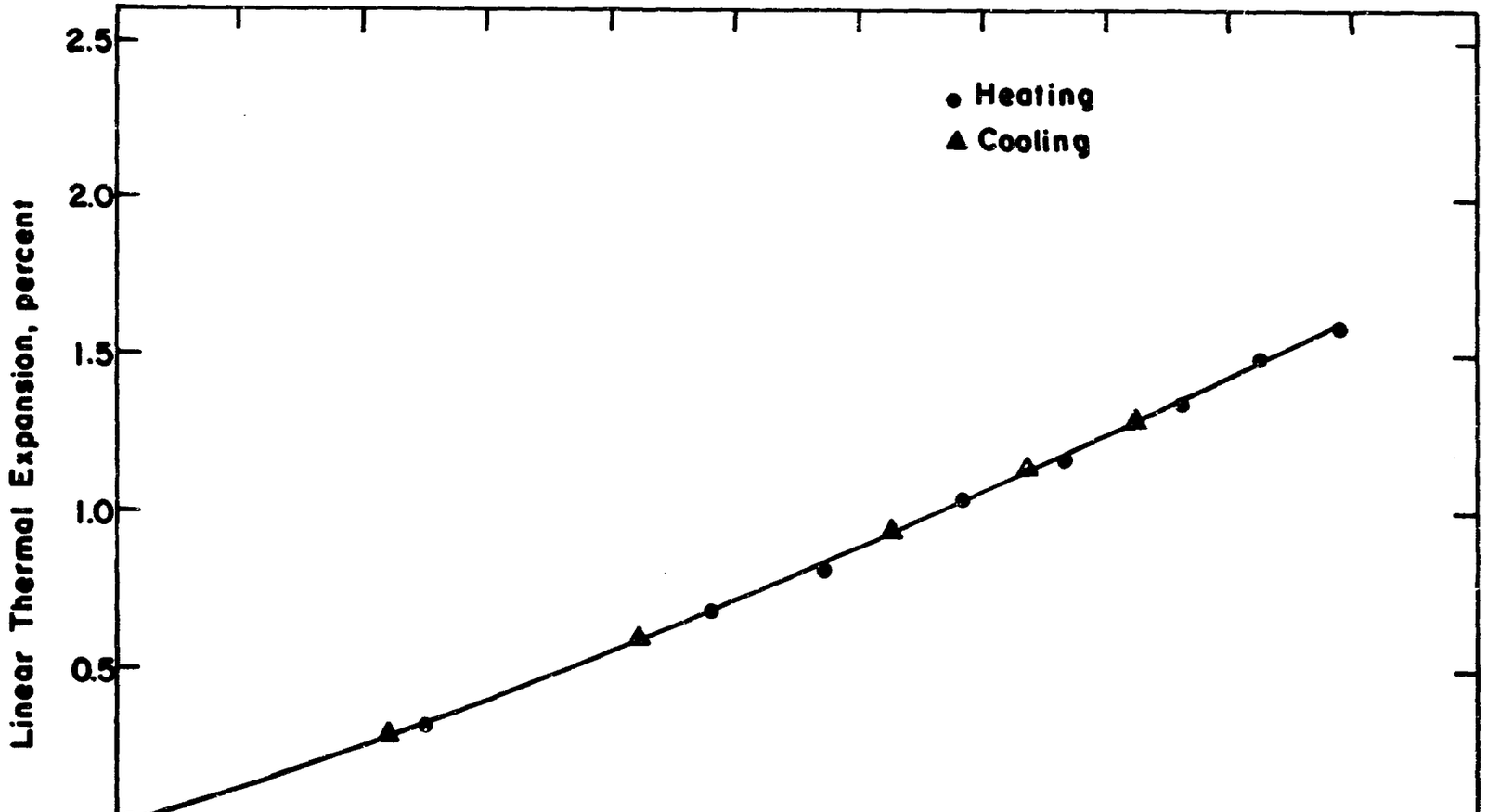

Figure 36. Direct-View Linear Expansion Data for Material XII(20)07F D0812K, 95% Dense.

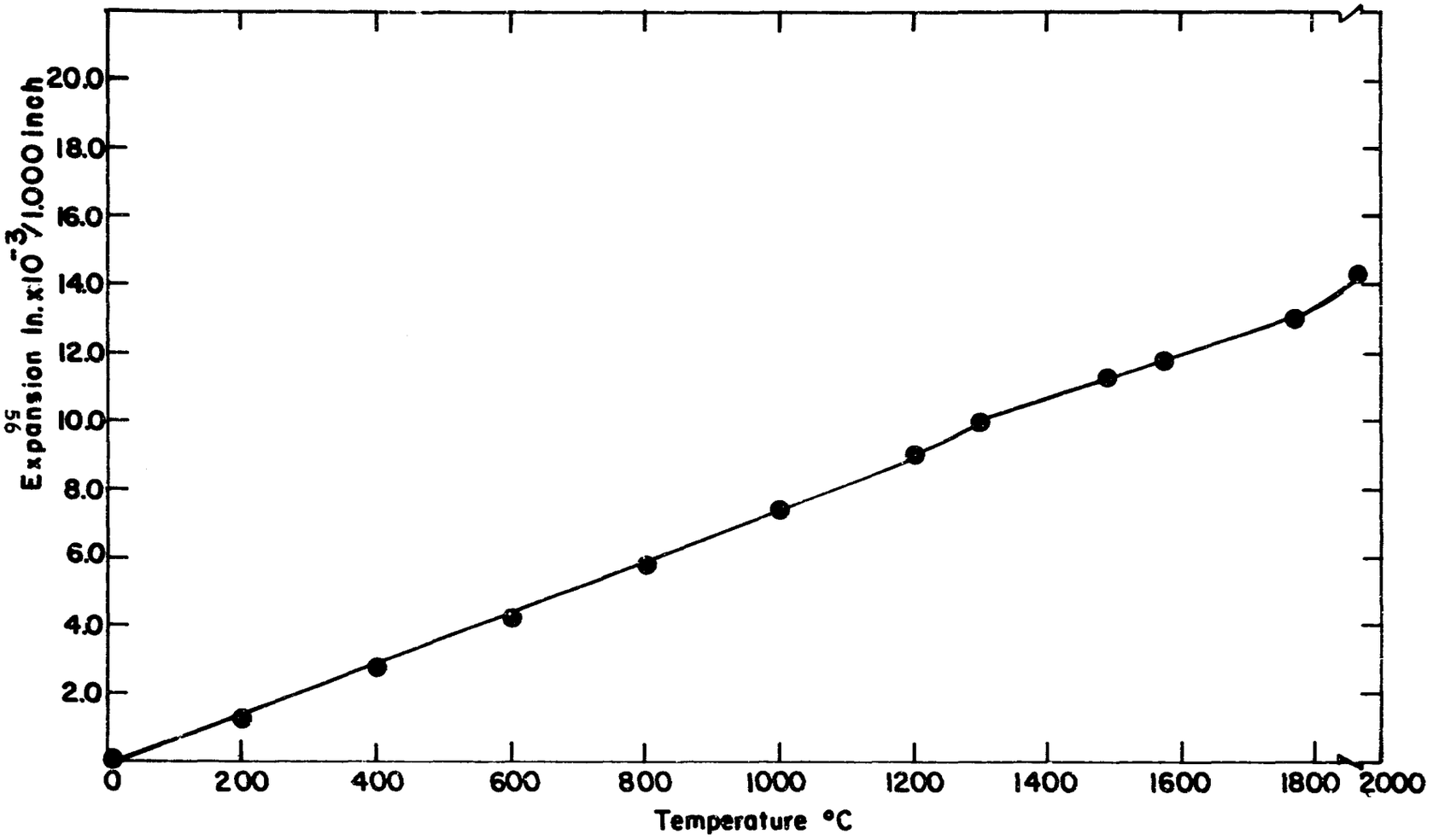

Figure 37. Differential Dilatometer Linear Expansion Data for Material I07F D0700K, 99 Percent Dense.

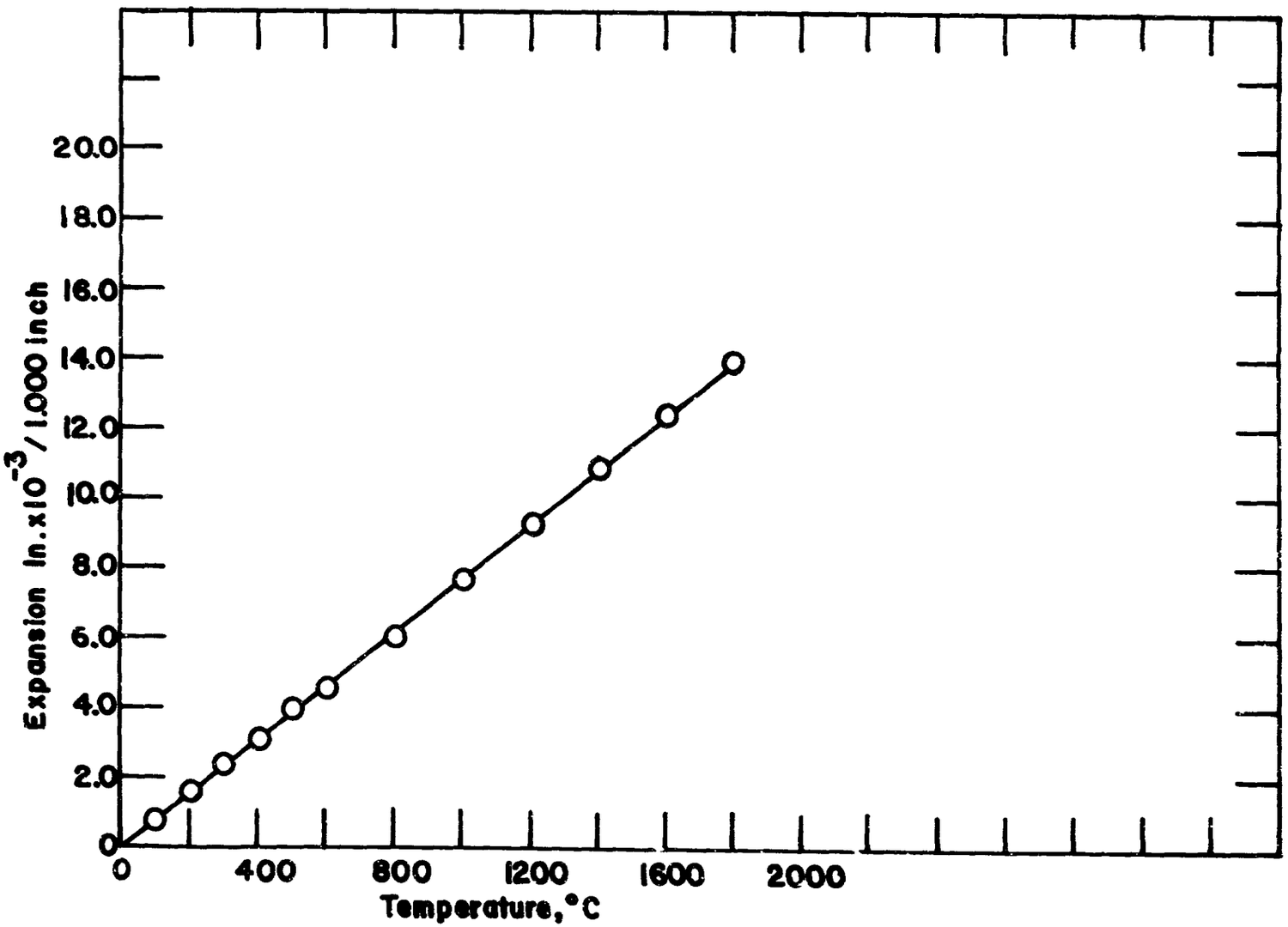

Figure 38. Differential Dilatometer Linear Expansion Data for Material V07F D0706K, 99 Percent Dense.

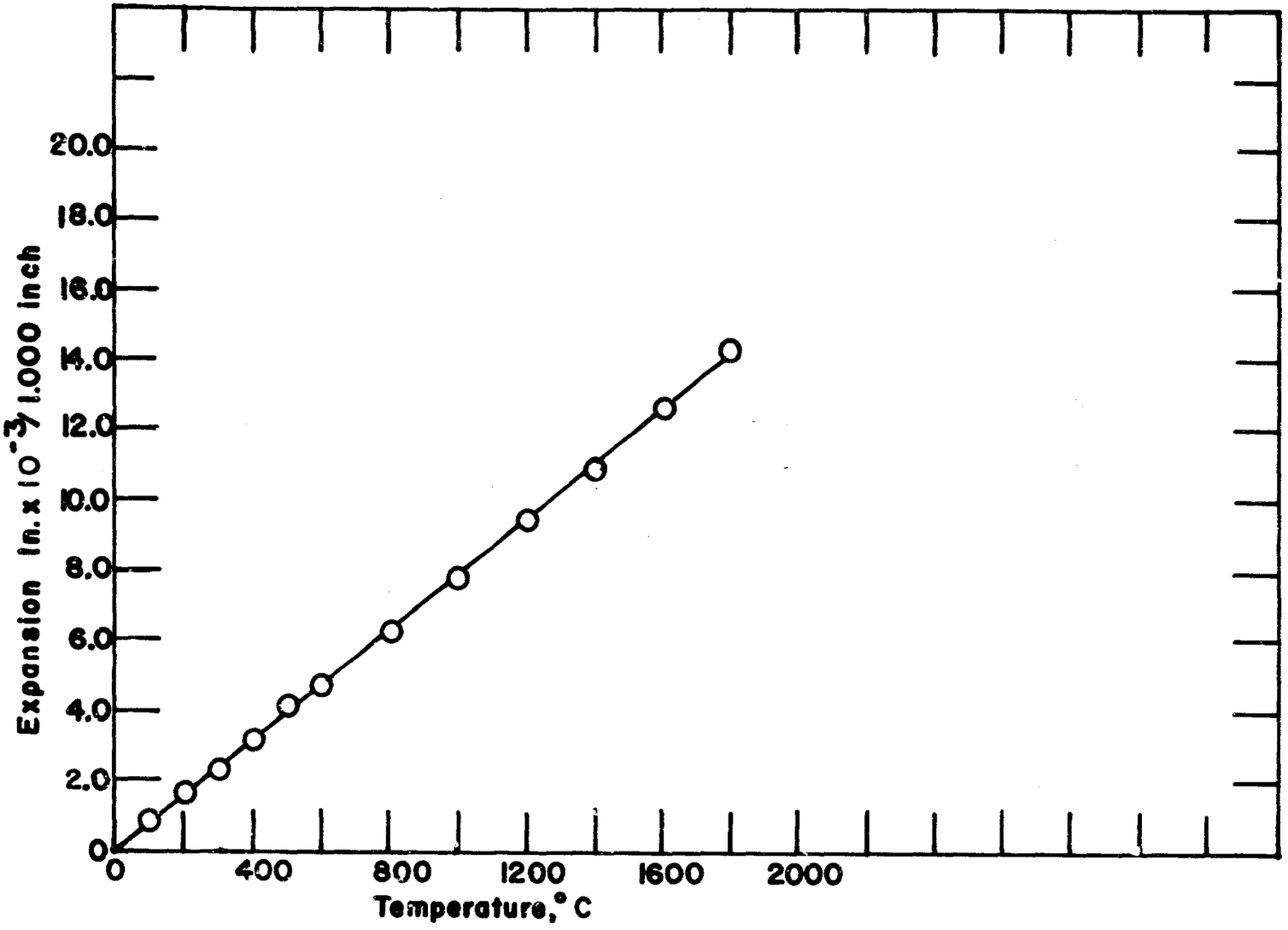

Figure 39. Differential Dilatometer Linear Expansion Data for Material V07F D0845K, 89 Percent Dense.

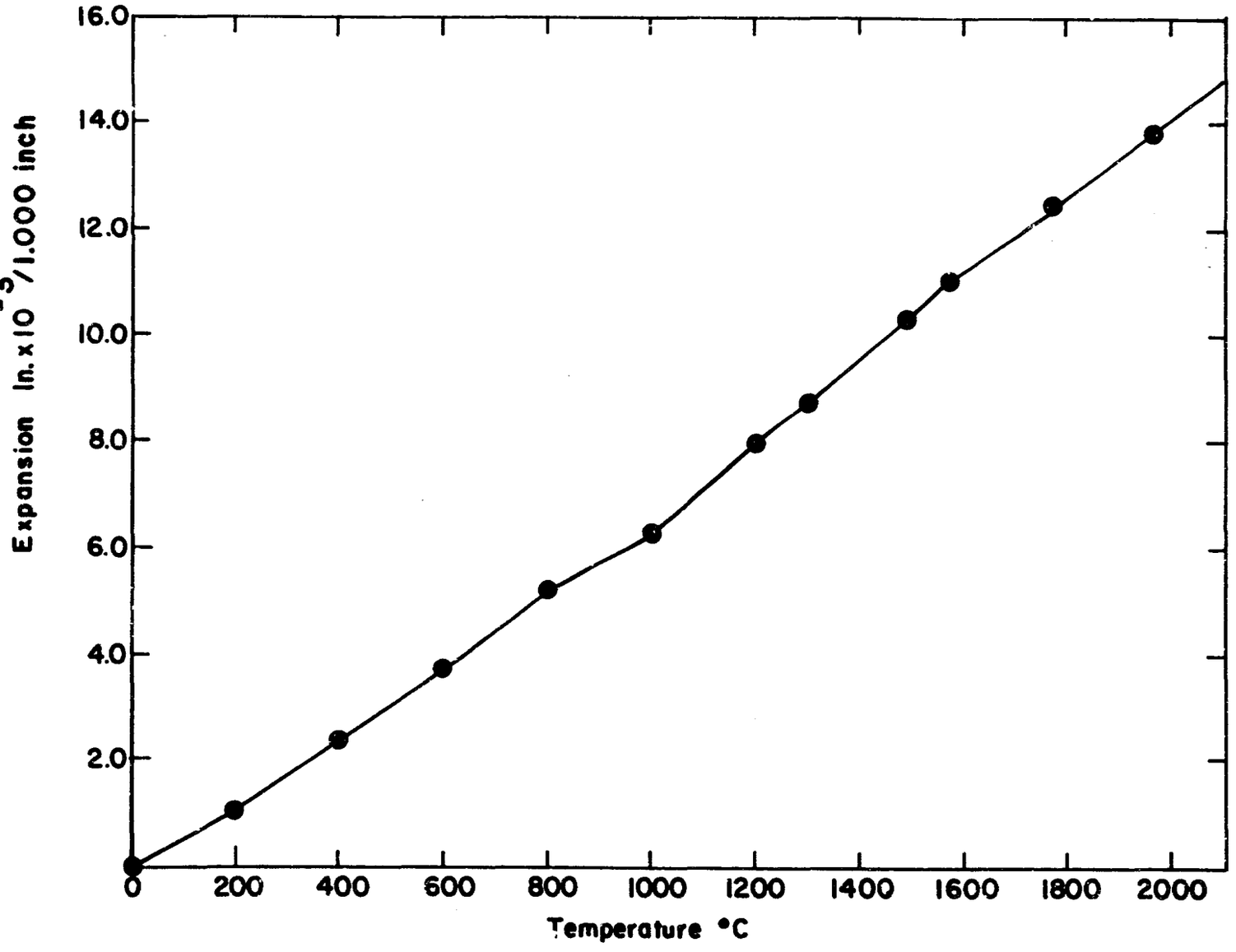

Figure 40. Differential Dilatometer Linear Expansion Data for Material VIII07F D0761K, 100 Percent Dense.

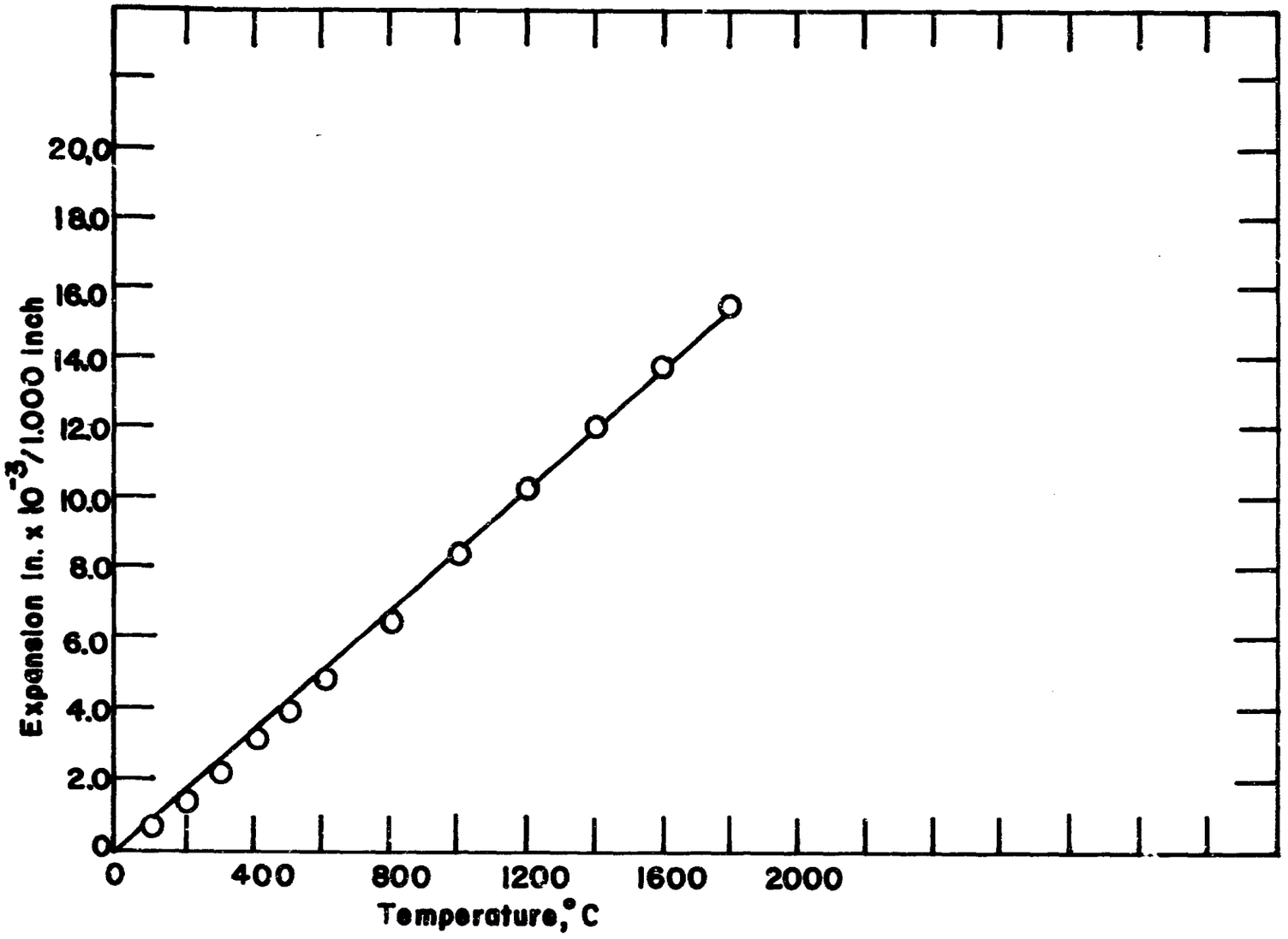

Figure 41. Differential Dilatometer Linear Expansion Data for Material XII(20)07F D0809K, 99 Percent Dense.

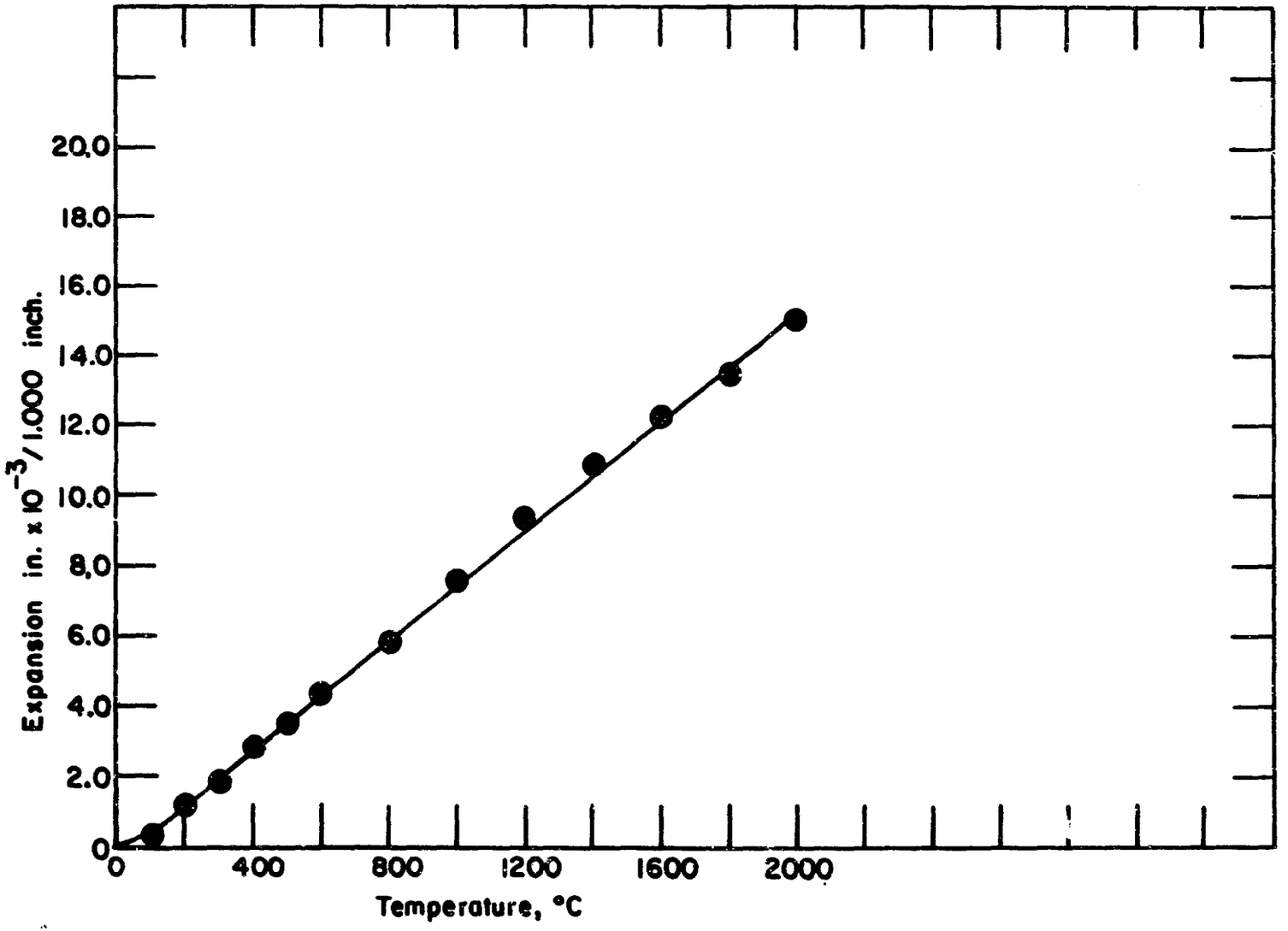

Figure 42. Differential Dilatometer Linear Expansion Data for Material IV09F D0804K, 100 Percent Dense.

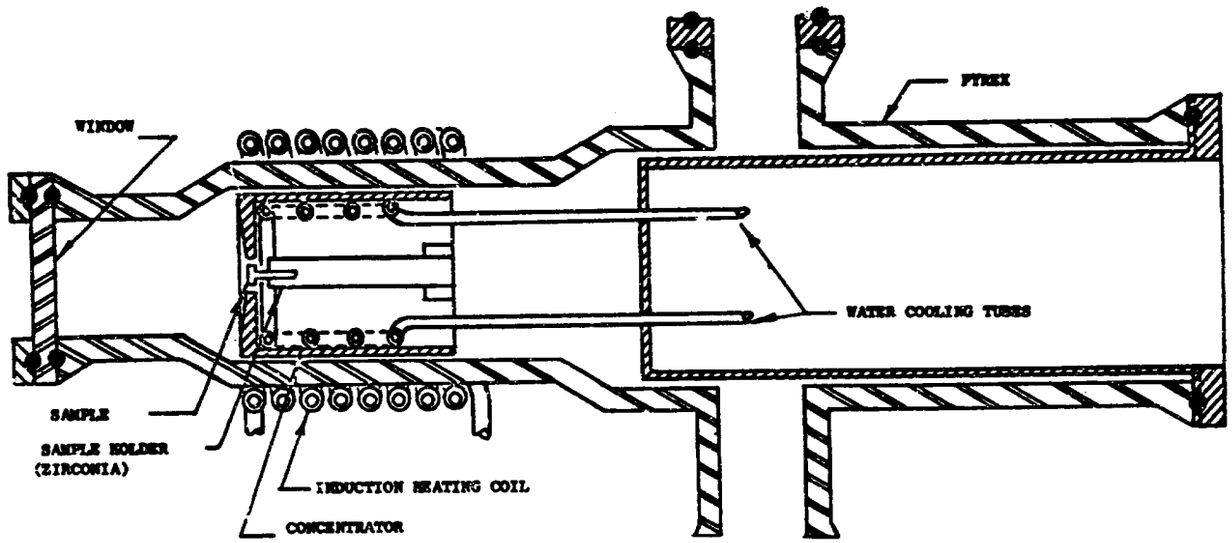

Figure 3. Total Normal Emittance Heating Apparatus

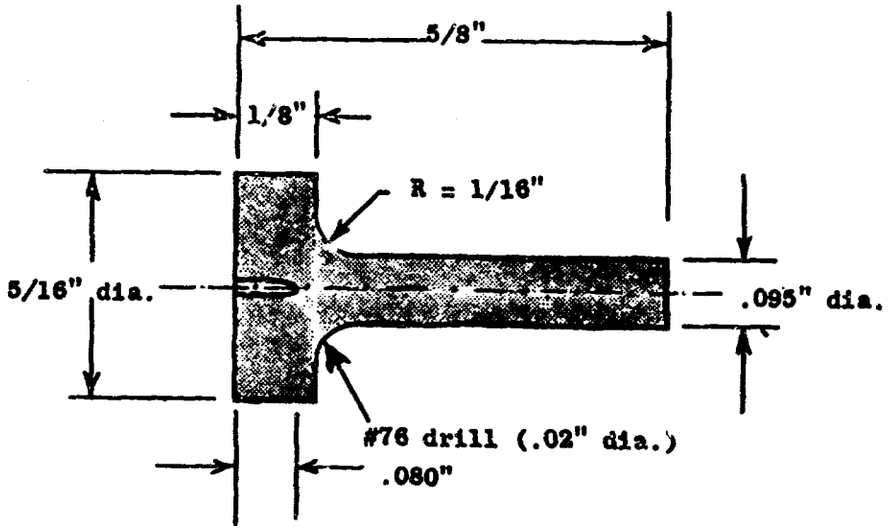

Figure 44. Cross-Section Schematic of Emittance Specimen

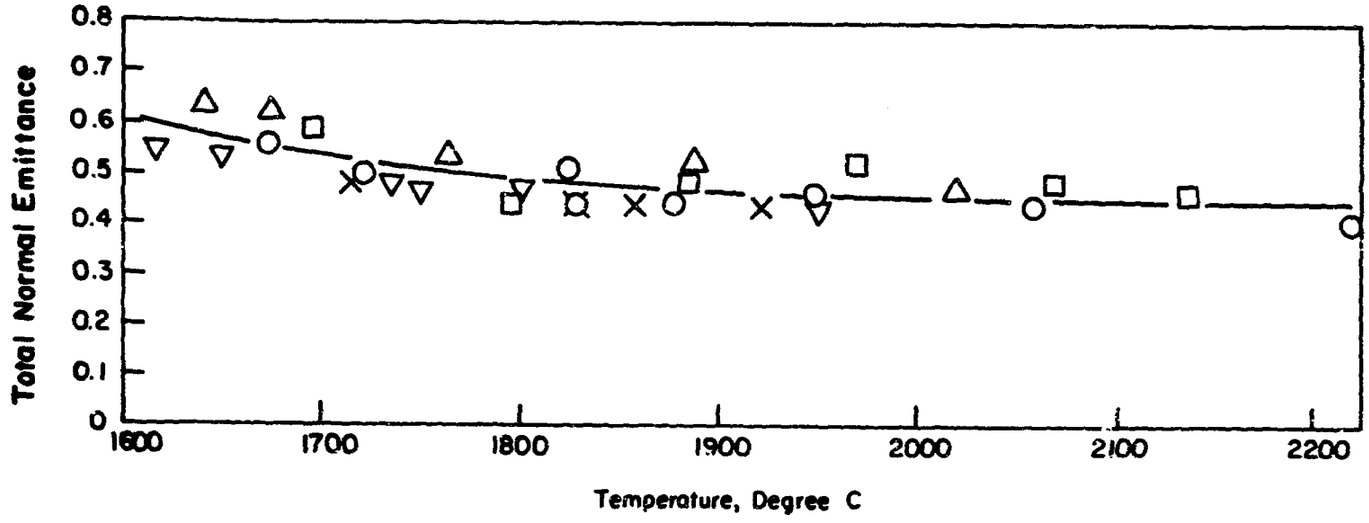

Figure 45. Total Normal Emittance of Material I (Billet I03 D0619K)

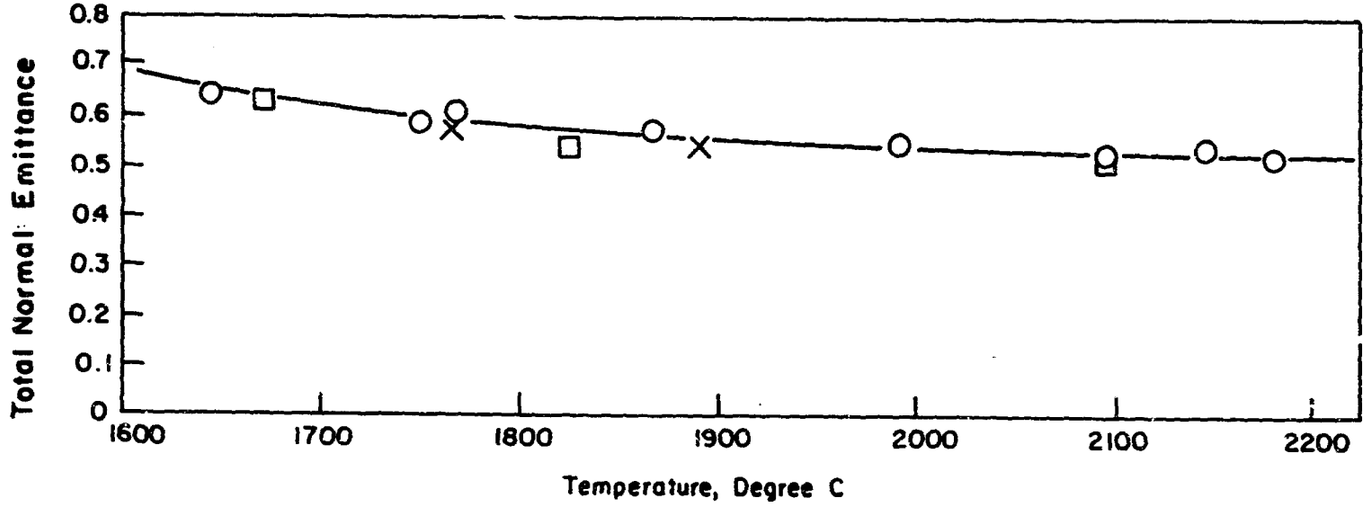

Figure 46. Total Normal Emittance of Material V (Billet V07 D0580K)

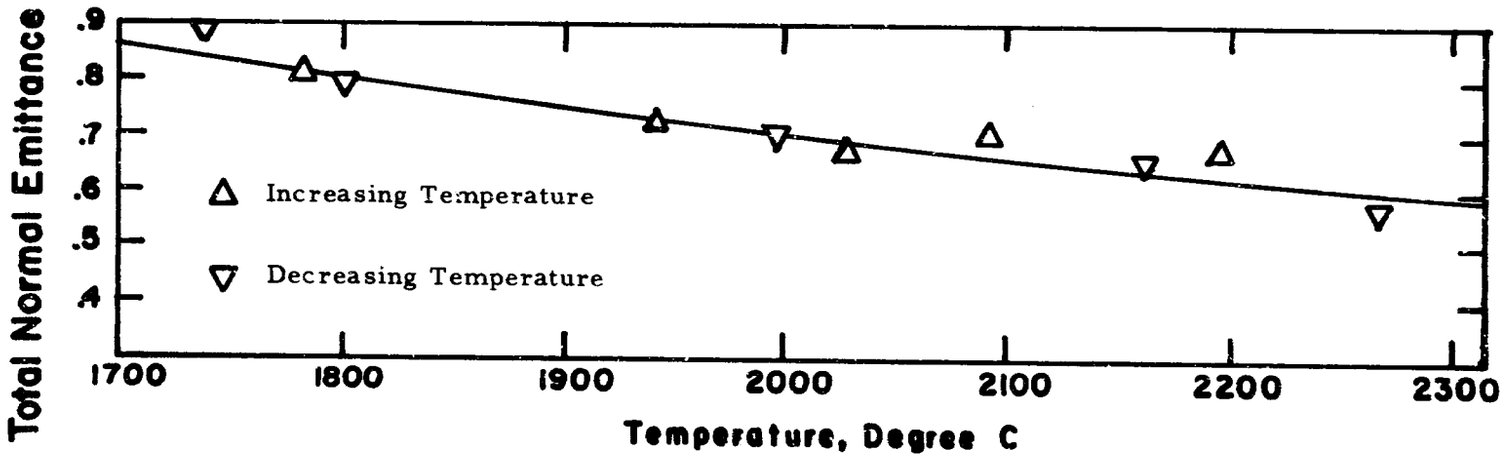

Figure 47. Total Normal Emittance of Material VIII (Billet VIII07F D0975K).

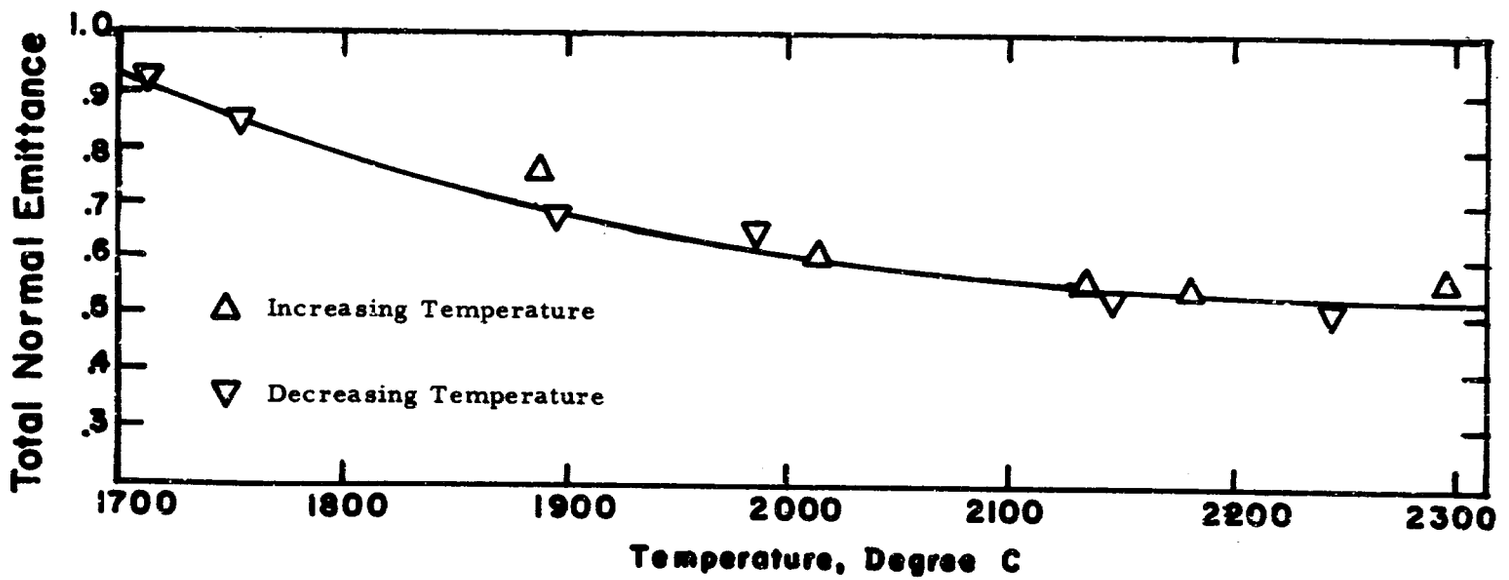

Figure 48. Total Normal Emittance of Material XII(20) (Billet XII(20)07F D0813K).

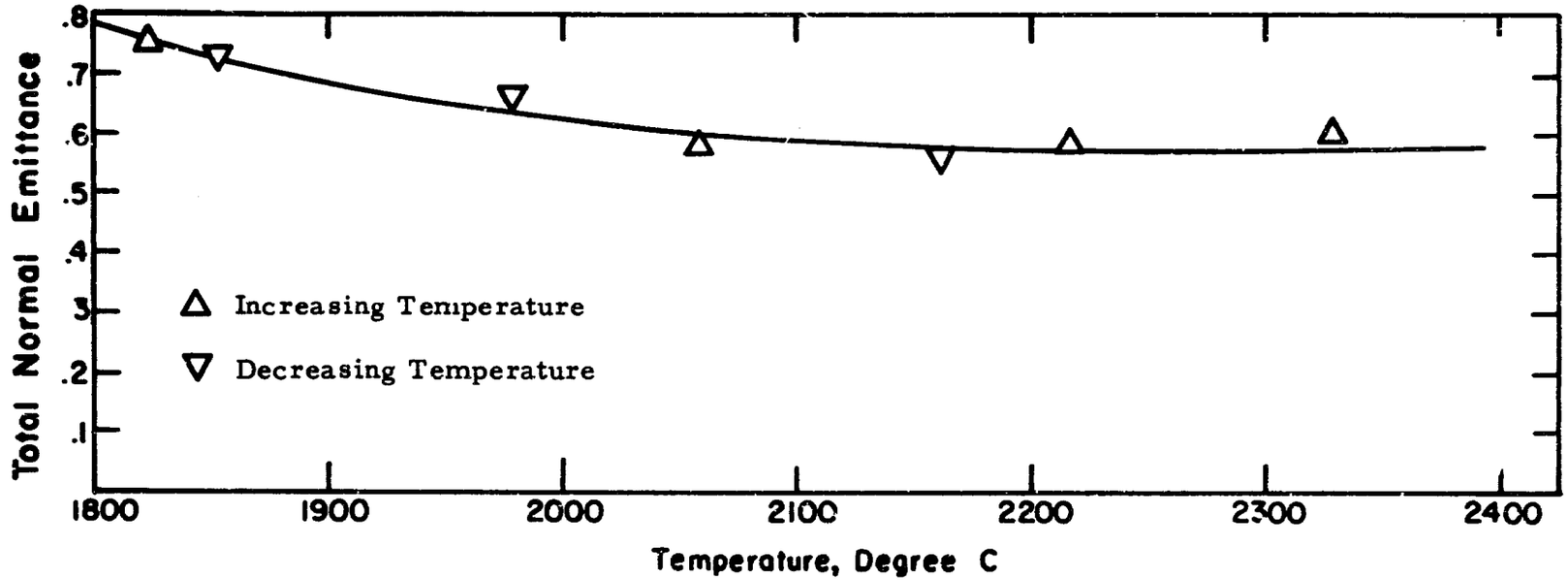

Figure 49. Total Normal Emittance of Material III (Billet III10 D0944K)

TABLE 1

DIBORIDE MATERIAL IDENTIFICATION: PHASE CONSTITUTION AND BASE COMPOSITION

Diboride Material	Designation	Remarks and Rationale for Specific Additives
I	ZrB_2	Zirconium diboride, no additive
II	HfB_2	Hafnium diboride, no additive
III	HfB_2+SiC	Hafnium diboride with twenty volume per cent silicon carbide to enhance oxidation resistance
IV	HfB_2+SiC	Hafnium diboride with thirty volume per cent silicon carbide to enhance oxidation resistance
V	ZrB_2+SiC	Zirconium diboride with twenty volume per cent silicon carbide to enhance oxidation resistance
VI	HfB_2+Hf-Ta	Hafnium diboride with four volume per cent hafnium tantalum alloy to provide an oxidation resistant metallic binder phase and enhance strength properties
VII	HfB_2+SiC	Boron rich hafnium diboride with silicon carbide additive to enhance oxidation resistance
VIII	ZrB_2+SiC+C	Zirconium diboride with fourteen volume per cent silicon carbide, thirty volume per cent carbon to enhance thermal stress resistance and maintain improved oxidation resistance relative to ZrB_2
IX	HfB_2+HfSi	Hafnium diboride with twenty volume per cent hafnium silicide to enhance oxidation resistance
X	ZrB_2+SiB_6	Zirconium diboride with twenty volume per cent silicon hexaboride to enhance oxidation resistance
XI	ZrB_2+Cr	Zirconium diboride with eight volume per cent chromium to enhance mechanical strength properties
XII	ZrB_2+C	Zirconium diboride with fifty volume per cent carbon to enhance thermal stress resistance
XIII	ZrB_2+W	Zirconium diboride with tungsten to enhance mechanical properties
XIV	HfB_2+SiC+C	Hafnium analogue of VIII
XV	HfB_2+C	Hafnium analogue of XII

TABLE 2

THERMAL CONDUCTIVITY OF PHASE TWO STRUCTURES

(Cut-Bar Method)

Material Designation / Percent Density, Grain Size	Thermal Conductivity (cal cm/cm^2 sec $^\circ$C) at T$^\circ$C									
	100°	200°	300°	400°	500°	600°	700°	800°	900°	1000°
I05 R44L 100%, 28.5μ	0.199	0.199	0.198	0.198	0.196	0.195	0.195	0.194	0.194	0.192
I07F D0905K 90.6%,	0.215	0.211	0.207	0.202	0.196	0.192	0.187	0.183	0.178	0.174
III(5)09F D1061 98.2%,	0.151	0.150	0.148	0.148	0.147	0.146	0.145	0.143	0.142	0.141
III10 D0943K 99%,	0.189	0.185	0.182	0.180	0.177	0.173	0.169	0.163	0.155	0.147
IV09F D0811K 100%,	0.187	0.181	0.175	0.168	0.162	0.155	0.149	0.145	0.141	0.138
V07F D0902K 99%,	0.236	0.220	0.211	0.204	0.202	0.199	0.195	0.193	0.190	0.187
V07F D0851K 88.5%, 9μ	0.211	0.204	0.193	0.185	0.178	0.169	0.162	0.154	0.148	0.140
VIII07F D0768K 99.6%	0.179	0.176	0.170	0.165	0.161	0.156	0.151	0.147	0.141	0.138
VIII(18, 10)07F D0920K 100%,	0.275	0.245	0.225	0.214	0.203	0.198	0.192	0.187	0.182	0.176
XII(20)07F D0812K 95%,	0.204	0.198	0.193	0.187	0.181	0.176	0.170	0.164	0.158	0.153
XIV(18, 10)09F D1033K 98.7%,	0.148	0.144	0.140	0.136	0.132	0.128	0.124	0.120	0.116	0.112
XV(20)10A D1027K 98.8%,	0.204	0.201	0.197	0.193	0.189	0.185	0.181	0.176	0.172	0.168

TABLE 3

THERMAL DIFFUSIVITY OF PHASE TWO STRUCTURES

Material Designation	THERMAL DIFFUSIVITY (cm^2/sec) at T^oC										
Per Cent Density, Grain Size	1000°	1100°	1200°	1300°	1400°	1500°	1600°	1700°	1800°	1900°	2000°
I05 R44L 100%, 28.5μ	0.205	0.202	0.199	0.197	0.194	0.191	0.188	0.186	0.183	0.180	0.178
III(5)09F D1061 98.2%	0.175	0.175	0.174	0.172	0.170	0.168	0.165	0.163	0.160	0.158	0.155
IV09F D0811K 100%	0.155	0.152	0.149	0.147	0.144	0.141	0.139	0.136	0.133	0.131	0.128
V07F D0902K 99%	0.213	0.207	0.195	0.189	0.184	0.180	0.176	0.172	0.169	0.166	0.163
V07F D0851K 88.5%, 9μ	0.172	0.167	0.162	0.157	0.154	0.150	0.147	0.144	0.141	0.138	0.135
VIII07F D0975K 98.7%	0.168	0.164	0.160	0.156	0.152	0.148	0.144	0.139	0.135	0.131	0.127
VIII(18,10)07F D0920K 100%	0.190	0.184	0.179	0.174	0.169	0.165	0.160	0.156	0.151	0.147	0.143
XII(20)07F D0812K 95%	0.179	0.175	0.172	0.169	0.165	0.162	0.159	0.155	0.152	0.149	0.145
XIV(18,10)09F D1037K 98.6%	0.160	0.156	0.151	0.148	0.145	0.142	0.140	0.138	0.135	0.134	0.131
XV(20)10 D1054K 97.4%	0.187	0.184	0.181	0.178	0.174	0.171	0.168	0.164	0.161	0.158	0.155

TABLE 4

DIMENSIONAL AND WEIGHT CHANGE DATA OF
THERMAL DIFFUSIVITY TEST SPECIMENS

Specimen	Before			After		
	Weight, grams	Thickness, in.	Diameter in.	Weight, grams	Thickness, in.	Diameter in.
I05 R44L	1.9205	0.1005	0.4933	1.9207	0.1005	0.4938
III(5)09F D1061	3.0950	0.1001	0.4976	3.0911	0.1000	0.4983
IV09F D0811K	2.5845	0.0998	0.4946	2.5765	0.1000	0.4952
V07F D0851K	1.5020	0.1014	0.4925	1.4844	0.1020	0.4916
V07F D0902K	1.7481	0.1001	0.4957	1.7308	0.1008	0.4969
VIII07F D0975K	1.4302	0.0985	0.4926	1.4322	0.0997	0.4944
VIII(18, 10)07F D0920K	1.6234	0.0990	0.4942	1.6232	0.1002	0.4950
XII(20)07F D0812K	1.6815	0.1006	0.4957	1.6808	0.1008	0.4956
XIV(18, 10)09F D1037K	2.6458	0.1007	0.4902	2.6402	0.1012	0.4906
XV(20)10 D1054K	2.8489	0.1001	0.4984	2.8481	0.1007	0.4992

TABLE 5

ENTHALPY, SPECIFIC HEAT, AND ENTROPY DATA FOR MATERIAL I*

Temperature $T^{\circ}C$	Enthalpy $H_T-H_0\ ^{\circ}C$ cal/gram	Specific Heat C_T cal/gram $^{\circ}C$	Entropy $S_T-S_0\ ^{\circ}C$ cal/gram $^{\circ}C$
1000	142.10	0.1685	0.00000
1100	159.00	0.1702	0.01278
1200	176.07	0.1718	0.02477
1300	193.30	0.1735	0.03609
1400	210.70	0.1753	0.04681
1500	228.30	0.1772	0.05703
1600	246.11	0.1793	0.06680
1700	265.13	0.1813	0.7617
1800	282.36	0.1833	0.08518
1900	300.79	0.1853	0.09386
2000	319.42	0.1873	0.10224

*Billet I05 R44L, room temperature density = 6.14 grams/cc (100 percent dense), linear expansion data provided in Table 11.

TABLE 6

ENTHALPY, SPECIFIC HEAT, AND ENTROPY DATA
FOR MATERIAL V*

Temperature $T^{\circ}C$	Enthalpy $H_T - H_0$ °C cal/gram	Specific Heat C_T cal/gram °C	Entropy $S_T - S_0$ °C cal/gram °C
1000	158.24	0.1712	0.00000
1100	175.46	0.1734	0.01303
1200	192.91	0.1756	0.02529
1300	210.59	0.1778	0.03690
1400	228.48	0.1800	0.04792
1500	246.59	0.1822	0.05843
1600	264.91	0.1843	0.6849
1700	283.44	0.1864	0.07813
1800	302.19	0.1885	0.08739
1900	321.15	0.1906	0.09632
2000	340.30	0.1926	0.10494

*Billet V07F D0902K, room temperature density = 5.52 grams/cc (99 percent dense), linear expansion data provided in Table 11.

TABLE 7

ENTHALPY, SPECIFIC HEAT, AND ENTROPY DATA
FOR MATERIAL VIII(18, 10)*

Temperature $T^{\circ}C$	Enthalpy $H_T-H_0{}^{\circ}C$ cal/gram	Specific Heat C_T cal/gram$^{\circ}C$	Entropy $S_T-S_0{}^{\circ}C$ cal/gram$^{\circ}C$
1000	164.43	0.1792	0.00000
1100	182.47	0.1818	0.01364
1200	200.79	0.1845	0.02652
1300	219.36	0.1871	0.03872
1400	238.20	0.1897	0.05032
1500	257.29	0.1923	0.06141
1600	276.65	0.1948	0.07203
1700	296.26	0.1973	0.08222
1800	316.12	0.1999	0.09204
1900	336.23	0.2023	0.10151
2000	356.58	0.2048	0.11067

*Billet VIII(18,10)07F D0920K, room temperature density = 5.25 grams/cc (100 percent dense), linear expansion data provided in Table 11.

TABLE 8

ENTHALPY, SPECIFIC HEAT, AND ENTROPY DATA
FOR MATERIAL XII(20)*

Temperature $T^{\circ}C$	Enthalpy $H_T - H_0{}^{\circ}C$ cal/gram	Specific Heat C_T cal/gram$^{\circ}C$	Entropy $S_T - S_0{}^{\circ}C$ cal/gram$^{\circ}C$
1000	160.18	0.1788	0.00000
1100	178.21	0.1819	0.01363
1200	196.54	0.1849	0.02651
1300	215.18	0.1880	0.03875
1400	234.13	0.1910	0.05043
1500	253.38	0.1940	0.06160
1600	272.93	0.1970	0.07233
1700	292.77	0.1999	0.08265
1800	312.91	0.2029	0.9261
1900	333.35	0.2058	0.10223
2000	354.07	0.2086	0.11155

*Billet XII(20)07F D0812K, room temperature density = 5.12 grams/cc (95 percent dense), linear expansion data provided in Table 11.

TABLE 9

CALCULATED THERMAL CONDUCTIVITY OF DIBORIDE
MATERIALS I, V, VIII(18,10) AND XII(20)

Material Designation / Percent Density, Grain Size	THERMAL CONDUCTIVITY, cal cm/cm^2 sec $^\circ$C										
	1000°	1100°	1200°	1300°	1400°	1500°	1600°	1700°	1800°	1900°	2000°
I05 R44L 100%, 28.5μ	0.206	0.205	0.203	0.202	0.201	0.199	0.198	0.197	0.196	0.196	0.195
V07F D0902K 99%,	0.196	0.190	0.185	0.181	0.178	0.175	0.173	0.171	0.169	0.167	0.165
VIII(18,10)07F D0920K 100%,	0.174	0.171	0.168	0.165	0.162	0.160	0.158	0.154	0.152	0.148	0.146
XII(20)07F D0812K 95%,	0.166	0.165	0.164	0.162	0.161	0.160	0.158	0.156	0.155	0.154	0.153

TABLE 10

CALCULATED AND MEASURED SPECIFIC HEAT VALUES FOR DIBORIDE MATERIALS I, V, VIII(18,10) AND XII(20)

Temp	Specific Heat, cal/gram °C							
	Material I		Material V		Material VIII(18,10)		Material XII(20)	
°C	Calc.	Obs*	Calc.	Obs*	Calc.	Obs*	Calc.	Obs*
1000	0.1709	0.1685	0.1867	0.1712	0.1964	0.1792	0.1927	0.1788
1200	0.1760	0.1718	0.1924	0.1756	0.2024	0.1845	0.1985	0.1849
1400	0.1814	0.1753	0.1983	0.1800	0.2084	0.1897	0.2041	0.1910
1600	0.1867	0.1793	0.2044	0.1843	0.2146	0.1948	0.2096	0.1970
1800	0.1920	0.1833	0.2103	0.1885	0.2204	0.1999	0.2149	0.2029
2000	0.1966	0.1873	0.2154	0.1926	0.2255	0.2048	0.2195	0.2086

*Observed data for Materials I, V, VIII(18,10) and XII(20) obtained from Billets I05 R44L, V07F D0902K, VIII(18,10)07F D920K and XII(20)07F D0812K, respectively.

TABLE 11

LINEAR THERMAL EXPANSION DATA FOR
MATERIALS I, V, VIII(18,10) AND XII(20)

Temperature °C	Material Designation, Percent Density				
	I05 R44L 100%	V07F R26L 99%		VIII(18,10)07F D0920 K 100%	XII(20)07F D0812K 95%
	Heating&Cooling	Heating	Cooling	Heating&Cooling	Heating&Cooling
20	0.000	0.0	-0.060	0.000	0.000
100	0.042	0.040	-0.023	0.040	0.044
200	0.100	0.090	0.018	0.100	0.110
300	0.163	0.145	0.095	0.162	0.175
400	0.227	0.203	0.158	0.227	0.242
500	0.292	0.264	0.220	0.295	0.315
600	0.359	0.336	0.284	0.363	0.385
700	0.428	0.400	0.358	0.435	0.460
800	0.498	0.473	0.425	0.505	0.540
900	0.569	0.545	0.495	0.583	0.621
1000	0.643	0.623	0.568	0.660	0.700
1100	0.718	0.704	0.644	0.740	0.786
1200	0.794	0.786	0.724	0.818	0.873
1300	0.870	0.874	0.807	0.900	0.960
1400	0.949	0.960	0.895	0.980	1.052
1500	1.030	1.048	0.983	1.063	1.140
1600	1.110	1.140	1.078	1.144	1.233
1700	1.193	1.228	1.177	1.232	1.323
1800	1.275	1.322	1.280	1.319	1.415
1900	1.360	1.420	1.392	1.404	1.510
2000	1.442	1.520	1.520	1.490	1.603

TABLE 12

SUMMARY OF LINEAR EXPANSION DATA

Material Designation	Measurement Technique*	Average CTE (inches/inch/°C) x 10^{-6} at T°C** 400°	800°	1200°	1600°
I05 R44L	DV	6.25	6.25	6.67	6.88
I07F D0700K	D	7.25	7.25	7.33	7.50
V07F R26L	DV	5.00	5.94	6.33	6.88
V07F D0706K	D	7.50	7.50	7.50	7.63
V07F D0845K	D	8.00	7.63	7.83	7.88
VIII(18, 10) D0920K	DV	6.25	6.29	7.29	7.19
VIII07F D0761K	D	6.00	6.13	6.25	6.25
XII(20)07F D0812K	DV	6.50	6.33	7.67	7.94
IV09F D0804K	D	7.00	7.25	7.50	7.50

*The letters DV and D refer to direct-view and differential dilatometry measurements, respectively.
**Tabulated CTE values refer to increments from room temperature to the tabulated temperature.

TABLE 13

SUMMARY OF DIBORIDE DENSITY DATA

Material Designation	Density, grams/cc
I05	6.33
I07F	5.96
V07F	5.56
VIII(18, 10)07F	5.26
VIII07F	4.44
XII(20)07F	5.43
II06B	10.95
II09F	10.39
II10	10.32
III10	9.34
IV09F	8.42
XIV(18, 10)09F	8.67
XV(20)10	8.95

TABLE 14

ELECTRICAL RESISTIVITY OF PHASE TWO STRUCTURES

Material Designation / Percent Density	Electrical Resistivity ($\mu\Omega$ cm) at T°C										
	20°	100°	200°	300°	400°	500°	600°	700°	800°	900°	1000°
I05 R44L 100%,	12.1	14.6	17.6	20.8	23.9	27.2	30.4	33.6	36.9	40.4	44.0
I07F R38L 90.8%,	11.6	14.4	18.2	22.2	26.1	30.1	34.0	38.0	42.5	47.3	52.0
III(5)09F D1061 98.2%,	12.8	15.9	19.9	23.8	27.6	31.7	35.9	40.3	45.0	49.4	53.6
III10 D0941K 99%,	9.6	13.2	17.8	22.4	27.0	31.6	36.5	41.8	47.2	52.4	57.8
IV09F D0811K 100%,	20.3	24.2	30.0	36.5	43.1	49.7	56.2	62.7	69.2	75.8	82.5
V07F D0902K 99%,	10.2	13.8	18.2	22.7	27.2	31.8	36.4	40.9	45.5	49.9	54.5
V07F D0851K 88.5%,	15.5	21.1	28.1	35.1	42.2	49.2	56.7	64.7	72.5	81.0	91.0
VIII07F D0975K 98.7%,	21.8	27.8	35.5	43.2	50.6	57.7	65.3	72.8	80.5	88.5	96.6
VIII(18, 10)07F D0920K 100%,	14.6	18.6	23.8	29.1	34.2	39.6	45.2	50.8	56.6	62.5	68.5
XII(20)07F D0812K 95%,	13.6	16.8	21.0	25.4	29.9	34.5	39.1	43.7	48.4	53.2	58.7
XIV(18, 10)09F D1037K 98.6%,	20.8	25.1	30.6	36.2	41.9	47.6	53.3	59.3	65.5	72.0	78.6
XV(20)10 D1054K 97.4%,	12.1	16.2	21.4	26.6	31.8	37.0	42.4	47.6	52.9	58.5	65.2

APPENDIX I

BILLET DESIGNATION SYSTEM

All Billets prepared in this program are designated by a series of letters and numbers to identify the powders and their relative amounts and the hot pressing billet. The designation system requires:

(1) a roman numeral to identify the base composition, Table 2, or a roman numeral followed by a parenthetically enclosed number or set of numbers to identify a compositional variation of the base composition, Table 3.

(2) an arabic number to identify a particular lot of the base powder, or an arabic number followed by the letter "F" to indicate a fluid energy milled base powder lot.

(3) a combination of a letter, and an arabic number or a letter, an arabic number and a letter to identify the billet pressing.

This is illustrated in the following examples:

(a) I07F D0701K designates Material I, ZrB_2; the 07 powder lot fluid energy milled, billet pressing D0701K where the D identifies the 75 ton Dake press and the K the billet size of 3 inch diameter by 1 inch high.

(b) V(5)05A D0829 designates Material V, ZrB_2 with 20 volume per cent SiC in the base composition but modified in this billet to 5 volume per cent as shown by "(5)" and billet pressing D0829 where the omission of a terminal letter indicates a billet size of 2 inch diameter by 0.7 inch high.

The letters for pressing or furnace identification include:

S, a 20 ton Dake Press;
D, a 75 ton Dake Press;
Q, a 125 ton press;
C, hot pressed at Carborundum;
B, vacuum furnace for sintering;
R, a 400 ton Rogers Press.

The letters for billet size identification include:

K, 3 inch diameter by 1 inch high;
N, 5 inch diameter by 1 to 2 inch high;
M, 6 inch diameter by 1 to 2 inch high;
L, 5.75 inch square by 1 to 2 inch high;
H, hollow cylindrical billet.

UNCLASSIFIED
Security Classification

DOCUMENT CONTROL DATA - R & D

(Security classification of title, body of abstract and indexing annotation must be entered when the overall report is classified)

1. ORIGINATING ACTIVITY (Corporate author) ManLabs, Inc. 21 Erie Street Cambridge, Massachusetts 02139	2a. REPORT SECURITY CLASSIFICATION UNCLASSIFIED 2b. GROUP N/A

3. REPORT TITLE

Research and Development of Refractory Oxidation Resistant Diborides: Part II, Volume V: Thermal, Physical, Electrical and Optical Properties

4. DESCRIPTIVE NOTES (Type of report and inclusive dates)

Technical Documentary Report, September 1967 to May 1969

5. AUTHOR(S) (First name, middle initial, last name)

Clougherty, Edward V., Wilkes, Kenneth, E., Tye, Ronald, P.

6. REPORT DATE	7a. TOTAL NO. OF PAGES	7b. NO. OF REFS
November 1969	90	20

8a. CONTRACT OR GRANT NO. AF33(615)-3671 b. PROJECT NO. 7350 c. Task No. 735001 d.	9a. ORIGINATOR'S REPORT NUMBER(S) N/A 9b. OTHER REPORT NO(S) (Any other numbers that may be assigned this report) AFML-TR-68-190, Part II, Vol. V

10. DISTRIBUTION STATEMENT

This document is subject to export controls and each transmittal to foreign governments or foreign nationals may be made only with prior approval of the Air Force Materials Lab. (MAMC), Wright-Patterson AFB, Ohio 45433.

11. SUPPLEMENTARY NOTES	12. SPONSORING MILITARY ACTIVITY
N/A	AFML (MAMC), WPAFB, Ohio 45433

13. ABSTRACT

Thermal conductivity data were measured from 100° to 1000°C and were calculated from thermal diffusivity, specific heat and density data from 1000° to 2000°C for compositional and microstructural variations of ZrB_2 and HfB_2 with SiC and/or C additives varying in total content from 20 to 34 volume percent. All compositions displayed a negative temperature dependence with values of the order of 0.20 and 0.10 cal. cm/cm^{2}sec°C at room temperature and 2000°C, respectively. The specific heat data were obtained from drop calorimetry methods for selected compositions and by calculations from constituent values for other compositions.

Linear expansion data were obtained from room temperature to 2000°C by direct-view and differential dilatometry for compositions of ZrB_2 with SiC and/or C additives. Average CTE values are of the order of 7.0×10^{-6} in/in/°C. Density data at room temperature showed the effects of SiC and C; the additions produce a significant reduction in the density of HfB_2 from 11 to 8 grams/cc.

Electrical resistivity data were obtained from room temperature to 1000°C; all compositions displayed positive temperature coefficients. Room temperature values of the order of 10 to 15 $\mu\Omega$ cm were measured for all compositions.

Total normal emittance data were measured from 1600° to 2300°C for unoxidized diboride compositions.

Unlimited distribution for this abstract.

DD FORM 1 NOV 68 1473 REPLACES DD FORM 1473, 1 JAN 64, WHICH IS OBSOLETE FOR ARMY USE.

UNCLASSIFIED
Security Classification

14. KEY WORDS	LINK A		LINK B		LINK C	
	ROLE	WT	ROLE	WT	ROLE	WT
Diboride						
Diboride and Carbon Compositions						
Diboride and Silicon Carbide Compositions						
Thermal Conductivity						
Thermal Diffusivity						
Thermal Expansion						
Electrical Resistivity						
Emittance						